

Evaluating the physical and insecticidal properties and the effects on grain flow properties of a synthetic amorphous zeolite intended for grain protection

by

Kouame Dominique Yao

B.S., University of Abobo-Adjame, 2004  
M.S., University Felix H. Boigny, 2009  
M.S., Kansas State University, 2014

AN ABSTRACT OF A DISSERTATION

submitted in partial fulfillment of the requirements for the degree

DOCTOR OF PHILOSOPHY

Department of Grain Science and Industry  
College of Agriculture

KANSAS STATE UNIVERSITY  
Manhattan, Kansas

2018

## Abstract

Alternatives to chemical grain protectants are needed that have low mammalian toxicity and high specificity to insects with no adverse environmental impacts. This project investigated the viability of using a synthetic amorphous zeolite as a potential alternative to chemical insecticides and phosphine in Australian grain. We evaluated the impacts of moisture content and application rates on dust and grain physical properties; compared registered dusts with this promising novel dust in terms of impact on grain flowability; investigated changes in bulk properties of inert-dust treated grain; and we constructed dynamic dewpoint isotherms of hard red winter wheat and amorphous silica dusts for a better understanding of moisture interactional behavior of the synthetic amorphous dust based on wheat initial moisture content.

Full sorption isotherms of zeolite and wheat obtained at 25, 35, and 45°C clearly exhibited the hysteresis phenomenon. The intensity of hysteresis remained unchanged with increasing temperatures for Hard Red Winter wheat (HRW), whereas, the intensity of hysteresis decreased with increased temperatures during water adsorption for the porous synthetic amorphous zeolite powder. Considering the IUPAC classification of isotherms, HRW had typical type II sigmoid shape isotherm, whereas, zeolite powder had a sorption isotherm close to resembling a type IV sigmoid shape isotherm. The hysteresis loops were of type H3 for HRW, and of type H4 for zeolite powder. Irrespective of sorption direction, DLP model was the best model to estimate zeolite and HRW sorption isotherms, followed by GAB and BET models, although BET model provided almost perfect fitting to sorption data in the water activity range 0-0.5. Particle size of the amorphous dust increased with increasing moisture content. Conversely, shape parameters (circularity, aspect ratio, convexity, and solidity) generally decreased with increasing dust moisture contents. When wheat was mixed with the amorphous dust at different rates and

moisture levels, the bulk density of wheat decreased, while the tapped density and the angle of repose increased, resulting in higher Hausner ratios and Carr Index values. Treating wheat with the amorphous dust caused the treated wheat to transition from an acceptable flowability to a poor flowability, based on angle of repose, Hausner ratio, and Carr index data, which do not account for the interaction of wheat with the storage vessel. Our data suggest that a range of moisture content (2-6%) and an application rate (0.5 g/kg) mitigate the adverse effects on wheat flowability. However, based on flow rate index and specific energy requirements, flowability of wheat was generally enhanced by admixing wheat with the amorphous dusts. Wheat treated with Odor-Z-Way was comparable with wheat treated with Celite or Diafil as they all exhibited low cohesion, moderate permeability, and moderate sensitivity to aeration. Wheat treated with each of the three dusts became almost unstable due to segregation, moisture uptake, lower adhesion, and coating of the blade and test vessel. A decrease in bulk density was however observed, although the decrease was smaller when wheat was admixed with Odor-Z-Way. The susceptibility to Celite, Diafil, and Odor-Z-Way varied among stored-product insect species and also among the type of substrate (wheat or concrete). Adults of the lesser grain borer, *Rhyzopertha dominica*, were generally least susceptible to all three amorphous silica dusts; however, a complete suppression of progeny production was possible using Celite. Adult emergence was generally not prevented by Celite, Diafil, and Odor-Z-Way which suggested a lower insecticidal efficacy of the three dusts against early developmental stages. On concrete, Odor-Z-way was particularly effective at controlling all stored-product insect species after 24 h of exposure. In view of the bulk and dynamic flow properties and the insecticidal activity, Odor-Z-Way has potential to become a grain protectant provided that segregation and the decrease in

bulk density are mitigated and that the insecticidal activity is not adversely affected by the seemingly low adhesion on wheat kernels.

Evaluating the physical and insecticidal properties and the effects on grain flow properties of a synthetic amorphous zeolite intended for grain protection

by

Kouame Dominique Yao

B.S., University of Abobo-Adjame, 2004

M.S., University Felix H. Boigny, 2009

M.S., Kansas State University, 2014

A DISSERTATION

submitted in partial fulfillment of the requirements for the degree

DOCTOR OF PHILOSOPHY

Department of Grain Science and Industry  
College of Agriculture

KANSAS STATE UNIVERSITY  
Manhattan, Kansas

2018

Approved by:

Major Professor  
Bhadriraju Subramanyam

# **Copyright**

© Kouame Yao 2018.

## Abstract

Alternatives to chemical grain protectants are needed that have low mammalian toxicity and high specificity to insects with no adverse environmental impacts. This project investigated the viability of using a synthetic amorphous zeolite as a potential alternative to chemical insecticides and phosphine in Australian grain. We evaluated the impacts of moisture content and application rates on dust and grain physical properties; compared registered dusts with this promising novel dust in terms of impact on grain flowability; investigated changes in bulk properties of inert-dust treated grain; and we constructed dynamic dewpoint isotherms of hard red winter wheat and amorphous silica dusts for a better understanding of moisture interactional behavior of the synthetic amorphous dust based on wheat initial moisture content.

Full sorption isotherms of zeolite and wheat obtained at 25, 35, and 45°C clearly exhibited the hysteresis phenomenon. The intensity of hysteresis remained unchanged with increasing temperatures for Hard Red Winter wheat (HRW), whereas, the intensity of hysteresis decreased with increased temperatures during water adsorption for the porous synthetic amorphous zeolite powder. Considering the IUPAC classification of isotherms, HRW had typical type II sigmoid shape isotherm, whereas, zeolite powder had a sorption isotherm close to resembling a type IV sigmoid shape isotherm. The hysteresis loops were of type H3 for HRW, and of type H4 for zeolite powder. Irrespective of sorption direction, DLP model was the best model to estimate zeolite and HRW sorption isotherms, followed by GAB and BET models, although BET model provided almost perfect fitting to sorption data in the water activity range 0-0.5. Particle size of the amorphous dust increased with increasing moisture content. Conversely, shape parameters (circularity, aspect ratio, convexity, and solidity) generally decreased with increasing dust moisture contents. When wheat was mixed with the amorphous dust at different rates and

moisture levels, the bulk density of wheat decreased, while the tapped density and the angle of repose increased, resulting in higher Hausner ratios and Carr Index values. Treating wheat with the amorphous dust caused the treated wheat to transition from an acceptable flowability to a poor flowability, based on angle of repose, Hausner ratio, and Carr index data, which do not account for the interaction of wheat with the storage vessel. Our data suggest that a range of moisture content (2-6%) and an application rate (0.5 g/kg) mitigate the adverse effects on wheat flowability. However, based on flow rate index and specific energy requirements, flowability of wheat was generally enhanced by admixing wheat with the amorphous dusts. Wheat treated with Odor-Z-Way was comparable with wheat treated with Celite or Diafil as they all exhibited low cohesion, moderate permeability, and moderate sensitivity to aeration. Wheat treated with each of the three dusts became almost unstable due to segregation, moisture uptake, lower adhesion, and coating of the blade and test vessel. A decrease in bulk density was however observed, although the decrease was smaller when wheat was admixed with Odor-Z-Way. The susceptibility to Celite, Diafil, and Odor-Z-Way varied among stored-product insect species and also among the type of substrate (wheat or concrete). Adults of the lesser grain borer, *Rhyzopertha dominica*, were generally least susceptible to all three amorphous silica dusts; however, a complete suppression of progeny production was possible using Celite. Adult emergence was generally not prevented by Celite, Diafil, and Odor-Z-Way which suggested a lower insecticidal efficacy of the three dusts against early developmental stages. On concrete, Odor-Z-way was particularly effective at controlling all stored-product insect species after 24 h of exposure. In view of the bulk and dynamic flow properties and the insecticidal activity, Odor-Z-Way has potential to become a grain protectant provided that segregation and the decrease in

bulk density are mitigated and that the insecticidal activity is not adversely affected by the seemingly low adhesion on wheat kernels.

## Table of Contents

List of Figures .....	xiv
List of Tables .....	xv
Acknowledgements.....	xvii
Dedication.....	xix
General Introduction.....	xx
References.....	xxvi
Chapter 1 - Dynamic dewpoint isotherms of hard red winter wheat and a synthetic amorphous zeolite intended for grain protection..... 1	
Introduction.....	2
Material & Methods.....	8
Wheat and zeolite preparation.....	8
Sorption isotherms .....	8
Water activity linear offset and weight calibration.....	9
Using DDI to investigate phase transitions.....	9
Isotherms models .....	10
DLP (Double Log Polynomial).....	10
GAB (Guggenheim-Anderson-de Boer).....	10
BET (Brunauer-Emmet-Teller).....	10
Error functions and assessment of goodness-of-fit.....	10
Coefficient of determination ( $R^2$ ) .....	11
The sum of the squares of the errors (SSE) .....	11
The Sum of the Absolute Errors (SAE) .....	11
The Mean Relative Deviation (MRD) .....	11
The Standard Error of prediction (SE).....	11
Optimal water activity and equilibrium moisture content (EMC) .....	11
Net isosteric heat of sorption, differential enthalpy, and differential entropy .....	12
Isokinetic temperature and free Gibbs energy .....	12
Water activity prediction: The Clausius-Clapeyron equation.....	13
Statistical analysis.....	13

Results & Discussion .....	15
Conclusions.....	21
References.....	22
Chapter 2 - Moisture content and application rates of inert dusts: Effects on dust and wheat	
physical properties.....	38
Introduction.....	39
Materials & Methods .....	42
Moisture effects on physical properties of amorphous silica dust .....	42
Sampling .....	42
Equilibration in controlled humidity chamber .....	42
True density analysis.....	42
Particle size and shape analysis .....	43
Circularity .....	43
Convexity.....	44
Solidity.....	44
Aspect ratio.....	44
Elongation.....	44
Moisture and application rates effects on wheat physical properties.....	44
Sampling .....	44
Static Angle of Repose (AoR) .....	45
Test weight.....	46
Tapped Density .....	46
Carr Index (CI) and Hausner Ratio (HR).....	46
Single Kernel Characterization System (SKCS).....	47
Statistical analyses .....	47
Results & Discussion .....	48
Conclusions.....	54
References.....	55
Chapter 3 - Using the FT4 Powder Rheometer to characterize bulk and dynamic flow properties	
of Hard Red Winter wheat (HRW) treated with three amorphous silica dusts .....	69
Introduction.....	70

Materials & Methods .....	74
Hard Red Winter Wheat (HRW).....	74
Inert dusts.....	74
Sample preparation .....	75
The FT4 Powder Rheometer.....	75
Bulk properties.....	76
Dynamic flow tests .....	76
Stability tests.....	76
Variable Flow Rate (VFR).....	77
Aeration tests .....	77
De-aeration tests.....	78
Tapped consolidation .....	78
Direct pressure consolidation.....	79
Statistical analyses .....	79
Results & Discussion .....	80
Conclusions.....	86
References.....	87
Chapter 4 - Efficacy of three amorphous inert dusts applied to wheat and concrete surfaces	
against eggs and adults of seven stored-grain insect species.....	103
Introduction.....	105
Materials & Methods .....	109
Organic Wheat .....	109
Concrete-poured Petri dishes .....	109
Inert dusts.....	109
Test insects.....	110
Bioassay on wheat.....	110
Adult mortality and progeny production.....	110
Egg-to-adult emergence of four insect species on wheat.....	111
Bioassay on concrete arenas .....	112
Statistical analyses .....	112
Results & Discussion .....	114

Adult mortality on wheat .....	114
Progeny production on wheat .....	115
Egg-to-adult emergence on wheat.....	116
Adult mortality on concrete .....	116
Conclusions.....	117
References.....	118
General conclusion and Recommendations .....	130

## List of Figures

Figure 1-1 Full sorption isotherms of zeolite powder at 25 (a), 35 (b), and 45°C (c). .....	35
Figure 1-2 Full sorption isotherms of Hard Red Winter wheat (HRW) at 25 (a), 35 (b), and 45°C (c). .....	36
Figure 1-3 Graphical determination of the net isosteric heat of sorption and the differential enthalpy of zeolite powder at different moisture contents .....	37
Figure 2-1 X-ray diffraction profile of a synthetic amorphous zeolite .....	67
Figure 2-2 Scanning electron microscopy of a synthetic amorphous zeolite at various moisture contents .....	68
Figure 3-1 Pressure drop across powder bed versus normal consolidation stress .....	95
Figure 3-2 Stability of untreated wheat and wheat treated with three amorphous silica dusts.....	96
Figure 3-3 Variable flow rate of untreated wheat and wheat treated with three amorphous silica dusts .....	97
Figure 3-4 Basic flowability energy versus number of de-aeration cycles.....	98
Figure 3-5 Flow Energy as a function of number of taps .....	99
Figure 3-6 Bulk density as a function of number of taps.....	100
Figure 3-7 Flow energy as a function of direct pressure .....	101
Figure 3-8 Bulk density as a function of direct pressure .....	102

## List of Tables

Table 1.1 Specifications of the Vapor Sorption Analyzer .....	25
Table 1.2 Estimated parameters of models for the sorption isotherms of hard red winter wheat (HRW).....	26
Table 1.3 Estimated parameters of models for the sorption isotherms of zeolite powder .....	28
Table 1.4 Best-fitting equations to sorption experimental data of zeolite powder and hard red winter wheat (HRW).....	30
Table 1.5 Critical water activity ( $A_{WC}$ ) and corresponding equilibrium moisture content (EMC) (% w.b.) for phase transition in zeolite powder and hard red winter wheat .....	31
Table 1.6 Recommended zeolite moisture content and water activity for grain (HRW) protection, at different grain moisture contents and storage temperatures .....	32
Table 1.7 Predicted water activity of HRW and zeolite powder at different moisture contents and temperatures .....	33
Table 1.8 Temperature effect: prediction of water activity of wheat and zeolite at different moisture contents .....	34
Table 2.1 Density and flow properties of an amorphous silica dust.....	57
Table 2.2 Equilibration parameters of zeolite powder and wheat in a controlled humidity chamber at 25°C.....	58
Table 2.3 Angle of repose and flowability.....	59
Table 2.4 Classification of powder flowability based on Hausner ratio.....	60
Table 2.5 Surface and volume mean diameters of zeolite powder at various moisture contents .	61
Table 2.6 Particle size distribution of zeolite powder at various moisture contents.....	62
Table 2.7 Median particle shape parameters of zeolite powder at various moisture contents.....	63
Table 2.8 Physical properties of zeolite-treated wheat at various dust moisture contents and application rates .....	64
Table 2.9 Single Kernel Characterization System (SKCS) data of wheat treated with an amorphous silica dust at various moisture contents and application rates.....	66
Table 3.1 Conditioned bulk density, Specific Energy, Stability Index, and Flow Rate Index of untreated wheat and wheat treated with three amorphous inert dusts at 1g/kg.....	90

Table 3.2 Aerated energy and aeration ratio of wheat treated with three amorphous inert dusts at 1g/kg. ....	91
Table 3.3 Basic flowability energy and percent recovery versus number of de-aeration cycles..	92
Table 3.4 Tapped consolidated energy and tapped consolidation index as a function of number of taps .....	93
Table 3.5 Direct pressure consolidated energy and direct pressure consolidation index as a function of direct pressure.....	94
Table 4.1 Mortality of adults of six species of stored-grain insects after 7 and 14 days on untreated wheat. ....	121
Table 4.2 Corrected adult mortality on wheat of six species of stored-grain insects exposed to various doses of Celite, Diafil, and Odor-Z-Way. ....	122
Table 4.3 Progeny production on untreated wheat exposed to six species of stored-grain insects .....	124
Table 4.4 Progeny production on wheat treated with various doses of Celite and Diafil.....	125
Table 4.5 Egg-to-adult emergence on wheat of four insect species of stored-grain exposed to various doses of Celite, and Diafil. ....	126
Table 4.6 Corrected percent knockdown of adults of six species of stored-grain insects exposed over time to concrete sprinkled with different rates of Celite and Diafil. ....	127
Table 4.7 Corrected mortality of adults of six species of stored-grain insects exposed over time to concrete sprinkled with different rates of Celite, Diafil, and Odor-Z-Way.....	128

## **Acknowledgements**

This dissertation would never have materialized without the financial support from the Government of Australia (Department of Industry and Science) and its affiliate, the Plant Biosecurity Cooperative Research Center (PBCRC). I think particularly of Dr. Michael Robinson (CEO), Dr. David Eagling (Research Coordinator and Safeguarding Trade Program Leader), Dr. Jo Luck (Director Research, Education & Training), Naomi Thompson (Project officer), Tony Steeper (Corporate Communications and Engagement Manager), John Austen (Project officer), Kylee Carpenter, Juanita Waters (Research coordinator), Devika Naidu-Ihms (Project officer), Ern Kostas (Internship supervisor), Guy Baxter (Grain Protection Coordinator, Kwinana Terminal), Shaugh Tomlinson (Grain Protection Coordinator, Metro Grain Centre), Mario Discenza and Casey Atkinson (Grain Protection, Merredin), Keith Andrews and Trevor Martin (Grain Protection, Albany Terminal) and all other staff I have not mentioned. They all have been very supportive and caring, and their respective dedication and talents were a great input in making that PhD venture more bearable.

The PBCRC offered a unique opportunity to broaden my networking through well-suited professional developments activities and annual meetings, conferences, and workshops. The summer 2018 internship that took place at Cooperative Bulk handling (CBH, Perth, Western Australia) was particularly a unique asset in bridging the gap between academia and the real job market.

Also, I would like to express my sincere gratitude to my academic advisor, Prof. Bhadriraju Subramanyam (Subi), for his unshakable patience, sustained motivation, perpetual enthusiasm, and immense knowledge. His guidance and, more importantly, the entire freedom I was given while working on this project, especially the ability to conduct my research at my own pace and,

sometimes, from my own perspective, helped me develop and reinforce my stature as an independent, self-starter scientist.

Besides, I would like to thank and express my heartfelt appreciation to the members of my research committee: Drs David Hagstrum (Department of Entomology), Kun Yan Zhu (Department of Entomology), Jennifer Anthony (Department of chemical engineering), and Ronaldo Maghirang (Department of Biological and Agricultural engineering). They spent hours editing this manuscript and providing me with insights into dealing with specific aspects of the project. Their proven expertise in their respective fields of study was genuinely invaluable.

## **Dedication**

To the memory of my beloved father.

You did not see the end, but You were at the very beginning.

## General Introduction

Australia's \$9 billion grain exports are protected with chemical insecticides that leave a residue, and the fumigant phosphine, that does not. With increasing market sensitivity to insecticide residues, development of resistance in grain pests, and potential changes in food security legislation, pest management agents are needed that have low mammalian toxicity and high specificity to insects with no adverse environmental impacts. Moreover, the 2008 de-regulation of the Australian export grain market has placed increasing pressure on the management of grain during transport, which is exacerbated by farmers storing larger volumes of wheat on the farm. Wheat is a major component of most diets of the world because of its agronomic adaptability, ease of storage, nutritional goodness, and the ability of its flour to produce a variety of palatable, interesting, and satisfying foods (Khan, 2016). The US Federal Grain Inspection Service (FGIS, 2013) defines wheat as grain that, before the removal of dockage, consists of 50 percent or more common wheat (*Triticum aestivum* L.), club wheat (*T. compactum* Host.), and durum wheat (*T. durum* Desf.) and not more than 10 percent of other grains and that, after the removal of the dockage, contains 50 percent or more of whole kernels of one or more of these wheats. During storage, wheat quality can deteriorate if insect infestation is not prevented, especially under environmental conditions such as high relative humidity and temperature (Le Patourel, 1986). Pest management strategies usually implemented to prevent grain infestation from several species of stored-grain insects encompass the use of sanitation of empty storage facilities and grain, contact insecticides (protectants), fumigation, and aeration (White & Leesch, 1996; Subramanyam & Roesli, 2000). The application of protectants on grain kernels is a preventive tactic used to treat uninfested grain as it is being loaded into bins. Grain protectants guarantee a residual protection of grain; however, they are not effective against all life stages of insects,

especially larvae that are developing internally. It is therefore important to kill adults of stored-grain insects before they have had a chance to mate and lay eggs on (internal insects) or within the grain kernels (external insects) (Hagstrum & Subramanyam, 2006). To ensure the delivery of wheat that meets the highest quality standards, wheat kernels are treated with chemical insecticides at the time of storage as grain is being loaded into the bin or silo. These conventional insecticides, despite their proven efficacy, pose food safety and environmental pollution concerns. Alternatives that are safe, effective, and cost-effective are thus needed. Inert dusts are promising and viable alternatives as they have low mammalian toxicity, do not leave harmful residues, are effective against chemical resistant species, and are persistent and stable at high and low temperatures (Subramanyam et al., 1994). Inert dusts are dry, chemically unreactive powders of different origins and have various industrial and agricultural uses (Ebeling, 1971). Inert dusts are primarily composed of amorphous silica, which should not be confused with crystalline silica such as quartz, cristobalite, and tridymite. Amorphous silica dusts are characterized by their unique ability to reversibly lose or gain water and adsorb molecules of appropriate cross-sectional diameter and exchange their inorganic cations without any major change of their structure (Dakovic et al., 2007). Inert dusts kill insects primarily by desiccation because of the abrasion of insect cuticle. It is believed that once insects come in contact with the inert dust particles, the inherent adsorption properties induce the dehydration of insect pests, keeping them from flourishing in stored-products. The main advantage of inert dusts is their low mammalian toxicity. Besides, inert dusts are effective for long durations and they do not affect end use quality of grain (Fields et al., 2003). Moreover, treating storage structures and handling machinery with inert dusts is more cost-effective compared with chemical treatments and provides effective, long-term protection (Desmarchelier & Dines, 1987; Desmarchelier et al.,

1993). Their main limitations are that they create a dusty environment, do not work well at high relative humidity (>60%), and they presumably adversely affect the physical properties of grain such as angle of repose and flowability (Korunic et al., 1996; Korunic et al., 1998). Literature on zeolites for use in stored-product insect control is scarce compared to that of earthed dusts. There are a limited number of studies that examined the effectiveness of natural zeolites applied to stored grain against stored-product insect pests. Earlier studies with natural zeolites did not evaluate the effectiveness of zeolites applied to concrete surfaces, such as those found in empty grain storage facilities, against stored-product insects.

Moisture uptake during dust storage prior to application onto grain negatively impacts the overall effectiveness of the dust. In fact, insects could better resist desiccation by taking advantage of the moisture already present within the moist dust to replenish the body water content loss induced by desiccation. Using dry powders with moisture as low as 1% is not enough to maximize the insecticidal efficacy, though. The limiting parameter is the  $A_w$  of the dust interacting with the grain. Optimal storage conditions can be defined as a combination of environmental parameters (storage temperature, water activity of dust and grain) that foster a maximum stability of the treated grain by considerably depressing the likelihood of water migration within the system “dust-grain”. At a given temperature, high differences in grain water activity relative to dust water activity will cause the dust to adsorb or desorb water. Moisture equilibration between grain and the moist dust results in a too moist grain that is easily prone to mold and fungi infestation, especially when grain moisture reaches 15% and beyond. On the other hand, a too dry dust can have a drying action on the stored grain. Stored grain is primarily sold based on weight and selling a too dry grain equates with a significant decrease in profitability. Hence, understanding the underlying mechanisms leading to the dramatic changes in the physical integrity of the dust

or how moisture migrates within the system “dust-grain” is crucial. A practical approach in determining moisture migration is the construction of sorption isotherms which help predict the moisture or water activity under specific storage conditions.

Wheat kernels treated with inert dusts form a granular system, which can transition between any of three distinct states: static, quasi-static, or dynamic (Lumay et al., 2012). A major concern, when applying any amorphous dust onto grain for quality preservation, is the change in the flow properties of the treated grain. A vast array of literature exists that stresses the relationship between flowability and grain physical properties such as particle size, particle shape, moisture, and environmental parameters such as temperature, and relative humidity (Fitzpatrick et al., 2004; Cooke & Freeman, 2006; Iqbal & Fitzpatrick, 2006; Freeman, 2007; Ganesan, 2008; Emery et al., 2009). Increasing grain moisture content generally causes a decrease in grain bulk density (Altuntas & Yildiz, 2007). However, the moisture content of the inert dust applied onto grain can also change grain moisture content, and hence grain bulk density. The extent of the decrease in bulk density may vary with the type and amount of dust, the particle size, and the moisture content of the dust. The changes in shape and size as well as surface roughness of particles of porous powders used as grain protectants are likely to alter the flow and abrasive properties of wheat kernels. However, it's unclear whether moisture content will affect the particle size and shape of porous inert dusts. Particle size analysis is often conducted to evaluate the modifications in particle size. Particle size analysis alone does not always discriminate between particles with different shapes, though. Particle shape has been shown to have a significantly higher impact on grain flowability (Guo et al., 1985; Fu et al., 2012). Thus, particle shape analysis is quite often carried out in addition to particle size analysis. Particle shape factors help shed light on subtle differences that may exist between particles with identical size, thus

contributing to a better understanding of flow properties (Masuda et al., 2006; Dietmar & Schultze, 2007). Minor changes in wheat flowability could result in dramatic changes in basic flowability energy, minimum fluidization energy, and the economic implications, for the entire supply chain, are higher energy consumption and a decreased profitability. The addition of inert dusts is not always detrimental to wheat flowability, though. Inert dusts may behave as flow additives and be desirable to improve grain processing by reducing the frictional resistance of particle to particle movement (Cooke & Freeman, 2006). Flowability is often mistakenly referred to as the ability of a powder to flow freely, in a regular and constant way (Masuda et al., 2006), with no reference to the surface properties of the specific vessel or the storage equipment the granular material is interacting with. A proper approach for powder flow characterization should embrace not only shear properties, but also bulk properties (density, compressibility) as well as the physical and process properties of the granular material (angle of repose, angle of avalanche, segregation, attrition, and agglomeration).

The objectives of this research were:

- To construct full boundary sorption isotherms of Hard Red Winter (HRW) wheat and Odor-Z-Way (Inert dust) and determine the critical water activity for phase transition;
- To determine the relationship between the critical  $A_w$  and storage temperature for wheat and zeolite;
- To assess the fitting of sorption experimental data with three isotherms models: Guggenheim-Anderson-de Boer (GAB), Double Log Polynomial (DLP), Brunauer-Emmet-Teller (BET);
- To determine the optimum dust moisture content, at a given storage temperature, for wheat protection;

- To determine the sorption kinetics of the synthetic amorphous zeolite;
- To determine the influence of inert dust moisture content on inert dust particle size, shape, and surface roughness;
- To determine the influence of inert dust moisture content and application rates on some physical properties of Hard Red Winter wheat (HRW);
- To determine the influence of three amorphous silica dusts on permeability and conditioned bulk density of Hard Red Winter wheat;
- To investigate the influence of three amorphous silica dusts on flow properties of Hard Red Winter wheat;
- To evaluate the insecticidal activity of three amorphous dusts (a synthetic zeolite and two registered DE dusts, Celite and Diafil) against eggs and adults of seven species of stored-grain insects on wheat and on concrete Petri dishes used to simulate floors of empty bins;
- To compare the insecticidal efficacy of the synthetic amorphous zeolite to two existing and registered DE products, Celite and Diafil; and
- To determine the influence of the rate, and the duration of exposure on insecticidal activity against adults on concrete.

## References

- Altuntaş, E., & Yıldız, M. (2007). Effect of moisture content on some physical and mechanical properties of faba bean (*vicia faba* L.) grains. *Journal of Food Engineering*, 78(1), 174-183.
- Athanassiou, C. G., Kavallieratos, N. G., Peteinatos, G. G., Petrou, S. E., Boukouvala, M. C., & Tomanović, Ž. (2014). Influence of temperature and humidity on insecticidal effect of three diatomaceous earth formulations against larger grain borer (coleoptera: Bostrychidae). *Journal of Economic Entomology*, 100(2), 599-603.
- Cooke, J., & Freeman, R. (2006). The flowability of powders and the effect of flow additives. Paper presented at the *World Congress on Particle Technology*, , 5
- Daković, A., Matijašević, S., Rottinghaus, G. E., Dondur, V., Pietrass, T., & Clewett, C. F. (2007). Adsorption of zearalenone by organomodified natural zeolitic tuff. *Journal of Colloid and Interface Science*, 311(1), 8-13.
- Desmarchelier, J. M., & Dines, J. C. (1987). Dryacide treatment of stored wheat: Its efficacy against insects, and after processing. *Australian Journal of Experimental Agriculture*, 27(2), 309-312.
- Desmarchelier, J. M., Wright, E. J., & Allen, S. E. (1993). Dryacide (R): A structural treatment for stored-product insects.
- Dietmar, S. (2007). Powders and bulk solids: Behavior, characterization, storage and flow.
- Ebeling, W. (1971). Sorptive dusts for pest control. *Annual Review of Entomology*, 16(1), 123-158.
- Emery, E., Oliver, J., Pugsley, T., Sharma, J., & Zhou, J. (2009). Flowability of moist pharmaceutical powders. *Powder Technology*, 189(3), 409-415.
- Fields, P., Allen, S., Korunic, Z., McLaughlin, A., & Stathers, T. (2003). (2003). Standardised testing for diatomaceous earth. Paper presented at the *Advances in Stored Products Protection. Proceedings of the Eighth International Working Conference on Stored Product Protection*. CABI International, Wallingford, 779-784.

- Fitzpatrick, J. J., Barringer, S. A., & Iqbal, T. (2004). Flow property measurement of food powders and sensitivity of Jenike's hopper design methodology to the measured values. *Journal of Food Engineering*, 61(3), 399-405.
- Freeman, R. (2007). Measuring the flow properties of consolidated, conditioned and aerated powders—a comparative study using a powder rheometer and a rotational shear cell. *Powder Technology*, 174(1-2), 25-33.
- Fu, X., Huck, D., Makein, L., Armstrong, B., Willen, U., & Freeman, T. (2012). Effect of particle shape and size on flow properties of lactose powders. *Particuology*, 10(2), 203-208.
- Ganesan, V., Rosentrater, K. A., & Muthukumarappan, K. (2008). Flowability and handling characteristics of bulk solids and powders—a review with implications for DDGS. *Biosystems Engineering*, 101(4), 425-435.
- Guo, A., Beddow, J. K., & Vetter, A. F. (1985). A simple relationship between particle shape effects and density, flow rate and Hausner ratio. *Powder Technology*, 43(3), 279-284.
- Hagstrum, D. W., & Subramanyam, B. (2006). *Fundamentals of stored-product entomology*. St. Paul, Minn.: AACC International. Retrieved from <http://www.loc.gov/catdir/toc/fy0612/2006920131.html>
- Handbook, G. I. (2013). Book II, chapter 13. federal grain inspection service. *US Department of Agriculture*.
- Iqbal, T., & Fitzpatrick, J. J. (2006). Effect of storage conditions on the wall friction characteristics of three food powders. *Journal of Food Engineering*, 72(3), 273-280.
- Khan, K. (2016). *Wheat: Chemistry and technology* Elsevier.
- Korunic, Z., Fields, P. G., Kovacs, M. I. P., Noll, J. S., Lukow, O. M., Demianyk, C. J., & Shibley, K. J. (1996). The effect of diatomaceous earth on grain quality. *Postharvest Biology and Technology*, 9(3), 373-387.
- Korunic, Z., Cenkowski, S., & Fields, P. (1998). Grain bulk density as affected by diatomaceous earth and application method. *Postharvest Biology and Technology*, 13(1), 81-89.

- Le Patourel, G. (1986). The effect of grain moisture content on the toxicity of a sorptive silica dust to four species of grain beetle. *Journal of Stored Products Research*, 22(2), 63-69.
- Lumay, G., Boschini, F., Traina, K., Bontempi, S., Remy, J., Cloots, R., & Vandewalle, N. (2012). Measuring the flowing properties of powders and grains. *Powder Technology*, 224, 19-27.
- Masuda, H., Higashitani, K., & Yoshida, H. (2006). *Powder technology handbook* CRC Press.
- Subramanyam, B., Swanson, C. L., Madamanchi, N., & Norwood, S. (1994). Effectiveness of insecto, a new diatomaceous earth formulation in suppressing several stored grain insect species. Paper presented at the *Proceedings of the 6th International Working Conference on Stored Product Protection*, , 2 650-659.
- Subramanyam, B., & Roesli, R. (2000). Inert dusts. *Alternatives to pesticides in stored-product IPM* (pp. 321-380) Springer.
- White, N. D., & Leesch, J. G. (1995). Chemical control. *Integrated Management of Insects in Stored Products*, 287-330.

# Chapter 1 - Dynamic dewpoint isotherms of hard red winter wheat and a synthetic amorphous zeolite intended for grain protection

## Abstract

Water-solid interactions play a key role in determining the efficacy of inert dusts. The critical water activity ( $A_{wc}$ ) for phase transition in amorphous materials is an important characteristic of amorphous inert dusts used as grain protectants. As water activity ( $A_w$ ) rises above  $A_{wc}$ , amorphous dusts undergo a transition from glassy or vitreous state to rubbery state. Such a transition induces dramatic changes in material properties, texture and structure, and hence impact their performance as grain protectants.

Full Dynamic Dewpoint Isotherms (DDI) of a synthetic amorphous zeolite intended for grain protection were generated using the Vapor Sorption Analyzer (VSA) to determine  $A_{wc}$  by investigating the relationship between moisture content and  $A_w$  at constant temperatures. Sorption experimental data was fitted using three sorption isotherm models: Guggenheim-Anderson-de Boer (GAB), Double Log Polynomial (DLP), and Brunauer-Emmet-Teller (BET). Water activity prediction was possible DLP models and the Clausius-Clapeyron equation. Critical water activities for phase transition in zeolite powder and Hard Red Winter (HRW) wheat were determined. Optimal moisture contents of zeolite required for wheat treatment were recommended.

**Keywords:** Dynamic dewpoint isotherm, Critical water activity, GAB, BET, DLP, Sorption kinetics, Amorphous dust

## **Introduction**

Inert dusts encompass various dry and chemically unreactive powders applied onto grain at the time of storage into silos or bins, on farm or off-farm. Prior to grain treatment, inert dusts are commonly stored in plastic sacks or bucket containers. Inert dusts are well-known for their hygroscopic nature and their tendency to quickly absorb ambient humidity. If not stored in tightly sealed containers, they can undergo a severe caking process as a result of particle agglomeration due to moisture migration. Natural or time consolidation of hygroscopic dust may also occur as a result of compaction created by the weight of the dust on itself. Consolidation of the dust also takes place as the dust is subjected to vibration during transport from the manufacturing plant to the farm, the elevator facility, or the production line. Caking is worsened by high ambient relative humidity, increased consolidation pressure and long-term powder storage (Hartmann & Palzer, 2011). Often times, by the time the inert dust reaches the farm, the elevator, or the laboratory, the moisture content has increased 5-10 times, and by the time the pest prevention is implemented, the moisture content would have increased 15-20 folds. The dust becomes very hard and difficult to remove from the container, delaying grain treatment, making necessary additional expenses, significantly reducing dust efficacy, and increasing the risk for greater deterioration of grain quality. Consolidation from gradual settling activity is not the only concern to reckon with while handling inert dusts. Even after a successful storage of an amorphous dust prior to application onto grain, consolidation can resurface while the treated grain is sitting inside the bin or silo. Caking occurring inside bins or silos is amplified as a result of the system “grain-dust” interacting with the ambient moisture and temperature. Caking inside a silo can amplify ratholing, especially if the silo is operating in funnel flow mode. In either case,

before or after grain treatment, inert dust caking is due to moisture migration. The main mechanism responsible for the caking of amorphous powders is sintering (Kamyabi et al. 2017).

The efficacy of inert dusts against insects derives from their ability to kill insects through desiccation (Subramanyam & Roesli, 2000). Consequently, the insecticidal activity that can be expected from a dust increases as the water activity ( $A_w$ ) of the dust and/or the ambient relative humidity decreases. Moisture uptake during dust storage prior to application onto grain negatively impacts the overall effectiveness of the dust. In fact, insects could better resist desiccation by taking advantage of the moisture already present within the moist dust to replenish the body water content loss induced by desiccation. Using dry powders with moisture as low as 1% is not enough to maximize the insecticidal efficacy, though. The limiting parameter is the  $A_w$  of the dust interacting with the grain. Optimal storage conditions can be defined as a combination of environmental parameters (storage temperature, water activity of dust and grain) that foster a maximum stability of the treated grain by considerably depressing the likelihood of water migration within the system “dust-grain”. At a given temperature, high differences in grain water activity relative to dust water activity will cause the dust to adsorb or desorb water. Moisture equilibration between grain and the moist dust results in a too moist grain that is easily prone to mold and fungi infestation, especially when grain moisture reaches 15% and beyond. On the other hand, a too dry dust can have a drying action on the stored grain. Stored grain is primarily sold based on weight and selling a too dry grain equates with a significant decrease in profitability. Hence, understanding the underlying mechanisms leading to the dramatic changes in the physical integrity of the dust or how moisture migrates within the system “dust-grain” is crucial. A practical approach in determining moisture migration is the construction of sorption isotherms which help predict the moisture or water activity under specific storage conditions.

A moisture sorption isotherm defines the relationship between  $A_w$  and moisture content at a constant temperature (Barbosa et al. 2008). The moisture sorption isotherm is an extremely valuable tool to predict stability at given moisture as it can be used to predict moisture gain or loss in a package with known moisture permeability (Bell and Labuza, 2000). A full isotherm comprises both an adsorption and a desorption curves. Adsorption isotherms are obtained by wetting a sample from a dry state, whereas, desorption isotherms are obtained by drying a sample from a wet state. Graphically, these two curves mismatch when they are superimposed. This phenomenon is called hysteresis and simply means that the moisture content at each water activity is higher during desorption than adsorption. The moisture sorption isotherm is useful for both processing and product stability (Reid, 2007). Besides allowing a rapid moisture content determination from water activity analysis through an isotherm curve, sorption isotherms can help decide on a safe water activity that maximizes the dust shelf-life and storage stability while avoiding over drying or over wetting. A rigorous investigation of kinetics of sorption properties of an inert dust, for instance, provides insight into proper packaging requirements. To preserve their intrinsic properties, inert dusts should be stored under specific environment conditions that would prevent them from reaching a specific water activity content known as the critical water activity. It's vital to have a clear understanding of the implications of the critical water activity with respect to phase transitions.

Several methods/equipment are available for isotherm construction. Recent technologies tend to emphasize automation and speed. The saturated salt slurry method or traditional desiccator method has long been a standard method of generating isotherms. This manual process is performed using sealed chambers such as desiccators and the equilibration process can take weeks or months. Basically, this method consists of determining equilibrium moisture content

over a series of saturated salt slurries of known water activity. The salt slurries are removed from the desiccator at fixed intervals and weighed to monitor the gradual change in moisture content. The state of equilibrium is achieved when the weight of the sample stops changing. Moisture content measurements can be inaccurate if temperature is not carefully monitored, and the possibility of mold growth at high humidity ( $A_w > 0.60$ ) is to be reckoned with. An alternative to this traditional method is the dynamic vapor sorption isotherm (DVS). DVS provides better accuracy and is less-time consuming. DVS is merely an automation of the traditional salt slurry method. Both the traditional method and DVS require the establishment of equilibrium between the sample and the ambient environment. In other words, both procedures generate static or equilibrium isotherms. As with the saturated salt slurries, the DVS method tracks sample weight change as the sample is exposed to different controlled humidity at a constant temperature. Once equilibrium is achieved, the sample is held at that controlled humidity for a preset time interval and moisture content is determined. The experiment proceeds and the sample is subjected to the next controlled humidity. DVS provides not only equilibrium moisture contents at a given water activity, but also kinetics of sorption and water vapor diffusion properties. Another procedure, the dynamic dew point isotherm (DDI), provides a greater resolution and is the least time-consuming method as there is no need for equilibrium to establish. DDI generates dynamic isotherms as opposed to equilibrium isotherms. The DDI method for dynamic isotherms is a water activity and gravimetric analysis method that controls neither water content nor water activity, but dries or wets the sample and measures water activity and water content during the wetting or drying process. Water content is determined using a high precision magnetic force balance and water activity is measured using a chilled-mirror dew point sensor. During the desorption cycle, dry air flows over the sample while during the adsorption cycle wet air passes

over the sample. After a short period of time, the VSA halts air flow and takes a snapshot of the sorption process by directly measuring the water activity and weight. The high resolution of dynamic isotherms makes them valuable for observing sudden changes in sorption properties associated with matrix changes such as glass transition. A correlation exists between the glass transition temperature and the critical water activity. In fact, to determine the glassy to rubbery transition, the Differential Scanning Calorimetry (DSC) approach consists of keeping the moisture content/ $A_w$  of the sample constant, while scanning the selected material property for heat capacity as a function of temperature. Determining phase transitions using isotherms is similar to determining glass transition temperature ( $T_g$ ) with DSC, except that instead of holding water activity constant and scanning temperature, the isotherm analysis holds temperature constant and scans water activity. The DDI approach keeps the temperature of the sample constant, while scanning relative humidity or water activity, resulting in the determination of the critical water activity of the material at the experimental temperature (Carter & Fontana, 2008).

The objectives of this study were:

- To construct full boundary sorption isotherms of Hard Red Winter (HRW) wheat and Odor-Z-Way (Inert dust) and determine the critical water activity for phase transition;
- To determine the relationship between the critical  $A_w$  and storage temperature for wheat and zeolite;
- To assess the fitting of sorption experimental data with three isotherms models: Guggenheim-Anderson-de Boer (GAB), Double Log Polynomial (DLP), Brunauer-Emmet-Teller (BET);

- To determine the optimum dust moisture content, at a given storage temperature, for wheat protection; and
- To determine the sorption kinetics of the synthetic amorphous zeolite.

## **Material & Methods**

### **Wheat and zeolite preparation**

It is necessary that the grain and the powder sub-samples that are used for analysis be representative of the initial lots or batches for valid and reproducible data. Wheat and zeolite samples sizes were reduced by pouring one 50-lb bag of wheat respectively into a Boerner Divider (Seedburo Boerner Divider) and into a chute splitter device (Gilson Co, Ohio, USA) and repeatedly halved until a sample of desired size was obtained. A total of ninety samples (250 g) were made and nine samples were systematically selected, of which, three samples were randomly assigned to each of three temperature levels (25, 35, and 45°C) considered for sorption isotherms. Hard red winter wheat was procured from Heartland Mills (Marienthal, KS, USA) and zeolite powder was supplied by Odor-Z-Way (Phillipsburg, KS, USA). The initial grain moisture content was determined using a Moisture Analyzer Model 930 (Shore Sales Co., Rantoul, IL). Zeolite powder was dried overnight at 25°C and moisture content was determined by thermogravimetric analysis (TGA) (Pyris 1 TGA, Perkin Elmer).

### **Sorption isotherms**

Separate sorption isotherms were constructed for the zeolite powder and for the samples of Hard Red Winter (HRW) wheat using a vapor sorption analyzer (VSA). The VSA is capable of generating both dynamic and equilibrium isotherms. Dynamic isotherms, however, are required to investigate phase transitions and to determine critical water activities. The performance characteristics and the operating specifications of the VSA are presented in Table 1.1. An isotherm standard test was run using a sample of microcrystalline provided by Decagon (data not shown). The kinetic and moisture sorption isotherm curves generated were compared to a

preloaded standard microcrystalline curve and less than one percent variation was the criterion to validate the working performance of the VSA.

Full dynamic dewpoint adsorption and desorption isotherms were obtained at 25, 35, and 45°C to fully investigate hysteresis phenomenon, to determine the critical water activity for phase transition, and to find optimal moisture content of zeolite needed for application onto HRW. Critical water activity provides useful information for maintaining textural properties and preventing caking and clumping. Three replications were done for each isotherm temperature and  $1.0 \pm 0.1$  g zeolite powder or grain was used for each run. Isotherms generated using the VSA typically yielded unique sets of data, so it was not possible to average the data.

#### **Water activity linear offset and weight calibration**

To ensure the accuracy of the isotherms generated, water activity capacitance and chilled mirror sensors and the instrument balance were verified for correct performance. Before running a new isotherm, water activity verification was conducted using the 0.76  $A_w$  (6 mol/kg NaCl) and the 0.25  $A_w$  (13.4 mol/kg LiCl) standards. Weight calibration was conducted against a NIST two-gram standard weight (National Institute of Standards and Technology, Maryland, USA) provided by Meter Group (formerly, Decagon).

#### **Using DDI to investigate phase transitions**

To investigate phase transition events using dynamic isotherms, a DDI test was performed with the following settings: initial water activity of 0.1  $A_w$ , final water activity of 0.90  $A_w$ , flow rate of 40 ml/min, resolution of 0.01  $A_w$ , and no timeout. These settings enabled the generation of isotherms with resolutions high enough to allow the detection of inflection points. Sharp inflection points in the isotherm indicate critical water activity for phase transition. The critical water activity for wheat or zeolite powder at constant temperature was determined by second

derivative curve smoothing strategies using the Excel spreadsheet developed by Meter Group, which is based on the Savitzky & Golay (1964) smoothing and differentiation method.

### **Isotherms models**

Three isotherm models were evaluated for their ability to fit the experimental data for HRW kernels and zeolite powder isotherms: Guggenheim-Anderson-de Boer (GAB), Double Log Polynomial (DLP), and Brunauer-Emmet-Teller (BET). The model equations are shown below:

#### ***DLP (Double Log Polynomial)***

$$m = b_3x^3 + b_2x^2 + b_1x + b_0 \quad (1.1)$$

Where  $m$  is the moisture content (%);  $x = \ln(-\ln(A_w))$ ;  $b_0, b_1, b_2,$  and  $b_3$  are empirical constants.

#### ***GAB (Guggenheim-Anderson-de Boer)***

$$m = \frac{c_1 k m_0 A_w}{(1 - k A_w)(1 - k A_w + c_1 k A_w)} \quad (1.2)$$

Where  $m$  is the moisture content (%);  $m_0$  is the monolayer moisture content (%);  $A_w$  is the water activity at moisture content  $m$ ;  $c_1, k,$  and  $m_0$  are empirical constants.

#### ***BET (Brunauer-Emmet-Teller)***

$$m = \frac{c m_0 A_w}{(1 - A_w)(1 + (c - 1) A_w)} \quad (1.3)$$

Where  $m$  is the moisture content (%);  $m_0$  is the monolayer moisture content (%);  $A_w$  is the water activity at moisture content  $m$ ;  $c$  and  $m_0$  are empirical constants.

### **Error functions and assessment of goodness-of-fit**

Five error functions were used to evaluate the goodness-of-fit of each isotherm model.  $V_{pred}$  is the moisture content calculated from the model,  $V_{obs}$  is the experimental moisture content,  $\overline{V_{obs}}$  is the average experimental moisture content, and  $n$  is the number of data points in the experimental sorption isotherm.

***Coefficient of determination ( $R^2$ )***

$$R^2 = \frac{\sum(V_{pred} - \overline{V_{obs}})^2}{\sum[(V_{pred} - \overline{V_{obs}})^2 + (V_{pred} - V_{obs})^2]} \quad (1.4)$$

***The sum of the squares of the errors (SSE)***

$$SSE = \sum_{i=1}^n (V_{pred} - V_{obs})^2 \quad (1.5)$$

***The Sum of the Absolute Errors (SAE)***

$$SAE = \sum_{i=1}^n |V_{pred} - V_{obs}| \quad (1.6)$$

***The Mean Relative Deviation (MRD)***

$$MRD = \frac{100}{n} \sum_{i=1}^n \frac{|V_{pred} - V_{obs}|}{V_{obs}} \quad (1.7)$$

***The Standard Error of prediction (SE)***

$$SE = \sqrt{\frac{\sum_{i=1}^n (V_{pred} - V_{obs})^2}{n-1}} \quad (1.8)$$

**Optimal water activity and equilibrium moisture content (EMC)**

The direction of moisture sorption for each entity in the mixture is important when grain is admixed with an amorphous dust. In fact, it's the water activity that dictates the direction of moisture migration until an equilibrium condition is achieved (Bell, 2007). To prevent moisture migration during storage, the water activity of the dust must be equal to that of HRW, at constant storage temperature. The water activity values and moisture content of HRW, at constant temperature, can either be calculated from the best-fitting adsorption or desorption equations or determined graphically from the sorption isotherms. The corresponding moisture content of the inert dust to meet this requirement is then obtained graphically or through the best-fitting adsorption equations of the zeolite powder. Once the water activity of the system wheat-inert

dust at equilibrium is determined, it is essential to verify that this value does not exceed the critical water activity for each component of the system.

### **Net isosteric heat of sorption, differential enthalpy, and differential entropy**

The relationship between the net isosteric heat of sorption ( $\Delta h_d$ ) and the differential entropy ( $\Delta S_d$ ) is given by:

$$\ln A_w = - \frac{\Delta h_d}{R} \cdot \left(\frac{1}{T}\right) + \frac{\Delta S_d}{R} \quad (1.9)$$

The differential entropy of sorption was obtained from the Y-axis intercept by plotting  $\ln (A_w)$  vs.  $1/T$ , while the net isosteric heat of sorption was obtained from the slope of the line resulting from plotting  $\ln (A_w)$  versus  $1/T$  at constant moisture content (Yazdani et al, 2006).

The relationship between the net isosteric heat of sorption ( $\Delta h_d$ ) and the differential enthalpy ( $\Delta H_d$ ) is given by:

$$\Delta h_d = \Delta H_d - \Delta H_{vap} \quad (1.10)$$

Where,  $\Delta H_{vap}$  is the latent heat of water vaporization.

### **Isokinetic temperature and free Gibbs energy**

The linear relationship between the net isosteric heat of sorption ( $\Delta h_d$ ) and the differential entropy ( $\Delta S_d$ ) is given by:

$$\Delta h_d = T_\beta \cdot \Delta S_d + \Delta G_\beta \quad (1.11)$$

The isokinetic temperature ( $T_\beta$ ) and constant ( $\Delta G_\beta$ ) were calculated using linear regression (Abdenouri et al. 2010).

### Water activity prediction: The Clausius-Clapeyron equation

The relationship between water activity and temperature is given by the Clausius-Clapeyron equation:

$$\ln \left( \frac{A_{w2}}{A_{w1}} \right) = - \frac{\Delta H}{R} \left( \frac{1}{T_2} - \frac{1}{T_1} \right) \quad (1.12)$$

Knowing the heat of sorption, water activity at a given temperature can be derived from the Clausius-Clapeyron equation:

$$A_{w2} = A_{w1} * e^{-\frac{\Delta H}{R} \left( \frac{1}{T_2} - \frac{1}{T_1} \right)} \quad (1.13)$$

Where,  $A_{w1}$  is the water activity at temperature  $T_1$  (K),  $A_{w2}$  is the water activity at temperature  $T_2$  (K),  $\Delta H$  = heat of sorption ( $\text{J mol}^{-1}$ ), and  $R$  is the universal gas constant ( $8.31 \text{ J.mol}^{-1}.\text{K}^{-1}$ ).

The heat of sorption ( $\Delta H$ ) is moisture-dependent and is calculated by dividing by  $R$  the slope of the line obtained by plotting  $\ln(A_w)$  vs  $1000/T$ . The heat of sorption ( $\Delta H$ ) in our study was automatically determined by using the Temperature Effect tool included in the Moisture analysis Toolkit 1.0.1328 (Meter group). Briefly, at least three isotherm files and three specific temperatures ( $^{\circ}\text{C}$ ) are uploaded in the software and one specific value of moisture (% d.b.) is specified as well as the direction of sorption. The heat of sorption generated is specific to that moisture content.

### Statistical analysis

The coefficients for the different models were obtained using Moisture Analysis Toolkit 1.0.1328 (Meter Group, Pullman, Washington, USA). The coefficient of determination ( $R^2$ ), the sum of squares of the errors (SSE), the sum of the absolute errors (SAE), the mean relative deviation (MRD), and the standard error of estimate (SE) were used to assess and compare the

goodness of fit of each model. Critical water values at different storage temperatures were compared using SAS One-way ANOVA.

## Results & Discussion

### 1) Full sorption isotherms

Water activities at the extremities of the sorption curve (below 0.1 and above 0.8) usually require much longer time for equilibrium to establish. Even though dynamic dewpoint isotherms (DDI) do not require equilibrium conditions to proceed, the amount of time required to complete the sorption analysis was significantly decreased by limiting the water activity range between 0.2 and 0.8. The full sorption isotherms of zeolite powder and wheat samples are shown in Fig. 1.1 and 1.2. According to BET classification (Brunauer et al. 1938) and the IUPAC classification (Rouquerol et al. 1994), HRW had typical type II sigmoid shape isotherm, whereas, zeolite powder had a sorption isotherm close to resembling a type IV sigmoid shape isotherm. Type II isotherms are exhibited by nonporous or macroporous solids (pore size  $> 50\text{nm}$ ) and represents unrestricted monolayer-multilayer adsorption, while Type IV isotherms are mostly characteristic of mesoporous solids (pore size 2-50 nm) and are indicative of multilayer adsorption followed by capillary condensation (Kruk & Jaroniec, 2001). Although the Brunauer and the IUPAC classifications of gas-solid adsorption are commonly used to determine the nature of adsorption, Donohue & Aranovich (1998) have found some limitations to these classifications because they are based on the absolute adsorption rather than the Gibbs adsorption, hence giving the incorrect impression that adsorption isotherms are always monotonically increasing functions of pressure.

Full sorption isotherms of zeolite and wheat obtained at 25, 35, and 45°C clearly showed the hysteresis phenomenon (Figure 1.1 and 1.2), resulting from lower equilibrium moisture contents during adsorption than during desorption. In fact, the hysteresis phenomenon does not occur in pores smaller than 2 nm. Hysteresis is rather observed when the pores are large enough for the adsorbing molecules to condense to a liquid (Ruthven, 1984; Myers, 2002). Moreover, the type

of hysteresis indicates the shape of the pores of the material being analyzed. Considering the IUPAC classification of isotherms, the hysteresis loops were of type H3 for HRW, and of type H4 for zeolite powder. Type H3 hysteresis are aggregates of plate-like particles forming slit-like pores, while type H4 hysteresis are narrow slit-like pores, particles with internal voids of irregular shape and broad size distribution, mostly hollow spheres with walls composed of ordered mesoporous silica (Sing, 1985; Kruk & Jaroniec, 2001; Lowell & Shields, 2013). Adsorption hysteresis in porous materials such as inert dusts is characterized both by the shapes of the hysteresis loops and by the way in which they depend on temperature (Burgess et al., 1989). The intensity of hysteresis remained unchanged for HRW, as hysteresis loop height and width did not change with increasing temperatures (Figure 1.2). Conversely, the intensity of hysteresis decreased with increased temperatures during water adsorption by porous zeolite powder (Figure 1.1). Similar observations were made by Dubinin (1960) during adsorption of CO<sub>2</sub> on porous silica gel. The explanation provided by Dubinin is that the hysteresis loops develop somewhat below the triple point temperature of the adsorptive, shrink as the temperature is raised and disappear some distance below the bulk critical temperature.

## 2) Isotherm models

Experimental data were fitted by means of GAB, DLP, and BET models. All three models are single-temperature models, meaning they do not involve temperature as a parameter. Estimated parameters of models for the sorption isotherms of HRW and zeolite powder are presented in Table 1.2 and 1.3. The coefficient of determination is often the first error function considered in isotherm sorption data fitting. The coefficient of determination ( $R^2$ ) is the square of the correlation ( $r$ ) between predicted and experimental values and it ranges from 0 to 1. While achieving  $R^2=1$  is most preferred, this is virtually impossible, and common values of  $R^2$  are

comprised between 0 and 1. The best fitting model should feature an  $R^2$  close to 1, which means the dependent variable can be predicted with minimal error from the independent variable. Other error functions reported in sorption data fitting include the Standard Error (SE), the Sum of the Absolute Errors (SAE), the Sum of the Squares of the Errors (SSE), and the Mean Square Error (MSE). Contrary to  $R^2$ , these four error functions must be kept as minimal as possible for the model to be meaningful. Error function values associated to adsorption and desorption data of zeolite powder and HRW are featured in Table 1.2 and 1.3. Irrespective of sorption direction, DLP model was the best model to estimate zeolite and HRW sorption isotherms, followed by GAB and BET models. As expected, BET model provided almost perfect fitting to sorption data, only in the water activity range 0-0.5 (Carter et al. 2015). Monolayer moisture content values ( $m_0$ ) for each sorption direction were provided only by GAB and BET models and indicated a decrease in monolayer moisture content with an increase in temperature (Table 1.2 and 1.3). The monolayer moisture content value is the value at which a food product is most stable. Duckworth and Smith (1963) demonstrated that solute movement was not detectable below the monolayer value but was detectable above it. Because reactant mobility is a prerequisite for reactivity, lower mobility at the monolayer translates into greater product stability. A faster determination of the moisture content of any sample of wheat or zeolite with known initial water activity can be achieved by using the DLP fitting equations generated for each sorption direction (Table 1.4).

### 3) Critical $A_w$ for phase transitions

The critical water activity ( $A_{wc}$ ) for phase transition is the water activity of hard red winter wheat or zeolite powder above which the rate of phase transition reactions is accelerated. Critical water activities are necessary for maintaining textural properties and preventing caking and clumping. If the water activity of the inert dust or the grain rises above the critical water activity for phase

transition, the stability will decrease as time dependent processes such as stickiness, structure collapse, and crystallization speed up significantly (Labuza et al. 2004; Carter & Campbell, 2008). Critical water activity values for zeolite powder increased from 0.639 to 0.657 as temperatures increased from 25 to 45°C. The same trend was observed with HRW as water activity values increased from 0.700 to 0.790 for the same temperature range (Table 1.5).

Plotting the second derivative of moisture content versus water activity yields the first matrix transition or glass transition, the second matrix transition (onset of crystallization), and the third matrix transition (the point of dissolution or deliquescence). Depending on the type of material being analyzed (amorphous, or crystalline), all or part of the transition matrices are present on the second derivative plot.

#### 4) Optimal storage $A_w$ and EMC

Wheat desorption isotherm at a specific temperature was used to find the corresponding water activity if we intended to store wheat at a specific moisture content. The corresponding water activity value was introduced into zeolite adsorption curve to determine the corresponding moisture content by linear extrapolation. The recommended storage moisture contents for inert dust and wheat at different temperatures are presented in Table 1.6. The linear relationship between zeolite (Z) and wheat (W) moisture contents is temperature dependent and expressed as:

- at 25°C  $Z = 0.8683W - 6.7822$  ( $R^2=0.98$ )

- at 35°C  $Z = 0.74W - 4.9456$  ( $R^2=0.99$ )

- at 45°C  $Z = 0.744W - 4.8124$  ( $R^2=0.98$ )

These linear equations can help determine faster and with at least 98% accuracy the moisture content of a synthetic amorphous dust required to protect grain of known moisture content under

a specific storage temperature. For instance, at 25°C if wheat is 12.0% moisture content (d.b.), the optimal moisture content for zeolite to be applied on wheat is computed as follows:

$$Z=0.8683*12-6.7822=3.6374.$$

A careful examination of optimal moisture contents of zeolites and wheat suggest that the water activity and the non-equilibrium moisture content of zeolite increased with increasing temperatures and wheat moisture content (Table 1.7).

#### 5) Temperature effect: Water activity prediction

Water activity was strongly linearly correlated ( $.995 < R^2 < .999$ ) with temperature at constant zeolite or wheat moisture contents (Table 1.8). The slopes of the lines obtained by plotting water activity as a function of temperature are higher during desorption than adsorption, which is a mathematical corroboration of the hysteresis phenomenon taking place in both wheat and zeolite samples. The equations presented in Table 1.8 allow an easy and quick determination of the water activity of zeolite or wheat samples of known moisture content stored under a specific temperature.

#### 6) Sorption kinetics

Sorption kinetics (isosteric heat of sorption and net isosteric heat of sorption) were determined for zeolite powder at different moisture contents (Figure 1.2). The net isosteric heats of sorption and the differential enthalpy of zeolite estimated by the Clausius–Clapeyron equation and determined graphically decreased with increasing moisture content of zeolite. Similar results were found by Bonner & Kenney (2013), Martinez-Las Heras et al. (2014) and Bennaceur et al. (2015), while investigating the net isosteric heat of sorption of dry persimmon leaves, Henna leaves, and energy sorghum, respectively, at various moisture contents. The explanation to that observation is that, at lower moisture content, water molecules are tightly bound to the active

polar sites by primarily the hydrogen bond. The differential enthalpy or isosteric heat of sorption ( $\Delta H_d$ ) indicates the state of absorbed water by the solid material and represent the total molar enthalpy change accompanying the phase change from vapor to sorbed water. In other words, the isosteric heat of sorption is the energy required for evaporating the adsorbed water from liquid to gas status at determined moisture content. The isosteric heat of sorption measures the energy changes that occur during the sorption process and is an indicator of the level of attractive or repulsive forces of the system. The net isosteric heat of sorption ( $\Delta h_d$ ) represents the quantity of energy exceeding the heat of vaporization of water ( $\Delta H_{\text{vap}}$ ) associated with the sorption process. The latent heat of vaporization of pure water is the energy required to evaporate pure water from liquid to gas state and is equal to 2,257 kJ/kg (40,626 J mol<sup>-1</sup>). The net isosteric heat of sorption is the differential enthalpy minus the latent heat of vaporization of pure water. The net isosteric heat of sorption gives a measure of the water-solid binding strength. The latent heat of vaporization of pure water is the energy required to change a gram of a liquid into the gaseous state at the boiling point. This energy breaks down the intermolecular attractive forces, and also must provide the energy necessary to expand the gas.

## Conclusions

Full sorption isotherms of zeolite and wheat obtained at 25, 35, and 45°C clearly exhibited the hysteresis phenomenon. The intensity of hysteresis remained unchanged with increasing temperatures for Hard Red Winter wheat (HRW), whereas, the intensity of hysteresis decreased with increased temperatures during water adsorption for the porous synthetic amorphous zeolite powder. Considering the IUPAC classification of isotherms, HRW had typical type II sigmoid shape isotherm, whereas, zeolite powder had a sorption isotherm close to resembling a type IV sigmoid shape isotherm. The hysteresis loops were of type H3 for HRW, and of type H4 for zeolite powder. Irrespective of sorption direction, DLP model was the best model to estimate zeolite and HRW sorption isotherms, followed by GAB and BET models, although BET model provided almost perfect fitting to sorption data in the water activity range 0-0.5.

## References

- Abdenouri, N., Idlimam, A., & Kouhila, M. (2010). Sorption isotherms and thermodynamic properties of powdered milk. *Chemical Engineering Communications*, 197(8), 1109-1125.
- Barbosa-CÃ, G. V., Fontana Jr, A. J., Schmidt, S. J., & Labuza, T. P. (2008). *Water activity in foods: Fundamentals and applications* John Wiley & Sons.
- Bell, L. N. (2007). Moisture effects on food's chemical stability. *Water activity in foods. fundamentals and applications* (pp. 173-198) Blackwell Publishing, Oxford.
- Bell, L. N., & Labuza, T. P. (2000). *Moisture sorption: Practical aspects of isotherm measurement and use* AACC Press.
- Bennaceur, S., Draoui, B., Touati, B., Benseddik, A., Saad, A., & Bennamoun, L. (2015). Determination of the moisture-sorption isotherms and isosteric heat of henna leaves. *Journal of Engineering Physics and Thermophysics*, 88(1), 52-62.
- Bonner, I. J., & Kenney, K. L. (2013). Moisture sorption characteristics and modeling of energy sorghum (sorghum bicolor (L.) moench). *Journal of Stored Products Research*, 52, 128-136.
- Brunauer, S., Emmett, P. H., & Teller, E. (1938). Adsorption of gases in multimolecular layers. *Journal of the American Chemical Society*, 60(2), 309-319.
- Burgess, C. G., Everett, D. H., & Nuttall, S. (1989). Adsorption hysteresis in porous materials. *Pure and Applied Chemistry*, 61(11), 1845-1852.
- Carter, B. P., Galloway, M. T., Campbell, G. S., & Carter, A. H. (2015). The critical water activity from dynamic dewpoint isotherms as an indicator of crispness in low moisture cookies. *Journal of food measurement and characterization*, 9(3), 463-470.
- Carter, B., & Fontana, A. (2008). Dynamic dewpoint isotherm verses other moisture sorption isotherm methods. *Application Note. Decagon Devices, Pullman, WA.*  
[https://pittcon.org/wp-content/uploads/2016/02/Aqualab\\_DDI-vs.-Other-Moisture-Sorption-Isotherm-Methods.pdf](https://pittcon.org/wp-content/uploads/2016/02/Aqualab_DDI-vs.-Other-Moisture-Sorption-Isotherm-Methods.pdf) (visited on March 24, 2017).

- Donohue, M. D., & Aranovich, G. L. (1998). Classification of Gibbs adsorption isotherms. *Advances in Colloid and Interface Science*, 76, 137-152.
- Dubinin, M. M. (1960). Theory of the physical adsorption of gases and vapors and adsorption properties of adsorbents of various natures and porous structures. *Russian Chemical Bulletin*, 9(7), 1072-1078.
- Duckworth, R. B., & Smith, G. M. (1963). The environment for chemical change in dried and frozen foods. *Proceedings of the Nutrition Society*, 22(2), 182-189.
- Hartmann, M., & Palzer, S. (2011). Caking of amorphous powders—Material aspects, modelling and applications. *Powder Technology*, 206(1-2), 112-121.
- Kamyabi, M., Sotudeh-Gharebagh, R., Zarghami, R., & Saleh, K. (2017). Principles of viscous sintering in amorphous powders: A critical review. *Chemical Engineering Research and Design*, 125, 328-347.
- Kruk, M., & Jaroniec, M. (2001). Gas adsorption characterization of ordered organic– inorganic nanocomposite materials. *Chemistry of Materials*, 13(10), 3169-3183.
- Labuza, T., Roe, K., Payne, C., Panda, F., Labuza, T. J., Labuza, P. S., & Krusch, L. (2004). Storage stability of dry food systems: Influence of state changes during drying and storage. Paper presented at the XIV International Drying Symposium. *Proceedings, Ourograf Gráfica E Editora, São Paulo, Vol. A*, 48-68.
- Lowell, S., & Shields, J. E. (2013). *Powder surface area and porosity* Springer Science & Business Media.
- Lowell, S., Shields, J. E., Thomas, M. A., & Thommes, M. (2012). *Characterization of porous solids and powders: Surface area, pore size and density*. Springer Science & Business Media.
- Martínez-Las Heras, R., Heredia, A., Castello, M. L., & Andres, A. (2014). Moisture sorption isotherms and isosteric heat of sorption of dry persimmon leaves. *Food Bioscience*, 7, 88-94.

- Myers, A. L. (2002). Thermodynamics of adsorption in porous materials. *AIChE Journal*, 48(1), 145-160.
- Reid, D. S. (2007). Water activity: Fundamentals and relationships. *Water activity in foods. fundamentals and applications* (pp. 15-28) Blackwell Publishing, Oxford.
- Rouquerol, J., Avnir, D., Fairbridge, C. W., Everett, D. H., Haynes, J. M., Pernicone, N., . . . Unger, K. K. (1994). Recommendations for the characterization of porous solids (technical report). *Pure and Applied Chemistry*, 66(8), 1739-1758.
- Ruthven, D. M. (1984). *Principles of adsorption and adsorption processes*. John Wiley & Sons.
- Savitzky, A., & Golay, M. J. (1964). Smoothing and differentiation of data by simplified least squares procedures. *Analytical Chemistry*, 36(8), 1627-1639.
- Sing, K. S. (1985). Reporting physisorption data for gas/solid systems with special reference to the determination of surface area and porosity (recommendations 1984). *Pure and Applied Chemistry*, 57(4), 603-619.
- Subramanyam, B., & Roesli, R. (2000). Inert dusts. *Alternatives to pesticides in stored-product IPM* (pp. 321-380) Springer.
- Yazdani, M., Sazandehchi, P., Azizi, M., & Ghobadi, P. (2006). Moisture sorption isotherms and isosteric heat for pistachio. *European Food Research and Technology*, 223(5), 577-584.

**Table 1.1** Specifications of the Vapor Sorption Analyzer

Water activity range	0.03-0.95 Aw for 15-50 °C, 0.03-0.90 for 50-60 °C
Water activity accuracy	±0.005 Aw (±0.02 Aw for volatiles)
Water activity repeatability	±0.003 Aw (±0.02 Aw for volatiles)
Temperature control range	15-60°C
Temperature and humidity operating range	0-60°C / 10-90% non-condensing
Sample weight range	500-5000 mg
Weight resolution	± 0.1 mg

**Table 1.2** Estimated parameters of models for the sorption isotherms of hard red winter wheat (HRW)

Model	Parameter	25°C		35°C		45°C	
		Adsorption	Desorption	Adsorption	Desorption	Adsorption	Desorption
DLP	b <sub>0</sub>	9.183	11.002	8.295	10.630	7.892	10.104
	b <sub>1</sub>	-0.341	-4.069	-0.872	-4.104	-1.288	-3.683
	b <sub>2</sub>	0.399	0.41	1.794	0.360	1.964	0.513
	b <sub>3</sub>	-0.597	0.329	0.035	0.180	0.090	0.092
	R <sup>2</sup>	0.999	0.999	0.994	0.999	0.999	0.999
	SE	0.058	0.089	0.248	0.123	0.087	0.132
	SSE	0.27	0.46	1.59	0.81	0.39	0.93
	SAE	3.66	4.99	7.53	6.26	3.30	6.26
	MRD	0.004	0.005	0.008	0.005	0.004	0.006
GAB	c <sub>1</sub>	10506.986	35.419	11475.395	53.059	12472.350	561.005
	k	0.588	0.542	0.7535	0.624	0.790	0.688
	m <sub>0</sub>	6.892	9.873	5.586	8.695	5.262	7.518
	R <sup>2</sup>	0.785	0.998	0.949	0.999	0.971	0.998
	SE	0.966	0.117	0.720	0.128	0.549	0.177
	SSE	74.7	0.87	40.00	0.96	20.61	2.14

	SAE	63.9	5.15	47.23	7.26	32.59	11.19
	MRD	0.07	0.004	0.06	0.01	0.05	0.01
BET	c	1997408.074	2195312.315	2875344.570	1070029.905	2625480.869	915530.879
	m <sub>0</sub>	5.826	6.910	5.198	6.663	4.924	6.364
	R <sup>2</sup>	0.953	.981	.968	0.981	0.963	0.979
	SE	1.262	.476	.841	0.433	0.705	0.460
	SSE	10011.5	24184.7	6491.6	22704.01	5203.67	19848.9
	SAE	582.9	794.5	445.1	756.03	387.04	701.46
	MRD	0.58	0.59	0.45	0.55	0.39	0.52

---

**Table 1.3** Estimated parameters of models for the sorption isotherms of zeolite powder

Model	Parameter	25°C		35°C		45°C	
		Adsorption	Desorption	Adsorption	Desorption	Adsorption	Desorption
DLP	b <sub>0</sub>	2.7318	3.837	2.887	3.381	2.777	2.469
	b <sub>1</sub>	-2.8808	-3.364	-2.584	-3.079	-2.113	-2.572
	b <sub>2</sub>	0.2802	2.530	-0.232	1.3660	-0.083	0.522
	b <sub>3</sub>	-1.6306	0.178	-1.718	-0.542	-1.272	-0.616
	R <sup>2</sup>	0.999	0.997	0.999	0.998	0.999	0.999
	SE	0.0787	0.203	0.084	0.174	0.051	0.103
	SSE	0.22	3.15	0.25	1.06	0.09	0.49
	SAE	2.52	12.56	2.49	4.31	1.50	3.30
	MRD	0.02	0.02	0.019	0.019	0.012	0.016
GAB	c <sub>1</sub>	3.883	4.667	6.654	5.551	14.661	3.713
	k	1.0454	0.951	1.039	0.984	1.021	0.968
	m <sub>0</sub>	2.2875	3.584	2.092	2.875	1.854	2.325
	R <sup>2</sup>	0.999	0.996	0.998	0.998	0.998	0.999
	SE	0.0809	0.230	0.128	0.186	0.09	0.109

	SSE	0.27	4.04	0.40	1.21	0.28	0.54
	SAE	2.71	13.93	3.28	4.23	2.75	3.97
	MRD	0.02	0.02	0.02	0.018	0.02	0.02
BET	c	2.582	6.861	3.991	6.174	7.971	3.381
	$m_0$	2.794	3.122	2.509	2.782	2.083	2.345
	$R^2$	0.999	0.995	0.989	0.998	0.998	0.995
	SE	0.024	0.056	0.085	0.031	0.029	0.05
	SSE	1.11	13.94	1.91	3.38	1.39	18.44
	SAE	4.46	17.92	6.17	7.32	5.05	17.84
	MRD	0.02	0.02	0.03	0.02	0.03	0.06

---

**Table 1.4** Best-fitting equations to sorption experimental data of zeolite powder and hard red winter wheat (HRW)

	Temperature (°C)	Direction of sorption	DLP fitting equations
HRW	25	Adsorption	$m = -0.597x^3 + 0.399x^2 - 0.341x + 9.183$
		Desorption	$m = 0.329x^3 + 0.410x^2 - 4.069x + 11.002$
	35	Adsorption	$m = 0.035x^3 + 1.794x^2 - 0.872x + 8.295$
		Desorption	$m = 0.180x^3 + 0.360x^2 - 4.104x + 10.630$
	45	Adsorption	$m = 0.090x^3 + 1.964x^2 - 1.288x + 7.892$
		Desorption	$m = 0.092x^3 + 0.513x^2 - 3.683x + 10.104$
Zeolite	25	Adsorption	$m = -1.631x^3 + 0.280x^2 - 2.881x + 2.732$
		Desorption	$m = 0.178x^3 + 2.530x^2 - 3.364x + 3.837$
	35	Adsorption	$m = -1.718x^3 - 0.232x^2 - 2.584x + 2.887$
		Desorption	$m = -0.542x^3 + 1.366x^2 - 3.079x + 3.381$
	45	Adsorption	$m = -1.272x^3 - 0.083x^2 - 2.113x + 2.777$
		Desorption	$m = -0.616x^3 + 0.522x^2 - 2.572x + 2.469$

m is the moisture content (%) and x is the water activity (Aw).

**Table 1.5** Critical water activity ( $A_{WC}$ ) and corresponding equilibrium moisture content (EMC) (% w.b.) for phase transition in zeolite powder and hard red winter wheat

Temperature (°C)	Zeolite*		HRW*	
	$A_{WC}$	EMC	$A_{WC}$	EMC
25	0.639	6.07	0.700	15.24
35	0.649	5.91	0.770	16.28
45	0.657	5.37	0.790	16.33

\* Data for zeolite and wheat was obtained from DLP models

**Table 1.6** Recommended zeolite moisture content and water activity for grain (HRW) protection, at different grain moisture contents and storage temperatures

25°C			35°C			45°C		
10.0	2.08	0.28	10.0	2.59	0.32	10.0	2.77	0.36
10.5	2.41	0.33	10.5	2.84	0.36	10.5	3.08	0.41
11.0	2.70	0.36	11.0	3.20	0.41	11.0	3.31	0.46
11.5	3.12	0.41	11.5	3.45	0.45	11.5	3.67	0.50
12.0	3.53	0.46	12.0	3.88	0.49	12.0	3.97	0.55
12.5	3.96	0.50	12.5	4.21	0.53	12.5	4.30	0.58
13.0	4.36	0.54	13.0	4.59	0.57	13.0	4.88	0.62
13.5	4.88	0.58	13.5	5.06	0.60	13.5	5.37	0.65
14.0	5.70	0.62	14.0	5.59	0.63	14.0	5.69	0.68

*For each storage temperature, the first column indicates wheat moisture content; the second column indicates recommended zeolite moisture; and the third column indicates the equilibrium water activity of the system "wheat-Zeolite".*

**Table 1.7** Predicted water activity of HRW and zeolite powder at different moisture contents and temperatures

	Moisture content	20°C	25°C	30°C	35°C	40°C	45°C	50°C
Zeolite	2%	.295	.284	.274	.264	.255	.246	.238
		.166	.175	.184	.193	.203	.212	.222
	4%	.485	.495	.505	.514	.524	.533	.543
		.337	.371	.407	.445	.485	.527	.571
	6%	.612	.624	.637	.649	.661	.673	.685
		.491	.526	.562	.599	.636	.676	.716
Wheat	10%	.638	.635	.633	.630	.627	.625	.623
		.254	.272	.291	.310	.330	.350	.371
	11%	.720	.709	.699	.690	.681	.672	.664
		.330	.353	.376	.400	.425	.450	.476
	12%	.770	.760	.750	.740	.731	.722	.714
		.425	.446	.468	.490	.512	.535	.558

**Table 1.8** Temperature effect: prediction of water activity of wheat and zeolite at different moisture contents

	Moisture (% d.b.)	Direction of sorption	Predicted Water activity vs Temperature	$R^2$
HRW	10	Adsorption	$A_w = -.0005 T + .6479$	.9955
		Desorption	$A_w = .0039T + .1746$	.9995
	11	Adsorption	$A_w = -.0019 T + .7557$	.9979
		Desorption	$A_w = .0049 T + .2312$	.9995
	12	Adsorption	$A_w = -.0019 T + .8068$	.9985
		Desorption	$A_w = .0044 T + .3353$	.9998
Zeolite	2	Adsorption	$A_w = -.0019 T + .3316$	.9977
		Desorption	$A_w = .0019 T + .1283$	.9997
	4	Adsorption	$A_w = .0019 T + .4469$	.9998
		Desorption	$A_w = .0078 T + .176$	.998
	6	Adsorption	$A_w = .0024 T + .5635$	.9999
		Desorption	$A_w = .0075 T + .3386$	.9994

**Figure 1-1** Full sorption isotherms of zeolite powder at 25 (a), 35 (b), and 45°C (c).

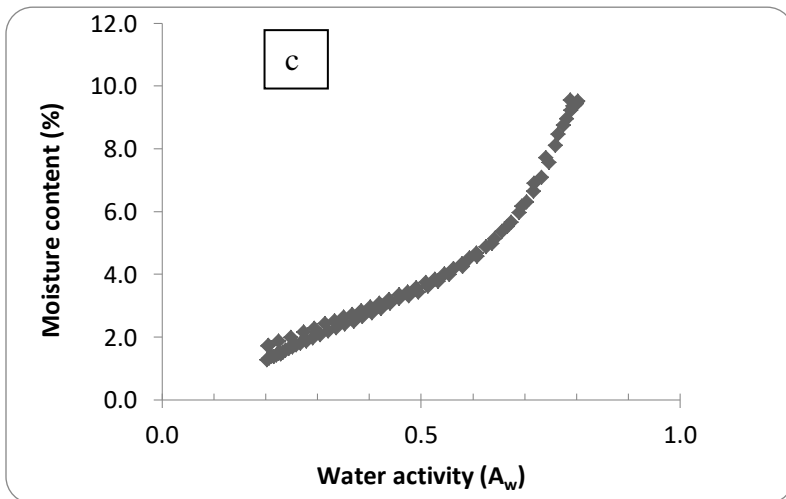
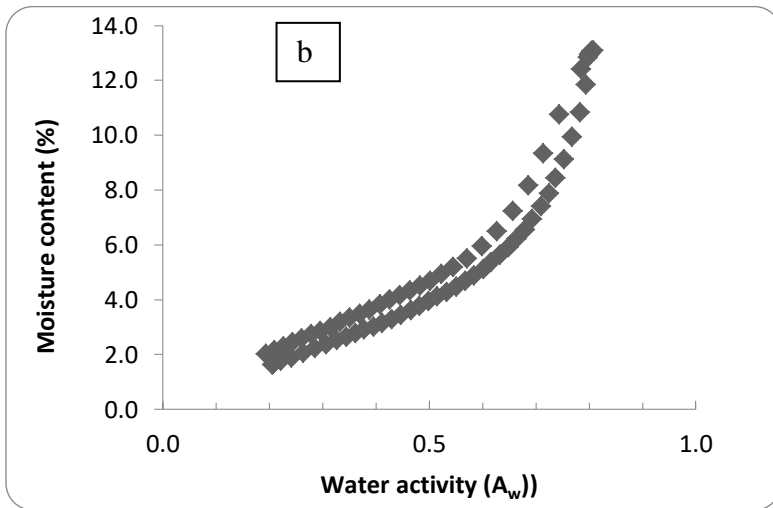
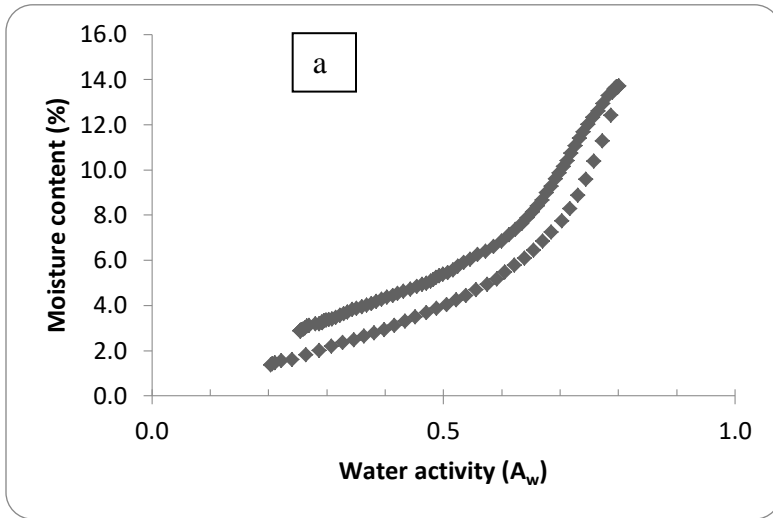


**Figure 1-2** Full sorption isotherms of Hard Red Winter wheat (HRW) at 25 (a), 35 (b), and 45°C (c).

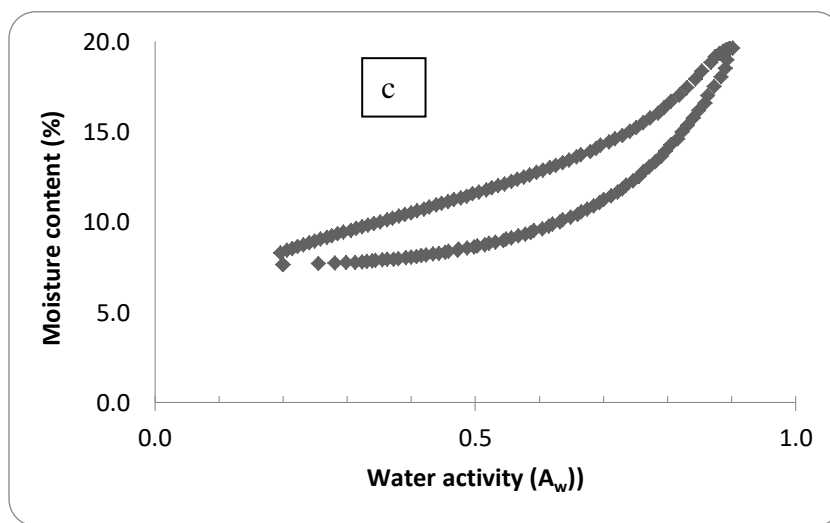
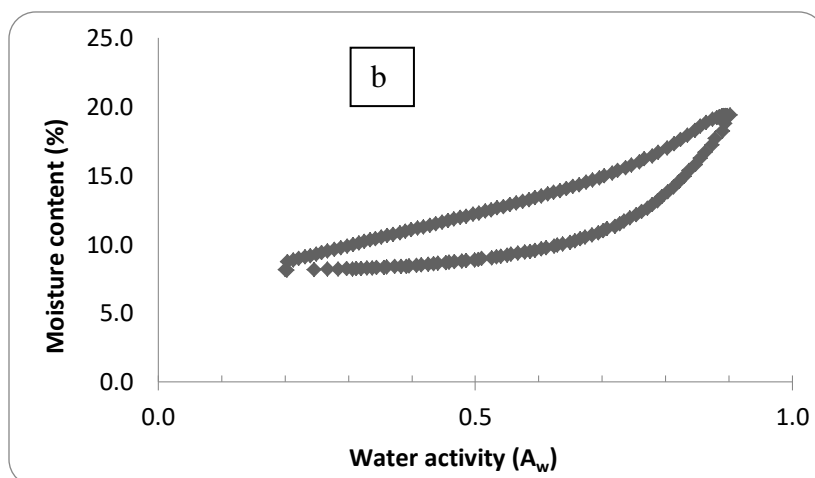
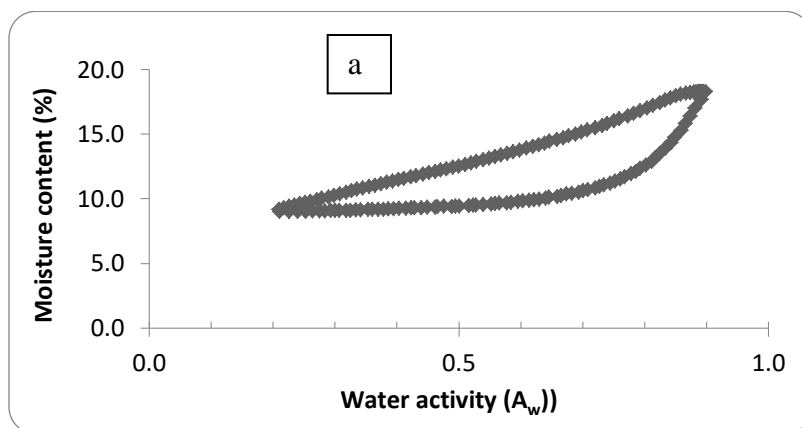
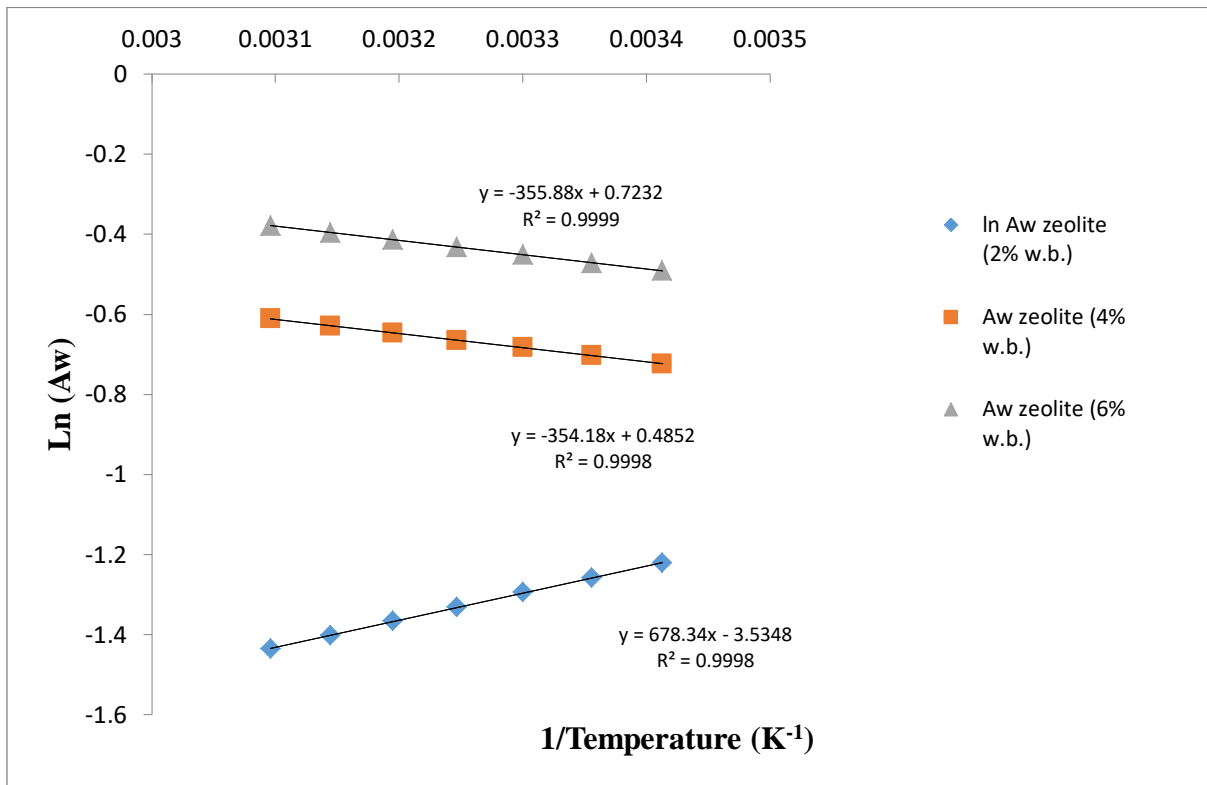


**Figure 1-3** Graphical determination of the net isosteric heat of sorption and the differential enthalpy of zeolite powder at different moisture contents



## **Chapter 2 - Moisture content and application rates of inert dusts: Effects on dust and wheat physical properties**

### **Abstract**

In the grain industry, amorphous silica dusts are often applied on wheat during storage to preserve grain quality. Adverse variations in bulk density and flow properties of wheat treated with inert dusts remain major concerns. Grain moisture content is known to greatly impact grain bulk density. However, the moisture content of the inert dust applied onto grain can also change grain moisture content, and hence grain bulk density. This research investigated the effects of the moisture content of a synthetic amorphous silica dust and the rates of application on some physical properties of the amorphous dust and wheat kernels. Three levels of moisture (2.0%, 6.0%, and 10.0%) of the dust were applied at three rates (0.5 g/kg, 1.0 g/kg, and 2.0 g/kg) on 100 g wheat samples (10% m.c, wet basis) in triplicates. Image analysis, laser diffraction, gas pycnometry, and the Single-Kernel Characterization System (SKCS) were used to characterize the physical properties of the dust and wheat kernels. The application of 0.5 g/kg of dust at 2-6% moisture content caused no significant changes in the physical properties of wheat and enhanced the flowability of wheat. This research suggests the existence of a range of moisture content and application rates that contribute positively to the flowability of grain treated with amorphous dust.

**Keywords:** Particle size, Particle shape, Surface roughness, Angle of repose, Test weight, SKCS, True density, Wheat

## Introduction

Inert dusts, like most powders, are not solely discrete solid particles, but rather a mixture of solid, liquid (surface moisture content), and gas (entrapped air). Wheat kernels treated with inert dusts form a granular system, which can transition between any of three distinct states: static, quasi-static, or dynamic (Lumay et al., 2012). A major concern, when applying any amorphous dust onto grain for quality preservation, is the change in the flow properties of the treated grain. A good flowability of wheat treated with inert dust and stored in bins is the ability of wheat to easily exit the bin by exhibiting low particle-to-particle friction, and low particle to bin inner wall surface friction. Ideally, wheat kernels with low surface friction, low angle of repose, low angle of internal friction, low angle of wall friction, and low compressibility are needed for optimal flow properties and minimal energy requirement during mechanical handling. When amorphous inert dusts are admixed with coarser materials such as grain kernels, the overall flow properties can be influenced by the amount of dust in the mixture, the particle shape and surface roughness of the dust, the moisture content of the dust, and the moisture content of grain kernels. Besides, the handling history, the state of compaction, the storage duration, and the process involved are important factors to consider. A vast array of literature exists that stresses the relationship between flowability and grain physical properties such as particle size, particle shape, moisture, and environmental parameters such as temperature, and relative humidity (Fitzpatrick et al., 2004; Cooke & Freeman, 2006; Iqbal & Fitzpatrick, 2006; Freeman, 2007; Ganesan, 2008; Emery et al., 2009). Increasing grain moisture content generally causes a decrease in grain bulk density (Altuntas & Yildiz, 2007). However, the moisture content of the inert dust applied onto grain can also change grain moisture content, and hence grain bulk density. Grain bulk density is a key indicator of wheat quality and is used to grade and assess the

commercial value of any class of wheat. For instance, the minimum bulk density to meet the requirements for U.S. grade No.1, is 60 pounds per bushel, except for Hard Red Spring wheat or White Club wheat (58 pounds per bushel) (FGIS, 2013). The extent of the decrease in bulk density may vary with the type and amount of dust, the particle size, and the moisture content of the dust. More importantly, a lower bulk density may not necessarily translate into poor flow performance. In other words, the magnitude of change in bulk density is not a good indicator of the magnitude of change in flow properties. The changes in shape and size as well as surface roughness of particles of porous powders used as grain protectants are likely to alter the flow and abrasive properties of wheat kernels. However, it's unclear whether moisture content will affect the particle size and shape of porous inert dusts. Particle size analysis is often conducted to evaluate the modifications in particle size. Particle size analysis alone does not always discriminate between particles with different shapes, though. Particle shape has been shown to have a significantly higher impact on grain flowability (Fu et al., 2012). Thus, particle shape analysis is quite often carried out in addition to particle size analysis. Particle shape factors help shed light on subtle differences that may exist between particles with identical size, thus contributing to a better understanding of flow properties. Several methods exist to quantify particle size and shape. Laser diffraction uses Mie theory of light scattering to calculate the particle size distribution, assuming a volume equivalent sphere model. Mie theory requires knowledge of the optical properties (refractive index and imaginary component) of both the dispersant and the sample being measured. A simplified approach is to use the Fraunhofer approximation, which does not require the optical properties of the sample. Automated image analysis is a counting technique which gives a number weighted distribution where each particle is given equal weighting irrespective of its size. No literature was found on the effects of the

moisture content of amorphous silica dusts on the size and shape of the dust and subsequently on the physical properties of wheat kernels mixed with the amorphous silica dust. Shape, size and surface roughness of porous powders influence flow properties of treated grain. Hence, understanding the relationship between powders moisture content and size and shape and surface roughness can help predict the flowability of the treated grain.

The objectives of this study were:

- To determine the influence of inert dust moisture content on inert dust particle size, shape, and surface roughness; and
- To determine the influence of inert dust moisture content and application rates on some physical properties of Hard Red Winter wheat (HRW).

## **Materials & Methods**

### **Moisture effects on physical properties of amorphous silica dust**

#### **Sampling**

A fresh batch of an amorphous silica dust, Odor-Z-Way®, available in the market as an odor absorbent, was purchased from a local manufacturer (Odor-Z-Way®, Phillipsburg, KS, USA). Measurements samples were obtained by passing gross samples through a chute splitter device. A total of 27 measurement samples were obtained and 9 samples were systematically selected and randomly assigned, in triplicates, to each of three moisture levels (2.0, 6.0, and 10.0%).

#### **Equilibration in controlled humidity chamber**

The initial moisture content determined by thermogravimetric analysis (TGA) (Pyris 1 TGA, Perkin Elmer) was about 35% (dry basis). Zeolite samples were then dried overnight at 25°C to remove excess moisture. Moisture content was re-determined by TGA and was about 1.29% (d.b.). Samples of zeolite were then allowed to equilibrate to  $2\pm.05\%$ ,  $6\pm.02\%$ , and  $10\pm.01\%$  moisture contents in controlled humidity chambers at 25°C under a specific relative humidity (Table 2.2). Each equilibrium relative humidity was chosen based on the adsorption isotherm of the silica dust at 25°C. Equilibrium was achieved when the relative change in sample weight did not exceed 1%. The samples were immediately analyzed once equilibrium was reached to minimize exposure to laboratory ambient conditions.

#### **True density analysis**

The true density of a particle is by definition the mass of a particle divided by its true volume, that is, excluding open and closed pores. True density was measured using a gas displacement pycnometer (Helium AccuPyc 1330, Micromeritics, Norcross, Georgia, USA). Helium gas was used to fill a chamber containing the sample and small voids (pores) within the sample to

determine the volume occupied by the particles. The principle is that Helium gas, under precisely-known pressure, occupies a fixed volume. The volume change of Helium in a constant volume chamber allows determination of solid volume. The ratio of sample mass to its true (solid) volume yields the true density. The data was collected through a RS-232 computer interface.

$$\text{True density} = \frac{\text{Weight (g)}}{\text{True volume (cm}^3\text{)}} \quad (2.1)$$

### **Particle size and shape analysis**

Particle size distribution, surface area moment mean, and volume moment mean were determined by laser diffraction (Mastersizer 3000, Malvern). Shape factors such as particle diameter (CE diameter), particle form (aspect ratio, elongation), particle outline (convexity, solidity), and a universal shape parameter (circularity) were determined by automated image analysis (Morphologi G3, Malvern). Image analysis allows a precise characterization of individual particles within pre-dispersed samples of dry powders, wet suspensions, and particulates deposited on filters. Statistically representative distributions are constructed by rapidly and automatically analyzing hundreds of thousands of particles per measurement, providing valuable information on the whole sample. Data from particle analysis and particle shape analysis fully characterizes both spherical and irregularly-shaped particles, enabling a deeper understanding of a sample's characteristics through precise detection of agglomerates, foreign particles and other anomalous materials.

### ***Circularity***

Circularity is the ratio of the circumference of a circle (with the area equal to that of the object's projected area) to the perimeter of the object; values range from 0 to 1.

$$\text{Circularity} = \frac{2 \times \sqrt{\pi \times \text{Area}}}{\text{Perimeter}} \quad (2.2)$$

### ***Convexity***

Convexity is a measurement of the surface roughness of a particle, that is, how much a particle curves in or bulges. Convexity is calculated by dividing the convex hull perimeter by the actual particle perimeter. A smooth shape like a circle has a convexity of 1, while a very 'spiky' or irregular object has a convexity closer to 0.

$$\text{Convexity} = \frac{\text{Convex Hull Perimeter}}{\text{Actual perimeter}} \quad (2.3)$$

Where, the convex hull perimeter is calculated from an imaginary elastic band which is stretched around the outline of the particle image.

### ***Solidity***

Solidity is the object's area divided by the area enclosed within the convex hull (border created by an imaginary rubber band wrapped around the object).

$$\text{Solidity} = \frac{\text{Area}}{\text{Convex Hull Area}} \quad (2.4)$$

### ***Aspect ratio***

The overall form of a particle can be characterized by the aspect ratio. A particle aspect ratio is obtained by dividing its width by its length. Aspect ratio values range from 0 to 1.

$$\text{Aspect ratio} = \frac{\text{Width}}{\text{Length}} \quad (2.5)$$

### ***Elongation***

Elongation helps identify needle-shaped particles in a sample. Elongation values range from 0 to 1.

$$\text{Elongation} = 1 - \text{Aspect ratio} = 1 - \frac{\text{Width}}{\text{Length}} \quad (2.6)$$

## **Moisture and application rates effects on wheat physical properties**

### **Sampling**

Bags of hard red winter wheat (HRW) were purchased from Heartland Mills (Marienthal, KS, USA) and kept in a freezer at  $-13^{\circ}\text{C}$  for 72 hours to kill any live insects. The initial grain moisture content determined using a portable moisture tester for Grain (Shore Model 930, Shore Sales Co., Rantoul, IL, USA) was about 11.8% (d.b). Grain was sifted through an aluminum sieve (Seedburo Equipment Company, Des Plaines, IL, USA) with a nominal aperture of 0.21 mm to remove dockage, shrunken, and broken kernels. Grain was further cleaned to remove foreign material, and damaged kernels. Wheat samples were obtained by emptying bags of HRW in a Boerner Divider (Seedburo Equipment Company, Des Plaines, IL, USA). The Boerner Divider meets USDA-FGIS (GIPSA) specifications for official inspections. Briefly, the sample is placed in the hopper and released by moving a slide gate located in the hopper throat, thus allowing an even dispersion over a 38 pockets-cone. The grain, after initial separation, is rejoined into two chutes which empty out of the bottom hopper. The principle is that the sample is poured into the divider and repeatedly halved until a sample of desired size is obtained. A total of 81 measurement samples were obtained and 27 samples were systematically selected and randomly assigned, in triplicates, to each of nine combinations of moisture and application rates. Treatments were formed by the combinations of three moisture levels ( $2.01\pm.05\%$ ,  $6.03\pm.02\%$ , and  $10.02\pm.01\%$  w.b) and three mixing ratios (0.5 g/kg, 1.0 g/kg, and 2.0 g/kg). Controls consisted of clean, sound, and dust-free HRW kernels. Wheat samples (100g;  $11.8\pm.2\%$  w.b) were allowed to equilibrate to  $10.0\pm.01\%$  moisture content (w.b) in a controlled humidity chamber (Table 2.1) based on wheat desorption isotherm at  $25^{\circ}\text{C}$ .

### **Static Angle of Repose (AoR)**

The angle of repose is related to particle size, shape, density, surface area, and coefficient of friction. Static angle of repose was determined using the conventional method described

elsewhere in the literature (Kurkuri et al., 2012). Briefly, samples of wheat (350 g) admixed with silica dust were poured onto an elevated plastic horizontal surface of 9cm-diameter through a funnel from a height of 6 cm (Kurkuri et al., 2012). The following formula was used to determine the angle of repose:

$$\text{Angle of Repose} = \tan^{-1}(2h / D) \quad (2.7)$$

where h is the height of the conical pile formed by the zeolite powder, and D is the diameter of the base of the horizontal surface (diameter of conical pile)

### **Test weight**

A Winchester cup arrangement (Seedburo Equipment Co., Des Plaines, IL, USA) was used to estimate the bulk density. Samples were made to fall from a hopper into a cup from a height of 10 cm. The cup was filled until excess of it began to overflow. The excess sample was removed by making three zig-zag motions with a scrapper. The cup had a volume of 473.18 ml. The bulk density was calculated from the weight and volume of the sample.

$$\text{Bulk density} = \frac{\text{Weight (kg)}}{\text{Volume (m}^3\text{)}} \quad (2.8)$$

### **Tapped Density**

A cylinder of known volume (250 ml) was filled with each sample (100 g) and the cylinder was tapped 750 times (260 taps/minute) using the Autotap Density Analyzer (Quantachrome Instruments, FL, USA). The tapped density was calculated from the tapped volume and weight of the samples.

$$\text{Tapped density} = \frac{\text{Weight (kg)}}{\text{Volume after tapping (m}^3\text{)}} \quad (2.9)$$

### **Carr Index (CI) and Hausner Ratio (HR)**

Carr Index (CI) and Hausner Ratio (HR) were obtained from bulk and tapped densities measurements and were determined as follows:

$$CI = 100 \times \frac{(Tapped\ density - Bulk\ density)}{(tapped\ density)} \quad (2.10)$$

$$HR = \frac{Tapped\ Density}{Bulk\ density} \times 100 \quad (2.11)$$

### **Single Kernel Characterization System (SKCS)**

The single-kernel characterization system (SKCS) (SKCS 4100, Perten instruments, Springfield, Ill.) was used to measure wheat kernel weight, moisture content, diameter, and hardness at a rate of two kernels per second and the results were reported as the average and standard deviation of these parameters from a 300-kernel sample. The working principle of the SKCS is detailed elsewhere in the literature (Martin et al., 1991).

### **Statistical analyses**

Two independent studies following a completely random experimental design (CRD) were subjected to:

- 1) One-way ANOVA using SAS PROC GLM procedure (SAS, 2009) to assess the significance of “dust moisture” main effect in particle size, and particle shape tests. Treatments means were separated by Bonferroni multiple comparisons test ( $\alpha=.05$ )
- 2) Two-way ANOVA using SAS PROC GLM procedure (SAS, 2009) to assess the significance of “dust moisture” main effect, “application rate” main effect, and their interaction (dust moisture x application rate) in physical tests related to wheat mixed with the amorphous dust. Treatments (the control was excluded) means were separated by Ryan-Einot-Gabriel-Welsch multiple comparisons test ( $\alpha=.05$ ). Dunnett’s multiple comparison procedure was used to compare the least squares means of all treatments to the control ( $\alpha=.05$ ).

## Results & Discussion

### *Preliminary analysis*

#### *X-ray diffraction*

The amorphous nature of the zeolite powder was confirmed by the absence of peak in the x-ray diffraction profile (Figure 2.1). Typical graphs for crystalline materials exhibit several peaks corresponding to specific minerals. The amorphous nature of the synthetic dust is required if we intend to use it as a grain protectant. Strict regulations exist that prohibit the application of crystalline powder onto grain intended for human consumption (Subramanyam & Roesli, 2000).

#### *Equilibration of dust and wheat*

Maintaining samples of dust and wheat in equilibrium conditions is essential to generate reproducible data in physical tests involving sorption properties. Wheat and dust required different amounts of time to reach equilibrium because of differences in their sorption properties (Table 2.1). Relative humidity in the controlled humidity chamber required for the samples to reach equilibrium was determined using wheat desorption isotherm and silica dust adsorption isotherm at 25°C. Sorption isotherms at 25°C were used as an approximation of the laboratory ambient conditions (26°C).

#### *Density and flow properties*

Three density indicators (bulk, tapped, and true densities) were determined at the time of reception of the silica dust. The moisture content of the silica dust at the time of reception was about 35% and density indicators were respectively 342.5kg/m<sup>3</sup>, 680.5 kg/m<sup>3</sup>, and 2.72g/cm<sup>3</sup> respectively for bulk density, tapped density, and true density. The corresponding values of Hausner ratio (HR) and Carr Index (CI) were respectively 1.987±.03 and 0.497±.05 (Table 2.2). The angle of repose measured at time of reception was about 47.2°±6.4. High variability

observed in values of angle of repose can be explained by the manner grain was handled before and during the formation of conical piles. A comparison of HR, CI, and AOR values to the reference values indicate that the silica dust is more likely to exhibit poor flowability (Table 2.3&2.4).

### ***Moisture effects on amorphous dust physical properties***

#### ***Particle size and size distribution***

Within the 2-35% moisture range, surface mean diameter significantly decreased ( $F=331$ ;  $P<.0001$ ) with increasing moisture content. Conversely, volume mean significantly increased ( $F=3807$ ;  $P<.0001$ ) with increasing dust moisture content (Table 2.6). Surface mean or Sauter diameter is relevant to specific surface area. Silica dusts with a high relative frequency of fines will have a larger specific area, which is directly related to their surface coverage. Theoretically, amorphous dusts with larger specific surface areas should perform better as grain protectants because of a better coverage of insect cuticle with the silica dust. Decreases in surface mean diameter values with increasing moisture content suggest the formation of agglomerates. Volume mean or De Brouckere mean diameter is indicative of the particle size which constitutes the most of the bulk of the sample volume. Increases in volume mean diameter with increasing moisture show that the proportion of large particulates is increasing in the particle size distribution. The particle size distributions of the silica dust reported as percentiles are presented in Table 2.7. The  $Dv_{10}$ ,  $Dv_{50}$ , and  $Dv_{90}$  represent the particle diameter below which 10%, 50%, and 90% respectively of the sample volume exists. In general, the one-way analysis of variance (ANOVA) indicated that all three percentiles determined at 35% moisture content were significantly higher than the percentiles determined at 2.0, 6.0, and 10.0% moisture contents, which implies a significant increase in the particle size when dust moisture reaches 35%. No significant

difference was found between median particle sizes ( $D_{v50}$ ) at 2% and 6% dust moisture content, but the median particle size at 10% was significantly higher than the median particle sizes at 2% and 6%. Our data suggest that significant changes in the median particle size begin to occur at 10% dust moisture content and the maximum change in particle size occur when the dust is at 35% moisture content, that is, at the time of reception. Also, changes at the extremes of the particle size distribution ( $D_{v10\%}$  and  $D_{v90\%}$ ) could be due to the presence of fewer fines, and more oversized particles or agglomerates, or a loss in texture and structure occurring above the critical water activity.

### ***Particle shape analysis***

Circularity quantifies the deviation of a particle shape from a perfect circle. A perfect circle has Circularity of 1.0, while a very narrow elongated object has circularity close to 0. Circularity values were comprised between 0.923 and 0.979 when the moisture of the dust ranged between 2 and 35%. Particles of the amorphous dust were not close to resembling a perfect circle (Table 2.7). A significant decrease in circularity values was observed at 10 and 35% moisture contents. No significant difference was observed between circularity at 2 and 6% moisture contents ( $P < .001$ ). Deviation from a perfect circle was significantly higher at 35% moisture content. These changes in circularity suggest possible changes in particle form and/or outline (surface roughness).

Aspect ratio ranged between 0.74 and 0.79 within the 2-35% moisture range, implying that the amorphous dust particles do not have regular symmetry, such as spheres or cubes and their shape is closer to ovoid particles (Figure 2.2). Solidity and convexity data provided more precise information about the outline of the particles. At 2% moisture content, convexity and solidity were respectively 0.977 and 0.978, whereas, at 35% moisture content, these values dropped at

0.958 and 0.975, respectively. As with circularity, the values determined for aspect ratio, convexity, and solidity did not significantly change at 2% and 6% moisture contents. Aspect ratio, convexity, and solidity values were significantly lower at 35 % moisture content, followed by 10% moisture content. These lower convexity/solidity values show that the amorphous dust particles possess rough outlines and they probably become agglomerated primary particles as moisture increases.

### ***Moisture and application rates effects on physical properties of wheat***

#### **Static angle of repose**

Values of static angle of repose can serve as an indirect assessment of flowability because the angle of repose relates to the inter-particulate friction. Changes in the bulk density of wheat were dependent on both the dust moisture and the rate of the application (Table 2.9). In fact, the moisture main effect ( $F=2489$ ;  $P<.0001$ ) and the rate main effect ( $F=117$ ;  $P<.0001$ ) were significant at the 5% level of significance. The moisture by rate interaction was also significant at 5% level ( $F=5.0$ ;  $P=.0018$ ). The lowest increase in static angle of repose was observed when wheat was admixed with dust at 2% moisture content and a rate of 0.5g/kg. The highest increase in static angle of repose was observed when wheat was admixed with dust at 35% moisture content and a rate of 2.0g/kg. A classification of flowability based on angle of repose by Carr (1965) suggests that angles of repose below  $30^\circ$  indicate good flowability,  $30^\circ$ - $45^\circ$  some cohesiveness,  $45^\circ$ - $55^\circ$  true cohesiveness, and  $>55^\circ$  sluggish or very high cohesiveness and very limited flowability. Based on this classification, wheat treated with the amorphous silica dust evolved from having “some cohesiveness” into exhibiting “true cohesiveness”.

### **Bulk and tapped density**

Tests on bulk density showed that the moisture main effect ( $F=8248.51$ ;  $P<.0001$ ), the rate main effect ( $F=662.69$ ;  $P<.0001$ ), and the moisture by rate interaction ( $F=57.11$ ;  $P<.0001$ ) were all significant at the 5% level of significance. Similarly, tests on tapped density indicated that the moisture main effect ( $F=50547.8$ ;  $P<.0001$ ), the rate main effect ( $F=3362.64$ ;  $P<.0001$ ), and the moisture by rate interaction ( $F=631.39$ ;  $P<.0001$ ) were all significant at the 5% level of significance. An increase in both the dust moisture and the rate of application significantly decreased wheat bulk density and significantly increased wheat tapped density (Table 2.9). Only minimal changes in bulk density (decrease) and in tapped density (increase) occurred when wheat was mixed with 0.5g/kg dust at 2% moisture content. As with the static angle of repose, the highest increase in tapped density of wheat and the highest decrease in the bulk density of wheat were observed when wheat was admixed with 2.0g/kg of dust at 35% moisture content.

### **Carr Index (CI) and Hausner Ratio (HR)**

There were a significant moisture main effect ( $F=8248.51$ ;  $P<.0001$ ), a significant rate main effect ( $F=662.69$ ;  $P<.0001$ ), and a significant interaction between moisture and rate ( $F=57.11$ ;  $P<.0001$ ) at 5% level of significance. In general, higher values of CI or HR were observed for combinations of higher dust moisture contents and higher rates of application. Carr Index (CI) and Hausner Ratio (HR) are single index parameters often used to indirectly assess the flowability of a given powder or granular material. An increase in both the CI and the HR are indicative of a cohesive material with a tendency to not flow easily or a tendency to resist flow. Carr Index (CI) and Hausner Ratio (HR) were linearly correlated to the static angle of repose (Fig 2.1 & 2.2).

### **Single Kernel Characterization System (SKCS)**

Table 2.10 shows the data for the SKCS of wheat treated with dust at various moisture and rates.

The two-way analysis of variance did not show any significant difference in wheat kernel diameter ( $F=1.47$ ;  $P=.206$ ), and in wheat hardness ( $F=.37$ ;  $P=.95$ ). However, data on wheat weight and moisture content showed a significant interaction between dust moisture and rate of application ( $P<.05$ ). Wheat moisture and wheat weight were significantly higher when dust moisture was 35%. No significant difference was found in wheat moisture and wheat weight between untreated wheat (control) and all treatments with dust at 2%. Average kernel weight and moisture were similar between all treatments with 2 and 6% amorphous dusts.

## Conclusions

In general, particle size of the amorphous dust increased with increasing moisture content. Conversely, shape parameters (circularity, aspect ratio, convexity, and solidity) generally decreased with increasing dust moisture contents. When wheat was mixed with the amorphous dust at different rates and moisture levels, the bulk density of wheat decreased, while the tapped density and the angle of repose increased, resulting in higher Hausner ratios and Carr Index values. Treating wheat with the amorphous dust caused the treated wheat to transition from an acceptable flowability to a poor flowability. However, our data suggest that a range of moisture content (2-6%) and an application rate (0.5 g/kg) mitigate the adverse effects on wheat flowability. Our data also highlight the importance of drying any amorphous dust or allowing a dust to equilibrate at the experiment temperature before conducting tests on physical properties. The improper handling of the amorphous dust before analysis may cause significant bias in the analysis of the flow and the physical properties of amorphous silica dusts and ultimately that of inert dust treated wheat.

## References

- Altuntaş, E., & Yıldız, M. (2007). Effect of moisture content on some physical and mechanical properties of faba bean (*Vicia faba* L.) grains. *Journal of Food Engineering*, 78(1), 174-183.
- Cooke, J., & Freeman, R. (2006). The flowability of powders and the effect of flow additives. In *World Congress on Particle Technology* (Vol. 5).
- Emery, E., Oliver, J., Pugsley, T., Sharma, J., & Zhou, J. (2009). Flowability of moist pharmaceutical powders. *Powder Technology*, 189(3), 409-415.
- FGIS. (2013). Book II, chapter 13. federal grain inspection service. *US Department of Agriculture*.
- Fitzpatrick, J. J., Barringer, S. A., & Iqbal, T. (2004). Flow property measurement of food powders and sensitivity of Jenike's hopper design methodology to the measured values. *Journal of Food Engineering*, 61(3), 399-405.
- Freeman, R. (2007). Measuring the flow properties of consolidated, conditioned and aerated powders—a comparative study using a powder rheometer and a rotational shear cell. *Powder Technology*, 174(1-2), 25-33.
- Freeman, R., & Cooke, J. (2006). Understanding powder behaviour by measuring bulk, flow and shear properties. *Pharmaceutical Technology Europe*, 18(11), 39.
- Fu, X., Huck, D., Makein, L., Armstrong, B., Willen, U., & Freeman, T. (2012). Effect of particle shape and size on flow properties of lactose powders. *Particuology*, 10(2), 203-208.
- Ganesan, V., Rosentrater, K. A., & Muthukumarappan, K. (2008). Flowability and handling characteristics of bulk solids and powders—a review with implications for DDGS. *Biosystems Engineering*, 101(4), 425-435.
- Iqbal, T., & Fitzpatrick, J. J. (2006). Effect of storage conditions on the wall friction characteristics of three food powders. *Journal of Food Engineering*, 72(3), 273-280.

Kurkuri, M. D., Randall, C., & Losic, D. (2012). New method of measuring the angle of repose of hard wheat grain. *Chemeca 2012: Quality of Life through Chemical Engineering: 23-26 September 2012, Wellington, New Zealand*, , 1814.

Lumay, G., Boschini, F., Traina, K., Bontempi, S., Remy, J., Cloots, R., & Vandewalle, N. (2012). Measuring the flowing properties of powders and grains. *Powder Technology*, 224, 19-27.

Martin, C. R., Rousser, R., & Brabec, D. L. (1991). *Rapid, Single Kernel Grain Characterization System U.S. Patent No. 5,005,774*. Washington, DC: U.S. Patent and Trademark Office.

Subramanyam, B., & Roesli, R. (2000). Inert dusts. *Alternatives to pesticides in stored-product IPM* (pp. 321-380) Springer.

**Table 2.1** Density and flow properties of an amorphous silica dust

<i>Density indicators</i>	
Bulk density (kg/m <sup>3</sup> )	342.5 ±12.5
Tapped density (kg/m <sup>3</sup> )	680.5 ±7.2
True density (g/cm <sup>3</sup> )	2.72±.03
<i>Flow indicators</i>	
Hausner ratio	1.987±0.03
Carr Index	0.497±0.05
Angle of Repose	47.2±1.4

*Density and flow indicators were determined at 35% moisture content (w.b)*

**Table 2.2** Equilibration parameters of zeolite powder and wheat in a controlled humidity chamber at 25°C

---

	Relative Humidity (%)	Equilibrium moisture contents (%)	Time to reach equilibration(h)
Zeolite	27.7	2.01	14.55
	63.6	6.03	17.0
	75.2	10.02	19.4
Wheat	28.3	10.0	10.1

---

**Table 2.3** Angle of repose and flowability

Flowability	Angle of Repose (degrees)
Excellent	25-30
Good	31-35
Fair	36-40
Passable	41-45
Poor	46-55
Very poor	56-65
Very, very poor	> 65

(Source: Carr, 1965)

**Table 2.4** Classification of powder flowability based on Hausner ratio

---

Flowability	Hausner ratio (HR)
Free flowing	$1.0 < HR < 1.1$
Medium flowing	$1.1 < HR < 1.25$
Difficult flowing	$1.25 < HR < 1.4$
Very difficult flowing	$HR > 1.4$

---

**Table 2.5** Surface and volume mean diameters of zeolite powder at various moisture contents

Moisture content (%)	Mean particle size ( $\mu\text{m}$ )	
	Surface mean diameter	Volume mean diameter
	( $D_{3,2}$ )	( $D_{4,3}$ )
2.0	21.3 $\pm$ 1.2 <sup><math>\alpha</math></sup>	33.3 $\pm$ 1.5 <sup><math>\gamma</math></sup>
6.0	20.8 $\pm$ 2.7 <sup><math>\beta</math></sup>	32.6 $\pm$ 4.1 <sup><math>\delta</math></sup>
10.0	20.0 $\pm$ 0.9 <sup><math>\gamma</math></sup>	37.8 $\pm$ 0.5 <sup><math>\beta</math></sup>
35.0	18.6 $\pm$ 1.9 <sup><math>\delta</math></sup>	46.8 $\pm$ 2.4 <sup><math>\alpha</math></sup>

*Mean particle sizes ( $n=3$ ), in the same column, followed by the same letter are not significantly different at 95% level of confidence.*

**Table 2.6** Particle size distribution of zeolite powder at various moisture contents

Moisture Content (%)	Size distribution		
	Dv10 ( $\mu\text{m}$ )	Dv50 ( $\mu\text{m}$ )	Dv90 ( $\mu\text{m}$ )
2.0	11.36	31.7	57.33
6.0	11.0	30.6	59.08
10.0	12.9	32.7	63.88
35.0*	18.84	37.38	71.84

*\*Indicate the moisture content at reception, before drying cycles*

**Table 2.7** Median particle shape parameters of zeolite powder at various moisture contents

Moisture content (%)	Shape parameters			
	Aspect ratio	Circularity	Convexity	Solidity
2.0	0.74	0.979	0.977	0.978
6.0	0.75	0.934	0.978	0.994
10.0	0.77	0.983	0.996	0.995
35.0	0.80	0.923	0.958	0.975

**Table 2.8** Physical properties of zeolite-treated wheat at various dust moisture contents and application rates

Dust moisture content (% d.b)	Dust application rate (g/kg)	Bulk density*	Tapped density*	Carr Index (CI)*	Hausner ratio* (HR)	Angle of repose * (AoR)
Control (HRW)	-	795.7	821.05	3.09	1.03	32.87
	0.5	790.8	828.89	4.55	1.05	33.19
	2.0					
	1.0	778.0	830.75	6.21	1.07	33.58
	2.0	763.8	835.85	8.68	1.10	34.47
6.0	0.5	729.7	872.14	16.5	1.20	37.44
	1.0	715.1	885.11	19.06	1.24	39.20
	2.0	704.2	898.77	21.5	1.27	40.67

10.0	0.5	696.0	900.92	22.6	1.29	42.70
	1.0	688.3	921.21	25.1	1.34	43.68
	2.0	686.1	946.53	27.3	1.38	45.62
	0.5	665.9	997.41	32.81	1.49	47.20
35.0	1.0	653.3	1063.4	38.6	1.63	47.99
	2.0	621.1	1081.76	42.53	1.74	49.04

---

*\*For each physical property, control (untreated wheat) was statistically different from all other treatments except treatment involving with treated with dust of 2.0% moisture content and applied at 0.5 g/kg.*

**Table 2.9** Single Kernel Characterization System (SKCS) data of wheat treated with an amorphous silica dust at various moisture contents and application rates

Dust moisture content (%)	Dust application rate (g/kg)	Hardness index	Weight (mg)	Moisture (%)	Diameter (mm)
Control	0	66.4	33.1	10.03	2.67
	0.5	66.3	31.2	10.06	2.65
2.0	1.0	66.4	31.4	10.03	2.67
	2.0	66.19	31.5	10.03	2.67
	0.5	66.4	32.1	10.56	2.66
6.0	1.0	66.4	32.6	10.43	2.67
	2.0	65.7	33.0	10.93	2.67
	0.5	65.4	34.2	11.72	2.67
10.0	1.0	65.4	33.5	11.14	2.68
	2.0	65.7	33.2	11.91	2.69
	0.5	62.4	36.2	13.23	2.67
35.0	1.0	62.1	37.7	13.75	2.67
	2.0	62.3	37.6	13.98	2.66

**Figure 2-1** X-ray diffraction profile of a synthetic amorphous zeolite

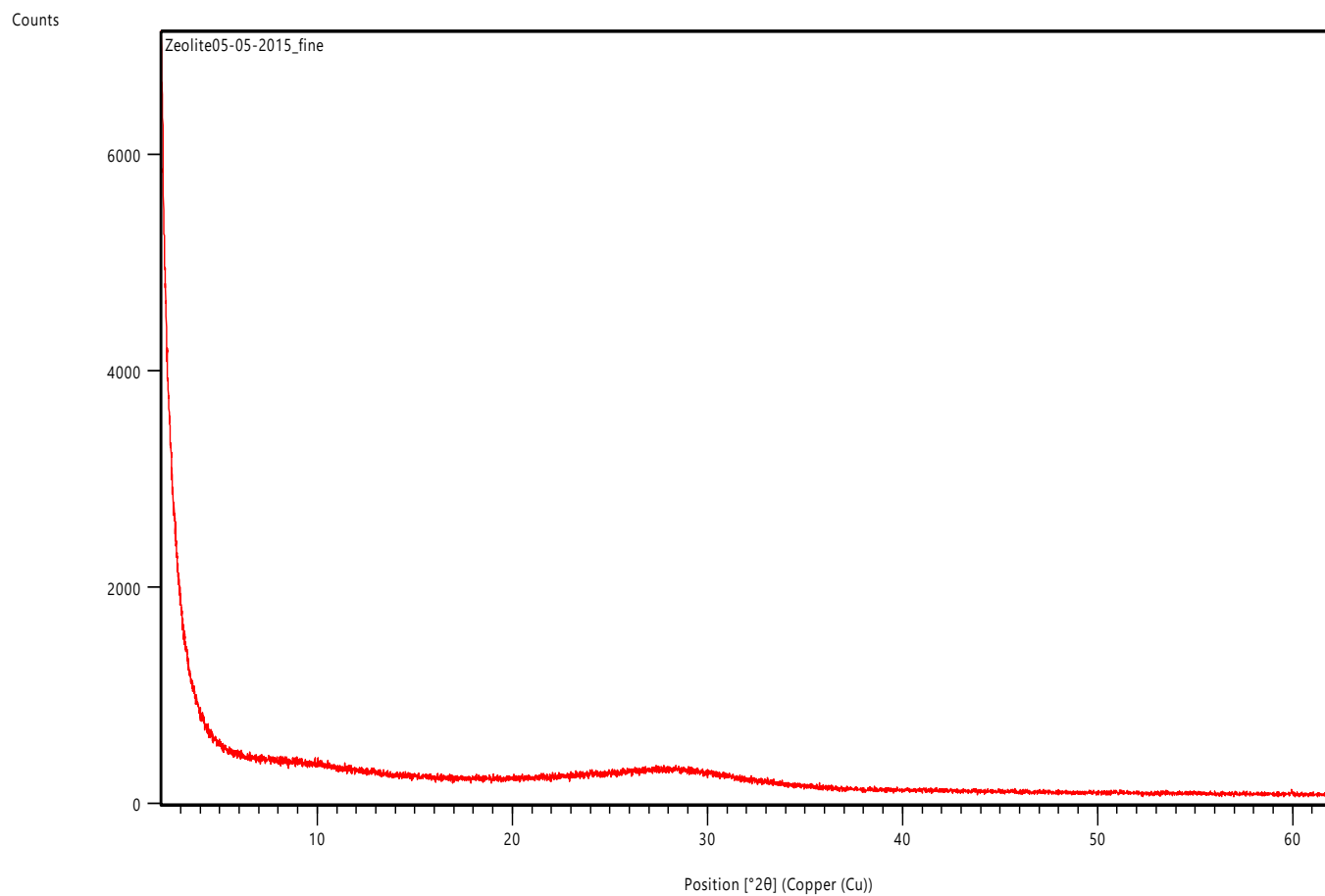
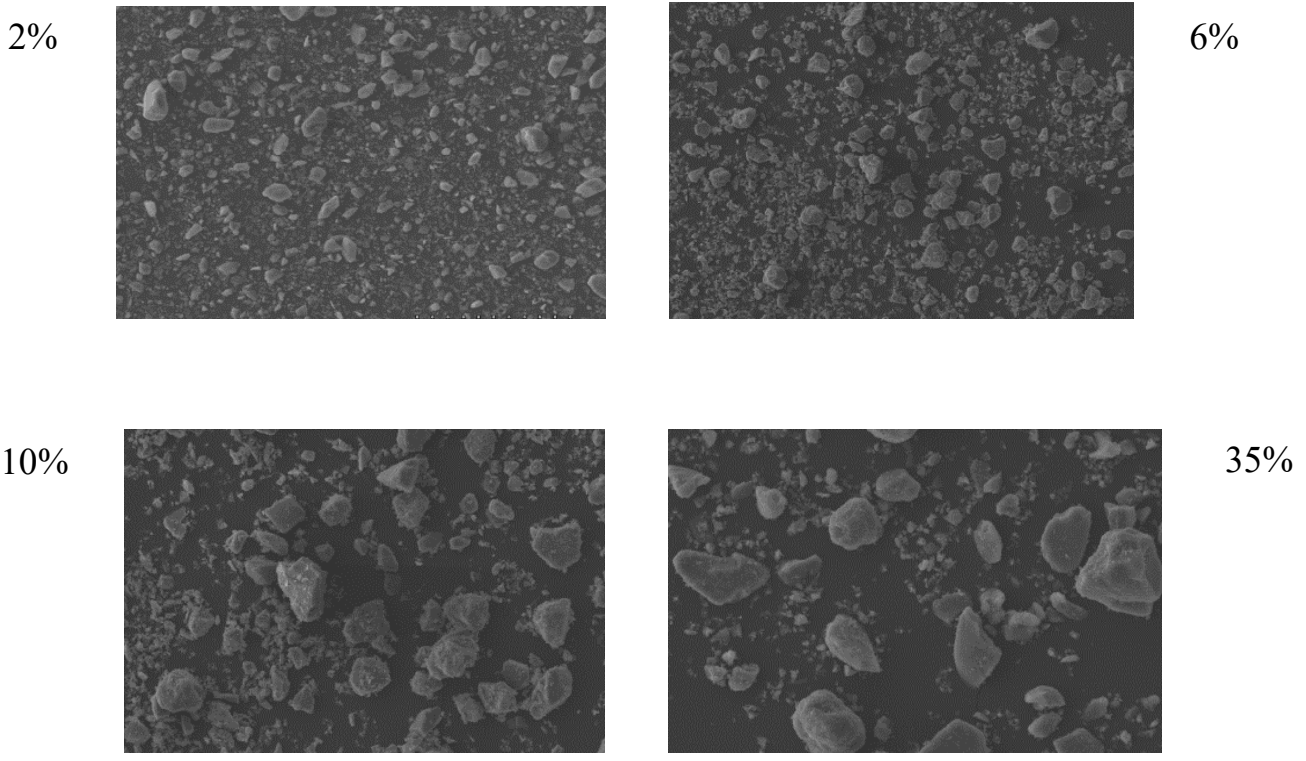


**Figure 2-2** Scanning electron microscopy of a synthetic amorphous zeolite at various moisture contents



*SEM images were obtained at 150X magnification*

**Chapter 3 - Using the FT4 Powder Rheometer to characterize bulk and dynamic flow properties of Hard Red Winter wheat (HRW) treated with three amorphous silica dusts**

**Abstract**

A series of laboratory tests using the FT4 Powder Rheometer was conducted to determine and compare the permeability, the conditioned bulk density and the dynamic flow properties of wheat treated with Odor-Z-Way®, a potential grain protectant or wheat treated with Diafil®, or Celite®, two registered amorphous silica dusts. Wheat was mixed, at the rate of 1g/kg, with each of three amorphous dusts dried down to 2% moisture content. Wheat treated with Odor-Z-Way was comparable to wheat treated with Celite and Diafil in terms of permeability, flow rate, cohesion, and sensitivity to aeration. However, wheat treated with Odor-Z-Way became almost unstable and exhibited a different de-aeration pattern. The conditioned bulk density generally decreased, but the decrease was lower when wheat was mixed with Odor-Z-Way. No minimum fluidization velocity was determined as the flow energy never stabilized in relation to air velocity. Tapped consolidated energy and direct pressure consolidated energy were not similar, suggesting different energy requirements during transport or storage in hoppers. This study suggests that the application of inert dusts on wheat as grain protectants can have desirable or adverse effects on the bulk and flow properties of wheat.

**Keywords:** Powder rheometer; Flowability; Permeability; Wheat; Inert dusts; Grain protection

## Introduction

Wheat is a major component of most diets of the world because of its agronomic adaptability, ease of storage, nutritional goodness, and the ability of its flour to produce a variety of palatable, interesting, and satisfying foods (Khan, 2016). The US Federal Grain Inspection Service (FGIS, 2013) defines wheat as grain that, before the removal of dockage, consists of 50 percent or more common wheat (*Triticum aestivum* L.), club wheat (*T. compactum* Host.), and durum wheat (*T. durum* Desf.) and not more than 10 percent of other grains and that, after the removal of the dockage, contains 50 percent or more of whole kernels of one or more of these wheats. Wheat is a primary crop for the US food industry, representing a major export and it is a common practice to store wheat in concrete or steel bins on farm or at commercial elevators for extended periods of time prior to shipping, sale, or processing. During storage, wheat quality can deteriorate if insect infestation is not prevented, especially under environmental conditions such as high relative humidity and temperature (Le Patourel, 1986). To ensure the delivery of wheat that meets the highest quality standards, wheat kernels are treated with chemical insecticides at the time of storage as grain is being augured into the bin or silo. These conventional insecticides, despite their proven efficacy, pose food safety and environmental pollution concerns.

Alternatives that are safe, effective, and cost-effective are thus needed. Inert dusts are promising and viable alternatives as they have low mammalian toxicity, do not leave harmful residues, are effective against chemical resistant species, and are persistent and stable at high and low temperatures (Subramanyam et al., 1994). Inert dusts are primarily composed of amorphous silica, which should not be confused with crystalline silica such as quartz, cristobalite, and tridymite. Crystalline silica is classified as a human lung carcinogen (IARC) and exposure to fine, respirable crystalline silica particles increases the risk of developing the symptoms of

silicosis, a lethal lung infection (Warheit, 2001). One major hurdle to guarantee the registration and the dissemination of inert dusts as grain protectants is their adverse effects on the bulk density (test weight), causing grain to be downgraded. In fact, wheat grading and pricing is primarily based on test weight per bushel, and secondarily on the level of defects such as damaged kernels, foreign materials, shrunken, and broken kernels (US Grain Council, 1986; FGIS, 2013). However, a decrease in bulk density can be corrected by performing a regular commercial cleaning of wheat or by the application technique (surface admixture in combination with aeration, capping in combination with fumigation). Desmarchelier & Dines (1987) were able to remove up to 98% of Dryacide on wheat, and no Dryacide could be detected in the flour, with no significant change in flour quality. The application of inert dust onto grain, if not as a slurry, may create an undesirable dusty environment. Also, the decrease in bulk density of inert dust treated grain was more significant when the inert dust applied was dry (Korunic et al., 1996). Another concern is the impact of inert dust application on wheat flow properties with regards to energy requirements in conveyance systems. Regardless of the type of conveyance system, even slight changes in wheat flowability could result in dramatic changes in basic flowability energy, minimum fluidization energy, and the economic implications, for the entire supply chain, are higher energy consumption and a decreased profitability. The addition of inert dusts is not always detrimental to wheat flowability, though. Inert dusts may behave as flow additives and be desirable to improve grain processing by reducing the frictional resistance of particle to particle movement (Cooke & Freeman, 2006). Various flow indicators are used to characterize powders flowability. Jenike's pioneering work showed that good powder flowability is often linked with a low angle of repose, a low angle of internal friction, and a low angle of wall friction (Jenike, 1961 & 1975). Generally, an angle of repose below 30° could be an

indicator of good flowability (Carr, 1965a). The Hausner ratio is a parameter that indicates how much a powder might compact with time, which correlates with flowability, and Hausner ratio values greater than 1.25 indicate that the powder will have poor flowability characteristics (Carr, 1965b). Geldart et al. (2006) established a correlation between angle of repose and Hausner ratio. Powders flowability is governed by intrinsic (particle size, shape) and external factors (temperature, moisture content, relative humidity). An increase in particle size usually increases the flowability up to a critical size range above which flowability does not show any improvement (Abdullah & Geldart, 1999). The correlation between particle shape and Jenike's classification of powders flow properties was investigated by Mellmann et al. (2014). They showed that a decrease in powder flowability, during unloading agricultural bulk materials from silos, was associated with an increase in particle elongation.

Powder flowability can be assessed through direct measurements using automated powder testers such as the FT4 powder Rheometer by investigating standard shear tests and wall friction tests, or indirectly through the determination of bulk properties such as compressibility and permeability. In a study involving distillers dried grain with solubles (DDGS) by Ganesan et al. (2008), compressibility increased with increasing solubles concentration and increasing moisture content. In other words, an increase in solubles concentration reduced the flowability. Similarly, an increase in moisture content from 10 to 20% resulted in a decrease of flowability. However, further increase in moisture to 25-30% improved the flow properties. The packing state or condition of a powder or granular material can also affect the flowability (Vasilenko et al., 2013). Besides, aeration and de-aeration of a granular material or the ability to trap or release air was correlated with flowability (Traina et al., 2013). Several direct or indirect techniques exist for flowability assessment. Lindberg et al. (2004) showed that five different techniques (Hausner

Ratio, Jenike tester, Powder rheometer, Angle of avalanche, uniaxial tester) yielded similar rank order correlation when used to assess the flowability of four pharmaceutical tablet formulations. However, the type of shear tester may also significantly impact the powder flowability and bulk density (Koynov et al. 2015).

The objectives of this study were:

- To determine the influence of three amorphous silica dusts on permeability and conditioned bulk density of Hard Red Winter wheat; and
- To investigate the influence of three amorphous silica dusts on flow properties of Hard Red Winter wheat

## **Materials & Methods**

### **Hard Red Winter Wheat (HRW)**

The moisture content of Hard Red Winter Wheat (Heartland Mills, Marienthal, KS, USA) determined using a portable moisture tester for grain (Shore Model 930, Shore Sales Co., Rantoul, IL, USA) was about 11.5% (w.b). Wheat was sifted through a 0.21 mm nominal aperture aluminum sieve (Seedburo Equipment Company, Des Plaines, IL, USA) to remove dockage, shrunken, and broken kernels. When necessary and after visual inspection, wheat samples were manually cleaned to remove foreign material and damaged kernels. Wheat samples (250g; 11.5±.2% m.c.) were obtained by emptying bags of HRW in a Boerner Divider (Seedburo Equipment Company, Des Plaines, IL, USA). The Boerner Divider meets USDA-FGIS specifications for official inspections. The principle is that the sample is poured into the divider and repeatedly halved until a sample of desired size is obtained.

### **Inert dusts**

Fresh batches of three commercial inert dusts made up of amorphous silica (Odor-Z-Way®, Celite® 610, and Diafil® 610) were purchased and kept in air-tight containers until analysis. Odor-Z-Way, a deodorizer agent, was supplied by a local manufacturer (Odor-Z-Way®, Phillipsburg, KS, USA). Diafil® 610, a diatomite functional filler, and Celite® 610, a diatomite filter aid, are registered Diatomaceous Earth (DE) products manufactured by Celite Corporation (Lompoc, CA, USA). Odor-Z-Way is not yet approved for grain and structural treatments.

## **Sample preparation**

Inert dust samples were analyzed for moisture content by thermogravimetric analysis (Pyris 1 TGA, Perkin Elmer). A sample of 1 mg was heated under nitrogen atmosphere (nitrogen purge rate of 20 mL/minute; balance purge rate of 30 mL/minute) with temperature set to increase from 100°C to 600°C at the rate of 50 °C/minute. The initial moisture contents determined by TGA were respectively about 35%, 30.5%, and 28.5% (d.b.) for Odor-Z-Way®, Diafil®, and Celite®, respectively (Table 3.1). Each sample was dried down through a maximum of three cycles of a mild heating procedure in an air oven for 45 min at 25°C and allowed to cool in a desiccator. The drying procedure was complete when variation in sample weight between drying cycles was less than 1%. Powder samples were equilibrated at specific relative humidity to ensure the final moisture contents of all three powders were similar (approximately equal to 2% d.b). Moisture content at the end of the drying procedure and equilibration process was re-determined using TGA. For sample size reduction, each gross sample of inert dust was passed through a chute splitter device to generate the actual sample size (250 mg) required for mixing with wheat (250 g) corresponding to 1g/kg treated grain sample. The chute splitter device allows a dynamic sampling of powders, which is preferred to static methods such as scooping or coning and quartering. Hard Red Winter wheat (HRW, 11.5 % m.c.) was mixed with each of three amorphous dusts at the rate of 1g/kg. Laboratory ambient temperature and relative humidity were respectively  $25.8 \pm 0.2^\circ\text{C}$  and  $62.5 \pm 2.1\%$  r.h. Controls consisted of clean, sound, and dust-free HRW. Permeability and dynamic flow properties were measured in triplicates.

## **The FT4 Powder Rheometer**

The FT4 Powder Rheometer is a fully automated rotational shear tester capable of measuring, with a high reproducibility, the bulk, shear, process, and dynamic flow properties of powders and

granular materials. The FT4 powder rheometer features an assortment of vessels, blades, pistons, and shear heads as well as a built-in, user-friendly software which facilitates the process of data collection, graphing and interpretation. A common stage in every analysis is conditioning which involves a gentle slicing action aimed at removing excess air, thus ensuring a uniformly packed powder bed. The working principle of the FT4 Powder rheometer is explained in detail elsewhere in the literature (Freeman, 2007; Hare et al. 2015).

### **Bulk properties**

The standard Permeability program was modified to suit the granular material. Test samples were conditioned (approximately 200 g), split to normalize the packing and provide accurate volume by rotating the upper part of the vessel away from the lower part, and then compressed under increasing normal consolidation stresses (3 to 15kPa), while air at constant velocity (2mm/s) was supplied through a distributor at the base of the granular bed. To allow the samples to fully equilibrate, 120 s normal stress hold time was maintained between steps. The powder remaining in the lower vessel was weighed using the FT4 in-built balance and the Conditioned Bulk Density was automatically calculated. Permeability was determined by plotting the pressure drop across the granular bed against the applied normal stress.

### **Dynamic flow tests**

#### **Stability tests**

Each of the three powders was tested for stability using a 48-mm diameter blade and a 160-mL powder sample contained in a 50 mm bore, borosilicate test vessel. Stability tests aimed at assessing whether the powder is likely to change in terms of flow energy requirement, as a result of being made to flow. The stability test is run at a constant blade tip speed (100 mm/s) and helix

angle (-5° helix downwards) and this test is a combination of 7 conditioning and 7 test cycles.

The following parameters were determined during stability testing:

- 1) Basic Flowability Energy, BFE (mJ): the energy needed to displace a conditioned and stabilized powder at a given flow pattern and flow rate.
- 2) Stability Index, SI: the factor by which the flow energy requirement changes during repeated testing.

$$SI = \frac{\text{Energy test 7}}{\text{Energy test 1}} \quad (3.1)$$

- 3) Specific Energy, SE (mJ/g): The energy needed to displace a conditioned powder using a gentle shearing and lifting mode of displacement. This energy is then divided by the split mass.

$$SE = \frac{(\text{Up Energy Cycle 6} + \text{Up Energy test 7})/2}{\text{Split Mass}} \quad (3.2)$$

### **Variable Flow Rate (VFR)**

The VFR test is a combination of 4 conditioning and 4 test cycles. The 4 test cycles were performed at decreasing flow rates: 100, 70, 40, and 10  $\text{mms}^{-1}$  blade tip speed. The flow rate index for each inert dust was determined and is defined as the factor by which the flow energy requirement is changed when the flow rate is reduced by a factor of 10.

$$FRI = \frac{\text{Energy test 4}}{\text{Energy test 1}} \quad (3.3)$$

### **Aeration tests**

A conditioned test sample (125 grams) in a 260 mL powder sample contained in a 50mm bore, borosilicate test vessel was subjected to increasing air velocities (from 0 to 40  $\text{mm.s}^{-1}$ ) at constant blade tip speed (100 mm/s). Changes in flow energy as a function of air velocity passing through the sample were measured and the following parameters were determined:

- 1) Aeration Ratio,  $AR_n$ : the factor by which the Basic Flowability Energy is reduced by aeration at an air velocity of  $n \text{ mms}^{-1}$ .  $AE_0$  is the aeration energy when the air velocity is  $0 \text{ mm.s}^{-1}$ .

$$AR_n = \frac{AE_0}{AE_n} \quad (3.4)$$

- 2) Aeration Energy,  $AE_n$  (mJ): the flowability energy at  $n \text{ mms}^{-1}$  air velocity.
- 3) Air velocity for fluidization: the air velocity when the flow energy is reduced to near zero.

### **De-aeration tests**

A conditioned test sample (125 grams) in a 260 mL powder sample contained in a 50mm bore, borosilicate test vessel was aerated using the minimum fluidization velocity from aeration tests. The aerated sample was then subjected to a series of measurements of BFE tests as a function of the number de-aeration cycles (conditioning cycles) performed before the BFE test. De-aeration was quantified by assessing the number of de-aeration cycles required to reach steady state (the BFE level) and the percentage recovery to BFE value after X de-aeration cycles.

### **Tapped consolidation**

A conditioned and stabilized test sample was initially tested for basic flowability energy. The test sample was then consolidated by tapping (100, 200, 400, and 800 times) using Autotap (QuantaChrome) and tested for BFE. The following parameters were determined:

- Tapped Consolidated Energy,  $CE_{\text{tapped, n}}$  (mJ): the flow energy measured after the powder has been tapped n times.
- Tapped Consolidation index ( $CI_{\text{tapped, n}}$ ): the factor by which the BFE is increased when the powder sample has been consolidated by tapping n times.

$$CI_{tapped,n} = \frac{CE_{tapped,n}}{BFE} \quad (3.5)$$

### **Direct pressure consolidation**

A conditioned test sample was consolidated by applying increasing direct pressures (3-15 kPa) and tested for BFE. The following parameters were determined:

- The Direct Pressure Consolidated Energy,  $CE_{DP, nkPa}$  (mJ): the flow energy measured after the powder has been consolidated by the application of a direct pressure of n kPa.
- Direct Pressure Consolidation Index ( $CI_{DP, nkPa}$ ) which is the factor by which the BFE is increased when the powder sample has been consolidated by applying a direct pressure of n kPa.

$$CI_{DP, nkPa} = \frac{CE_{DP, nkPa}}{BFE} \quad (3.6)$$

### **Statistical analyses**

Data was collected using the FT4 Data Analysis software v4.00.0009 (Freeman Technology Ltd., Tewkesbury, UK). The study was a completely randomized experimental design (CRD) subjected to one-way ANOVA using SAS PROC GLM procedure (SAS, 2009). Treatments means were separated by Scheffe multiple comparisons procedure ( $\alpha=.05$ ).

## Results & Discussion

### BULK PROPERTIES

#### Permeability

Fig 3.1 shows the pressure drop across the powder bed versus normal consolidation stress for untreated wheat and wheat treated with three amorphous dusts. A minimal pressure drop (high permeability) across the powder bed was observed for untreated wheat while moderate permeability was observed for wheat treated with each of the three amorphous dusts: Celite, Diafil and Odor-Z-Way. Compression had little or no effect on the permeability of untreated wheat, which is typical of non-cohesive, large particle size or granular material. However, pressure drop increased with increased compression in all samples of wheat treated with the amorphous dusts, suggesting a reduction in the size and number of available channels for air to pass. Moderate permeability is typical of granular material with some cohesion and a wide particle size distribution.

#### Conditioned bulk density (CBD)

As expected, the conditioned bulk density (CBD) of wheat was significantly lower when wheat was mixed with 1g/kg Celite, Diafil, or Odor-Z-Way (Table 3.1). The fine dust particles occupy the voids and small interstices between coarse grains kernels, causing a reduction in the weight of kernels needed to fill the same volume. The bulk density was similar between Wheat+Celite ( $688.03 \text{ kg/m}^3$ ) and Wheat+Diafil ( $697.09 \text{ kg/m}^3$ ), but significantly different to Wheat+Odor-Z-way ( $718.11 \text{ kg/m}^3$ ). Similar drops in bulk density of a variety of grains across Dryacide rates of 0.01-0.5 grams per kilogram was 8.9% for maize, 7.7% for hard wheat, 7.5% for feed wheat, 7.2% for barley, 6.6% for rye corn, 5.9% for chick pea, 5.4% for field pea, 3.9% for oats, 3.7% for sorghum, 3.3% for canola, and 2% for sunflower (Jackson & Webley, 1994). The same

authors noticed the same trend with inert dusts such as silica aerogel (Cabosil), diatomite, and rice husk ash (Amosil). Similar significant decrease in bulk density of grain treated with amorphous dusts such as Diafil and Celite was also reported by Korunic et al. (1996, 1998). Particle sizes and shapes of Celite and Diafil along with a better adhesion on wheat kernels could explain the higher decrease in bulk density of wheat kernels. Among the three dusts, Odor-Z-Way caused the minimum decrease in bulk density which could be explained by a lower adhesion on wheat kernels. The extent of decrease in bulk density of wheat following the addition of a given dust may serve as an indicator of flowability as shown by Abdullah & Geldart (1999).

## **DYNAMIC FLOW PROPERTIES**

### **Stability Index (SI)**

The stability test of untreated wheat and wheat admixed with three amorphous dusts at 1g/kg is shown in Fig 3.2. The stability indexes for wheat and each wheat mixture are presented in Table 3.1. The criterion for classifying wheat stability was as follows:  $SI=1$ , stable material,  $SI<1$  or  $SI>1$ , unstable material. According to this classification, untreated wheat ( $SI=.98$ ) was a robust material, not being affected by being made to flow. The one-way analysis of variance showed a significant difference in SI ( $F=95.61$ ;  $P<.0001$ ). Admixing wheat with Odor-Z-way caused the SI to increase to 1.24. The  $p$ -values for the pair-wise ANOVA t-tests showed that the SI for Wheat+Odor-Z-Way ( $SI=1.24$ ;  $P<.0001$ ) was higher than the SI for untreated wheat. The SI of Wheat+Celite ( $SI= 0.85$ ;  $P=0.0052$ ) was statistically lower than the SI of untreated wheat. The SI of and Wheat+Diafil ( $SI= 0.94$ ;  $P=0.5504$ ) was not statistically different from the SI of untreated wheat. Treating wheat with each of the three dusts caused wheat to become unstable. The deviation from stability observed in wheat treated with Celite ( $SI<1$ ) could be attributed to

coating of the blade and vessel, causing a reduction in flow energy due to a reduction in friction. On the other hand, the deviation from stability observed in wheat treated with Odor-Z-Way (SI>1) was more likely caused by segregation (coarser kernels remaining on top and dust particles sinking to the bottom of the test vessel), and moisture uptake by the hygroscopic dust particles. Powders that are hygroscopic may take on moisture during the test, resulting in swelling of particles in size and in an increase in the surface frictional forces due to moisture adhering to the surface of the particles. Wheat mixed with amorphous silica dust is a granular system with a very wide particle size distribution. During the stability test, amorphous dust particles fill the voids between the large kernels, causing the granular system to segregate as a function of particle size. A visual inspection of test vessels showed a less pronounced segregation when wheat was mixed with Celite and Diafil, more likely due to their smaller particle sizes or better adhesion to wheat kernels, which were not determined.

### **Flow rate index (FRI)**

Table 3.1 shows the flow rate index (FRI) of untreated wheat and wheat treated with each of three amorphous dusts. Because there was some uncertainty about the stability of the granular system, the stability program and the variable flow rate program were run simultaneously to measure both stability and flow rate sensitivity. There was a significant difference between the flow rate index measured for untreated wheat and wheat treated with amorphous dusts ( $F=85.18$ ;  $P<0.0001$ ). The criterion for classifying wheat flow rate sensitivity was as follows: FRI=1, flow rate insensitive, FRI<1.0, pseudoplastic flow rate,  $1.5<FRI<3.0$  moderate flow rate sensitivity, and FRI>3.0, high flow rate sensitivity. Generally, treating wheat with amorphous dusts caused the FRI to decrease (Fig 3.3). The flow rate index of wheat+Odor-Z-Way was 0.97, which is typical of powders with large particle size and insensitive to flow rate. Only wheat+Celite

(FRI=0.85) and wheat+Diafil (FRI=0.87) showed pseudoplastic flow rates (FRI<1.0), usually seen in powders with flow enhancers. The flowability of wheat was apparently enhanced by the addition of 1g/Kg of Celite or Diafil. Mixing wheat with all three amorphous dusts somewhat improved the flowability within the range of dust rate tested. The low adhesion of Odor-Z-Way on wheat kernels as determined by visual evaluation caused most of the dust to sink to the bottom of the test vessel, resulting in a much lower kernel to kernel surface friction and a higher blade-dust friction expressed by a relatively higher energy requirements to initiate flow.

### **Specific energy (SE)**

The specific energy of wheat significantly decreased as a result of being admixed with amorphous silica dusts ( $F=129.85$ ;  $P<.0001$ ). The criterion for classifying wheat specific energy was as follows:  $SE<5$ , low cohesion,  $5<SE<10$ , moderate cohesion, and  $SE>10$ , high cohesion. The specific energy measured ranged between 1.94 and 2.33 mJ/mg (Table 3.1), indicating that even after treating wheat with amorphous dusts, the cohesion remained low. The observations about the specific energy are consistent with the flow rate index and confirm that the three amorphous dusts somewhat improved the flow performance of wheat by acting as lubricants.

### **Aeration**

The ability of powder to become aerated depends heavily on the cohesive forces acting between particles. The Aeration Ratio (AR) measured during the aeration program was respectively 2.19, 2.45, 3.66, and 3.15 for wheat, wheat+Odor-Z-way, wheat+Celite, and wheat+Diafil (Table 3.3). The criterion to evaluate the sensitivity of wheat samples to aeration was as follows:  $AR=1$  for cohesive,  $2<AR<20$  for powders with moderate sensitivity, and  $AR>20$  for high sensitivity. Untreated wheat and wheat treated with each of the three amorphous dusts exhibited moderate sensitivity to aeration, which means they did not behave as cohesive materials, nor did they

become easily fluidized. In fact, even at maximum air velocity ( $40 \text{ mm}\cdot\text{s}^{-1}$ ), fluidization was never achieved, since the flow energy never stabilized in relation to air velocity (Data not shown).

### **De-aeration tests**

Table 3.4 shows the flow energy and the percent recovery to the basic flowability energy after several de-aeration cycles. Approximately 98% recovery to the BFE was observed in untreated wheat, after 5 de-aeration cycles, while 68-80% recovery was observed in wheat treated with the amorphous dusts. Despite having similar permeability, the dusts caused wheat to exhibit different de-aeration patterns. BFE generally increased with increased number of de-aeration cycles (Fig. 3.4). Differences in de-aeration patterns can be attributed to the level of adherence of dust on wheat kernels, to the porosity of the dust particles, and to the particle size and shape of the different dusts, which were not determined.

### **Tapped and direct pressure consolidations**

The tapped consolidated energy increased with increased number of taps (Fig 3.5). The actual tapped consolidation indexes are presented in Table 3.4. The bulk density also increased with increased number of taps (Fig 3.6). The tapped consolidated energy increased by 14.0-25.6% for a corresponding 2-5% increase in bulk density. After 400 taps, the bulk density of untreated wheat increased by 2%, the bulk density of Wheat+Odor-Z-Way increased by 4%, and the bulk density of both Wheat+Celite and Wheat+Diafil increased by about 5%. Similarly, the direct pressure consolidated energy increased with increased direct pressure (Fig. 3.7), and so did the bulk density measured after direct pressure (Fig 3.8). Direct pressure consolidation indexes are presented in Table 3.5. The direct pressure consolidated energy increased by 21-47% for a corresponding 9-14% increase in bulk density. Changes in flow energy and bulk density were

higher after direct pressure (3-15Kpa) than after tapping (0-400 taps). The changes in flow energy measured after tapping and direct pressure simulate the change in flow energy that would occur after vibration or mechanical oscillation (like during transportation, process, and storage) or during storage in hopper under different normal stress. The magnitude of increase in bulk density was dissimilar to the magnitude of change in flowability.

## Conclusions

Wheat treated with Odor-Z-Way was comparable with wheat treated with Celite or Diafil as they all exhibited low cohesion, moderate permeability, and moderate sensitivity to aeration. Wheat treated with each of the three dusts became almost unstable due to segregation, moisture uptake, lower adhesion, and coating of the blade and test vessel. Flowability of wheat was generally enhanced by admixing wheat with the amorphous dusts. A decrease in bulk density was however observed, although the decrease was smaller when wheat was admixed with Odor-Z-Way. In view of the bulk and dynamic flow properties, Odor-Z-Way has potential to become a grain protectant provided that segregation and the decrease in bulk density are mitigated and that the insecticidal activity is not adversely affected by the seemingly low adhesion on wheat kernels.

## References

- Abdullah, E. C., & Geldart, D. (1999). The use of bulk density measurements as flowability indicators. *Powder Technology*, 102(2), 151-165.
- Carr, R. L. (1965a). Classifying flow properties of solids. *Chem.Eng.*, 1, 69-72.
- Carr, R. L. (1965b). Evaluating flow properties of solids. *Chem.Eng.*, 18, 163-168.
- Cooke, J., & Freeman, R. (2006). The flowability of powders and the effect of flow additives. In *World Congress on Particle Technology* (Vol. 5).
- Council, U. G. (1986). *Grain Quality and US Standards, Importer Manual. Chapter 4.*
- Desmarchelier, J. M., & Dines, J. C. (1987). Dryacide treatment of stored wheat: Its efficacy against insects, and after processing. *Australian Journal of Experimental Agriculture*, 27(2), 309-312.
- FAO (2013). *FAOSTAT Database. Food and Agriculture Organization of the United Nations, Rome, Italy.*
- FGIS. (2013). Book II, chapter 13. federal grain inspection service. *US Department of Agriculture.*
- Freeman, R. (2007). Measuring the flow properties of consolidated, conditioned and aerated powders—a comparative study using a powder rheometer and a rotational shear cell. *Powder Technology*, 174(1-2), 25-33.
- Ganesan, V., Muthukumarappan, K., & Rosentrater, K. A. (2008). Flow properties of DDGS with varying soluble and moisture contents using Jenike shear testing. *Powder Technology*, 187(2), 130-137.
- Geldart, D., Abdullah, E. C., Hassanpour, A., Nwoke, L. C., & Wouters, I. (2006). Characterization of powder flowability using measurement of angle of repose. *China Particuology*, 4(03n04), 104-107.

- Hare, C., Zafar, U., Ghadiri, M., Freeman, T., Clayton, J., & Murtagh, M. J. (2015). Analysis of the dynamics of the FT4 powder rheometer. *Powder Technology*, 285, 123-127.
- Jackson, K., & Webley, D. (1994, April). Effects of Dryacide on the physical properties of grains, pulses and oilseeds. In *Proceedings of the 6th International Working Conference on Stored-Product Protection*. CAB, Wallingsford, Canberra, Australia (pp. 635-637).
- Jenike, A. W. (1961). Gravity flow of bulk solids. *Bull. Utah Engng Exp. Station*, 108
- Jenike, A. W. (1975). A measure of flowability for powders and other bulk solids. *Powder Technology*, 11(1), 89-90.
- Khan, K. (2016). *Wheat: Chemistry and technology* Elsevier.
- Korunic, Z., Fields, P. G., Kovacs, M., Noll, J. S., Lukow, O. M., Demianyk, C. J., & Shibley, K. J. (1996). The effect of diatomaceous earth on grain quality. *Postharvest Biology and Technology*, 9(3), 373-387.
- Korunic, Z., Cenkowski, S., & Fields, P. (1998). Grain bulk density as affected by diatomaceous earth and application method. *Postharvest Biology and Technology*, 13(1), 81-89.
- Koynov, S., Glasser, B., & Muzzio, F. (2015). Comparison of three rotational shear cell testers: Powder flowability and bulk density. *Powder Technology*, 283, 103-112.
- Le Patourel, G. N. J. (1986). The effect of grain moisture content on the toxicity of a sorptive silica dust to four species of grain beetle. *Journal of Stored Products Research*, 22(2), 63-69.
- Lindberg, N., Pålsson, M., Pihl, A., Freeman, R., Freeman, T., Zetzener, H., & Enstad, G. (2004). Flowability measurements of pharmaceutical powder mixtures with poor flow using five different techniques. *Drug Development and Industrial Pharmacy*, 30(7), 785-791.
- Mellmann, J., Hoffmann, T., & Fürll, C. (2014). Mass flow during unloading of agricultural bulk materials from silos depending on particle form, flow properties and geometry of the discharge opening. *Powder Technology*, 253, 46-52.

- Subramanyam, B., Swanson, C. L., Madamanchi, N., & Norwood, S. (1994). Effectiveness of Insecto, a new diatomaceous earth formulation in suppressing several stored grain insect species. In *Proceedings of the 6th International Working Conference on Stored Product Protection* (Vol. 2, pp. 650-659).
- Traina, K., Cloots, R., Bontempi, S., Lumay, G., Vandewalle, N., & Boschini, F. (2013). Flow abilities of powders and granular materials evidenced from dynamical tap density measurement. *Powder Technology*, 235, 842-852.
- Vasilenko, A., Koynov, S., Glasser, B. J., & Muzzio, F. J. (2013). Role of consolidation state in the measurement of bulk density and cohesion. *Powder technology*, 239, 366-373.
- Warheit, D. B. (2001). Inhaled amorphous silica particulates: what do we know about their toxicological profiles?. *Journal of environmental pathology, toxicology and oncology*, 20 (Suppl.1).

**Table 3.1** Conditioned bulk density, Specific Energy, Stability Index, and Flow Rate Index of untreated wheat and wheat treated with three amorphous inert dusts at 1g/kg.

	CBD (kg/m <sup>3</sup> )	SE (mJ/mg)	SI	FRI
Wheat	776 <sup>a</sup>	2.33 <sup>a</sup>	0.98 <sup>b</sup>	1.02 <sup>a</sup>
Wheat + Odor-Z-Way	718 <sup>b</sup>	1.94 <sup>c</sup>	1.24 <sup>a</sup>	0.99 <sup>cd</sup>
Wheat + Celite®	688 <sup>c</sup>	2.15 <sup>b</sup>	0.85 <sup>c</sup>	0.95 <sup>bc</sup>
Wheat + Diafil®	697 <sup>c</sup>	1.97 <sup>c</sup>	0.94 <sup>b</sup>	0.87 <sup>d</sup>

Each mean is based on  $n=3$  replications.

*Means followed by different letters within the same column indicate significant differences according to Scheffe test ( $P<.05$ ).*

**Table 3.2** Aerated energy and aeration ratio of wheat treated with three amorphous inert dusts at 1g/kg.

	Wheat	Wheat + Odor-Z-Way	Wheat + Celite®	Wheat + Diafil®
AE <sub>0</sub> (mJ)	2,850	2,800	2,550	2,820
AE <sub>40</sub> (mJ)	1,300	1,550	1,125	1,043
AR <sub>40</sub>	2.19 <sup>d</sup>	2.45 <sup>c</sup>	3.66 <sup>a</sup>	3.15 <sup>b</sup>

*\*BFE was obtained using 50mm\*260ml vessels*

Each mean is based on  $n=3$  replications.

Means followed by different letters on the same row indicate significant differences according to Scheffe test ( $P<.05$ ).

**Table 3.3** Basic flowability energy and percent recovery versus number of de-aeration cycles

De-aeration cycles	Wheat	Wheat +Odor-Z-Way	Wheat+Celite®	Wheat+Diafil®
1	1,680 (59)	1,455 (52)	1,315 (52)	1,231 (44)
2	1,945 (68)	1,556 (56)	1,555 (61)	1,474 (52)
3	2,045 (72)	1,689 (60)	1,745 (68)	1,787 (63)
4	2,125 (75)	1,909 (68)	1,978 (78)	1,899 (67)
5	2,795 (98)	2,103 (75)	2,045 (80)	1,918 (68)
<b>BFE*</b>	<b>2,850</b>	<b>2,800</b>	<b>2,550</b>	<b>2,820</b>

*\*BFE was obtained using 50mm\*260ml vessels*

*The standard program was modified to suit the granular material. Maximum air velocity was set at 40 mm/s and 5 de-aeration cycles were completed.*

*Data in parentheses represent percent recovery (%) to the BFE.*

**Table 3.4** Tapped consolidated energy and tapped consolidation index as a function of number of taps

Number of Taps	Wheat	Wheat +Odor-Z-Way®	Wheat+Celite®	Wheat+Diafil®
0 (BFE)	765	733	806	773
50	807 (1.05)	765 (1.04)	858 (1.06)	805 (1.04)
100	841 (1.10)	798 (1.09)	897 (1.11)	889 (1.15)
200	859 (1.12)	856 (1.17)	932 (1.16)	922 (1.19)
400	872 (1.14)	908 (1.24)	956 (1.19)	971 (1.25)
<i>% Increase in BFE( 400 taps)</i>	14.0	23.9	18.6	25.6

*\*BFE and bulk density were obtained using 50\*85 vessels  
Data in parentheses represent the tapped consolidation index*

**Table 3.5** Direct pressure consolidated energy and direct pressure consolidation index as a function of direct pressure

Consolidation pressure (kPa)	Wheat	Wheat +Odor-Z-Way	Wheat+Celite®	Wheat+Diafil®
0	765	733	806	773
3	804 (1.05)	814 (1.11)	887 (1.10)	889 (1.15)
6	832 (1.09)	872 (1.19)	975 (1.21)	920 (1.19)
9	845 (1.10)	931 (1.27)	1,016 (1.26)	951 (1.23)
12	896 (1.17)	953 (1.30)	1,056 (1.31)	982 (1.27)
15	925 (1.21)	995 (1.36)	1,185 (1,47)	1,074 (1.39)
<i>% Increase in BFE (15 Kpa)</i>	20.91	35.7	47.02	38.94

*\*BFE and bulk density were obtained using 50×85 vessels  
Data in parentheses represent the direct pressure consolidation index*

**Figure 3-1** Pressure drop across powder bed versus normal consolidation stress

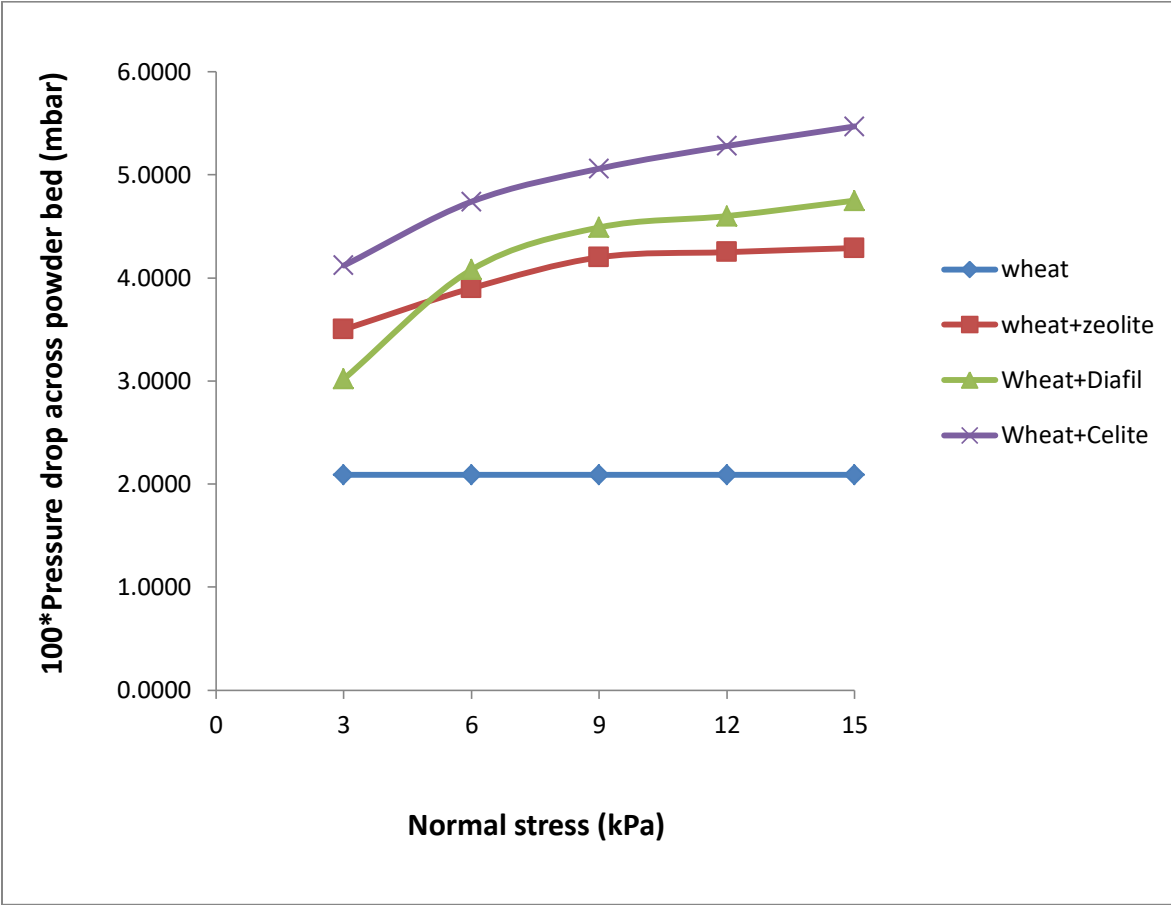
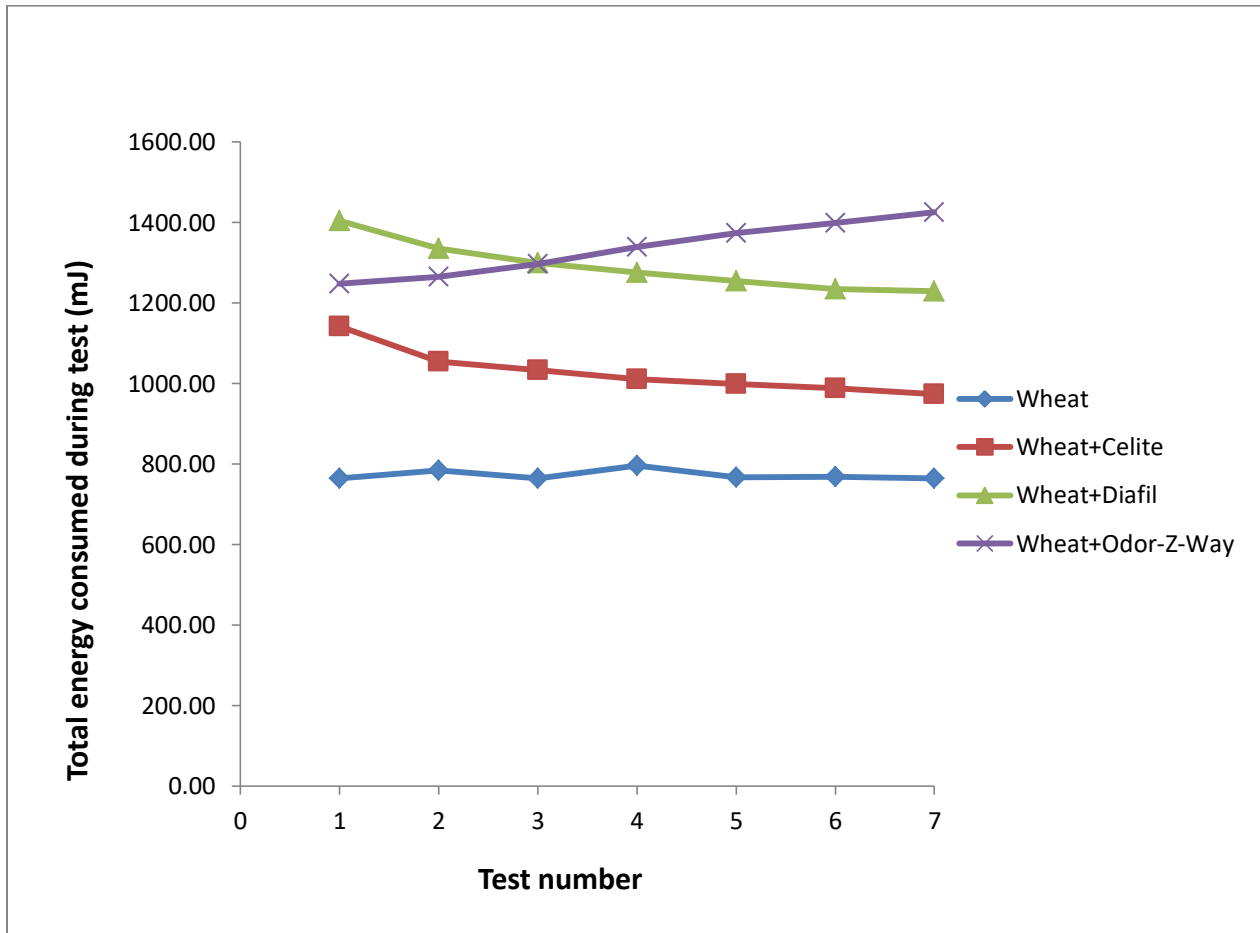


**Figure 3-2** Stability of untreated wheat and wheat treated with three amorphous silica dusts



*Stability tests were conducted using 50mm x 160 ml Split vessels*

**Figure 3-3** Variable flow rate of untreated wheat and wheat treated with three amorphous silica dusts

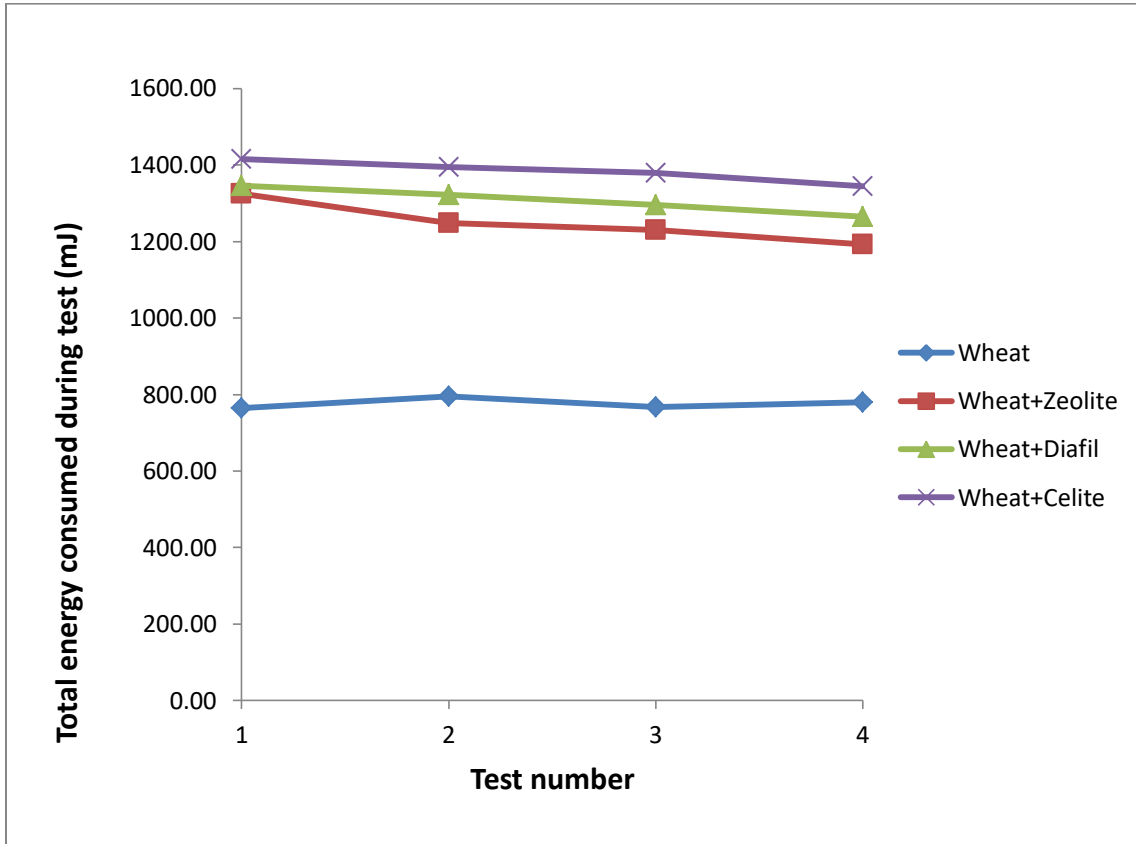


**Figure 3-4** Basic flowability energy versus number of de-aeration cycles

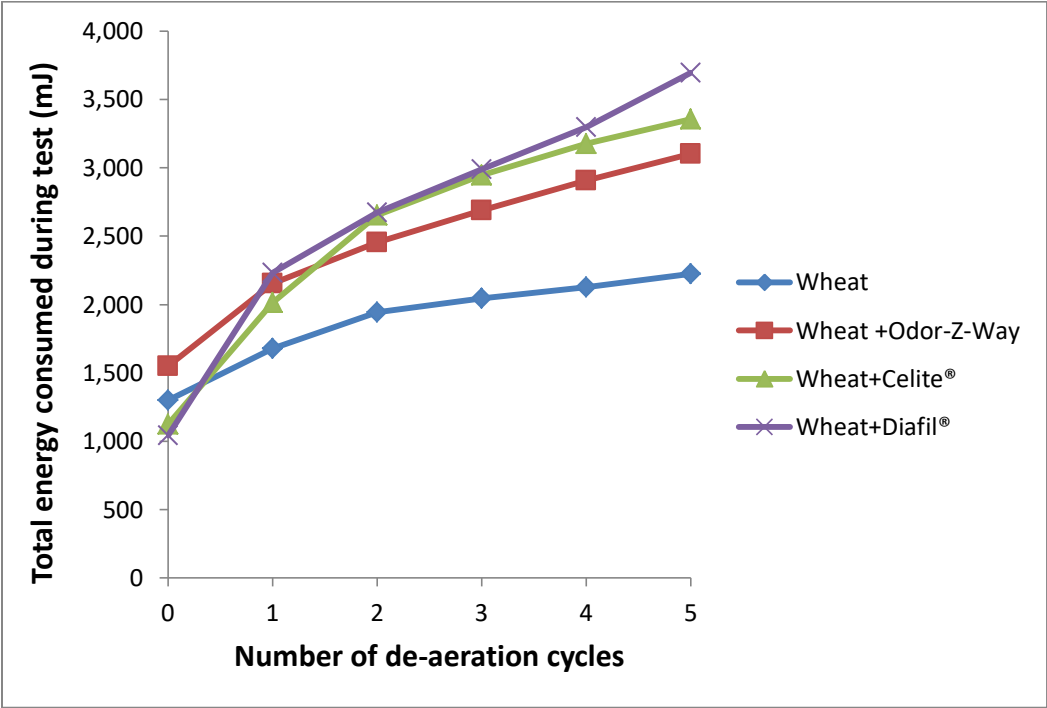


**Figure 3-5** Flow Energy as a function of number of taps

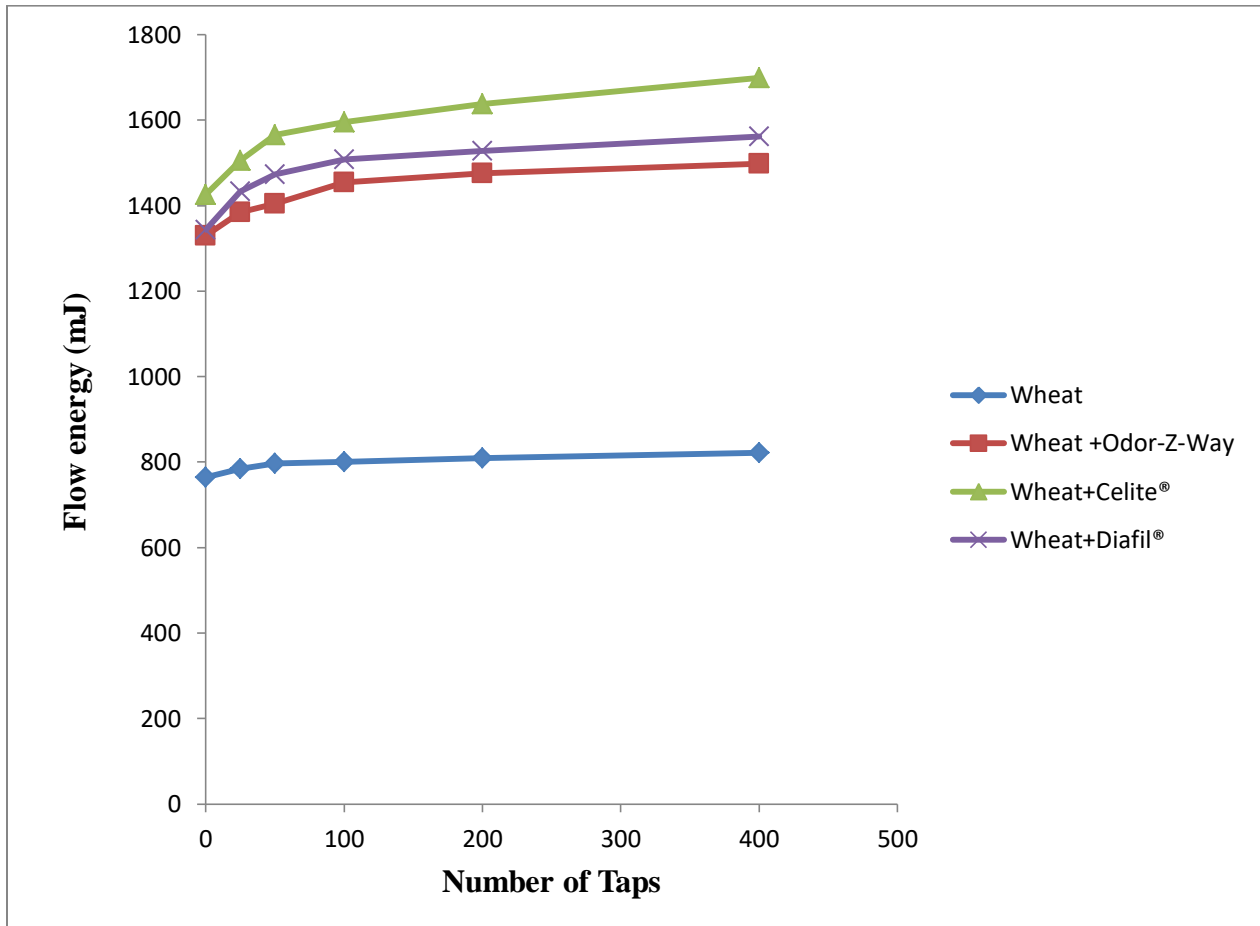


**Figure 3-6** Bulk density as a function of number of taps

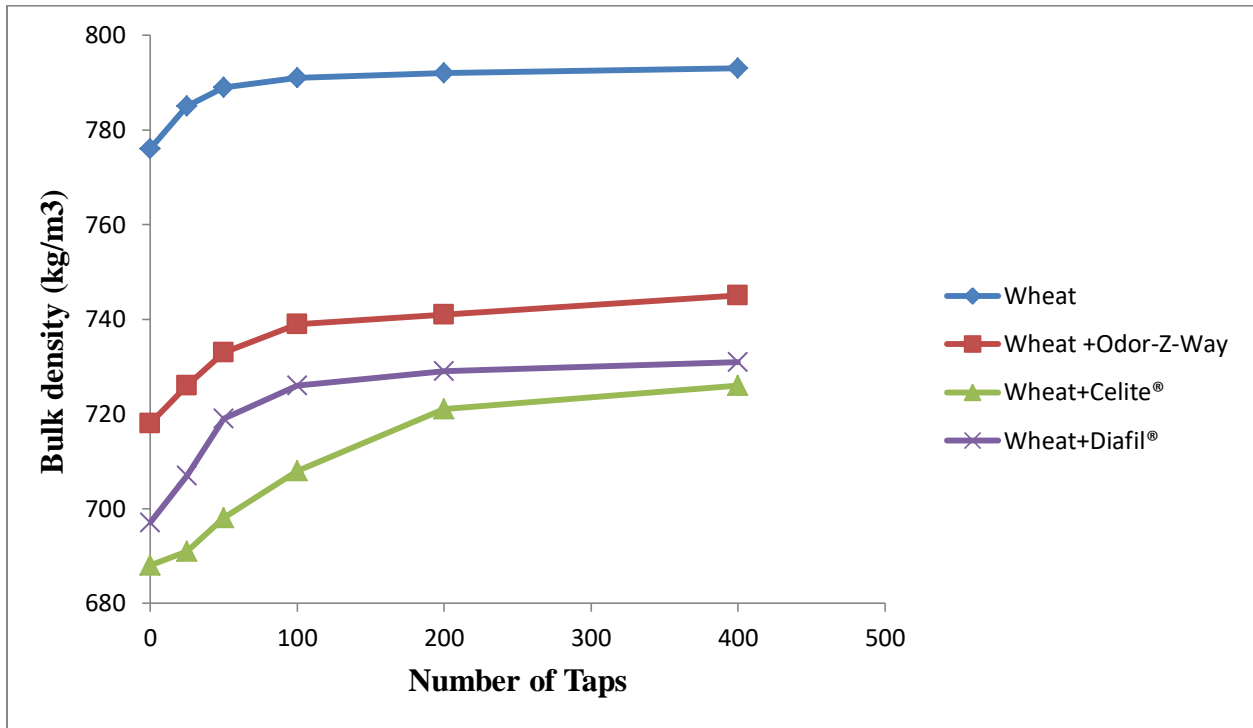


**Figure 3-7** Flow energy as a function of direct pressure

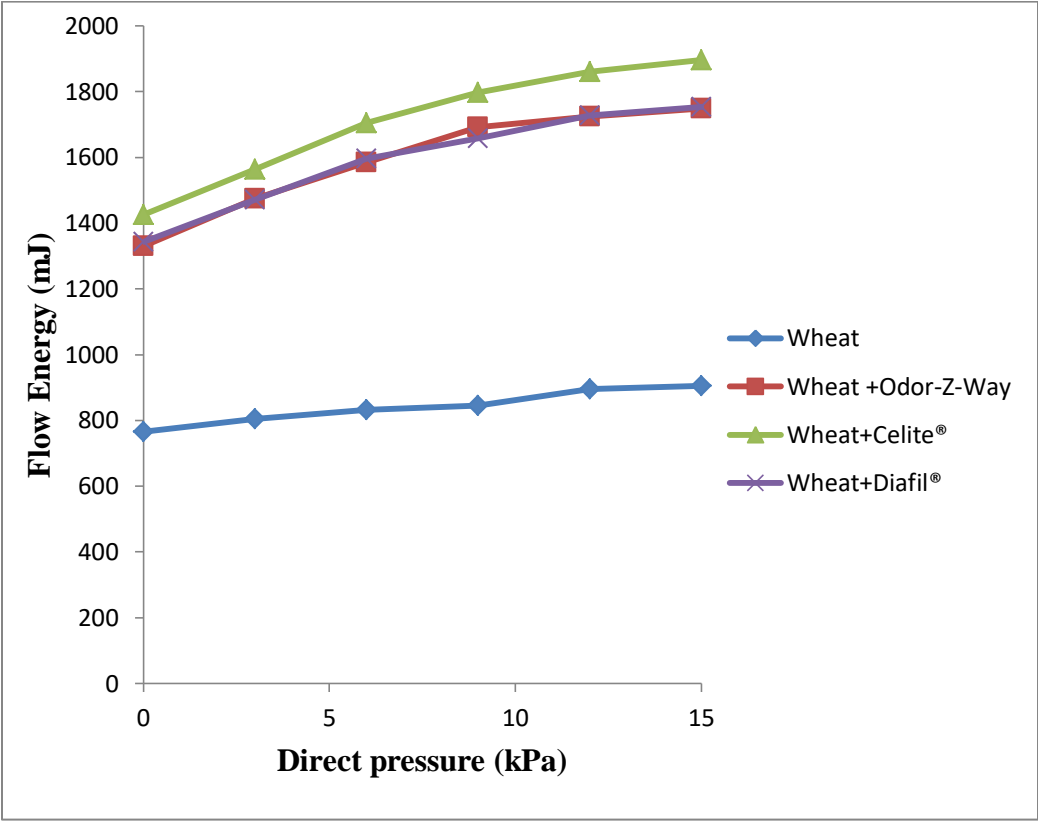
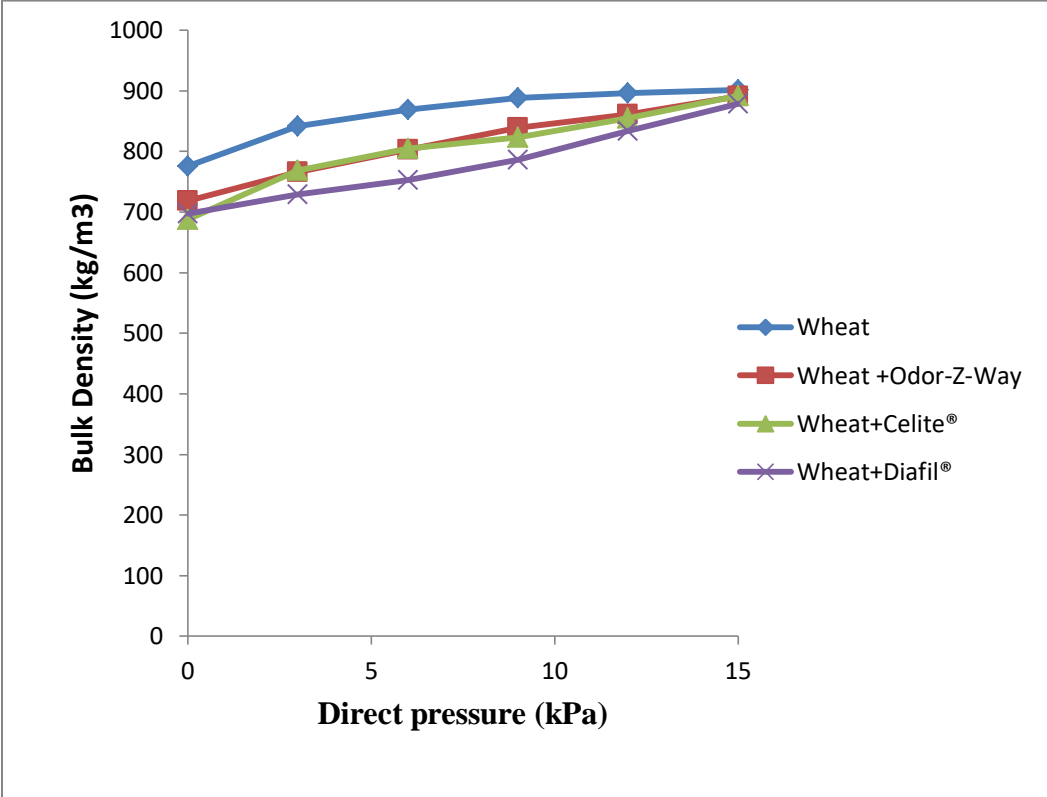


**Figure 3-8** Bulk density as a function of direct pressure



# **Chapter 4 - Efficacy of three amorphous inert dusts applied to wheat and concrete surfaces against eggs and adults of seven stored-grain insect species**

## **Abstract**

Alternatives to chemical insecticides used in grain protection are needed to mitigate adverse effects on the environment and to minimize effects on worker health and safety. Three amorphous silica dusts (Odor-Z-Way®, Celite®, and Diafil®) were tested for their ability to control eggs and adult stages of seven major species of stored-grain insect on wheat and on concrete surfaces. Insect species tested included unsexed adults (50) of the lesser grain borer, *Rhyzopertha dominica* (F.); rice weevil, *Sitophilus oryzae* (L.); maize weevil, *Sitophilus zeamais* (Motschuslky); red flour beetle, *Tribolium castaneum* (Herbst); sawtoothed grain beetle, *Oryzaephilus surinamensis* (L.); granary weevil, *Sitophilus granarius* (L.), and the Indianmeal moth, *Plodia interpunctella* (Hubner).

Adult mortality was assessed 7 and 14 days post-infestation of wheat treated at 0.2-2.0 g/kg and progeny production was determined 42 days post-infestation. Egg-to-Adult emergence on wheat was assessed at 21 and 42 days using wheat treated at 0.2 and 0.5 g/kg for *Rhyzopertha dominica*, *Tribolium castaneum*, and *Oryzaephilus surinamensis*, and at 1.0 and 2.0 g/kg for *Plodia interpunctella*. On concrete, arenas in 9-cm diameter Petri dishes were sprinkled with the synthetic zeolite to provide deposits of 1, 2 and 5 g/m<sup>2</sup>. Mortality on concrete was assessed 24 and 48 hours post-treatment followed by 48 hours recovery on clean wheat.

Adults of *Rhyzopertha dominica* were generally least susceptible to all three amorphous silica dusts, although a complete suppression of progeny production was possible using Celite. Adult

emergence was generally not prevented by Celite, Diafil, and Odor-Z-Way which suggested a lower insecticidal efficacy of the three dusts against early developmental stages. On concrete, Odor-Z-way was particularly effective at controlling all stored-product insect species after 24 h of exposure. This study suggests that Odor-Z-Way possesses insecticidal activity and could be effectively used to prevent insect pests from flourishing on wheat and concrete floors of empty bins.

**Keywords:** Amorphous dusts; Concrete surface; Wheat; Stored-grain insects; Pest management.

## **Introduction**

Prior to being sold or processed, grain is held on farm or off-farm inside grain storage structures. Favorable environmental conditions such as excess moisture and high temperature speed up the development of stored-product insects. Farmers and grain managers routinely monitor grain for visible signs or indirect signs of insect infestation. Insects are known to be the predominant cause of food and feed supplies deterioration and grain infestation remains a major concern despite the widespread use of chemical insecticides. Pest management strategies usually implemented to prevent grain infestation from several species of stored-grain insects encompass the use of sanitation of empty storage facilities and grain, contact insecticides (protectants), fumigation, and aeration (White and Leesch, 1996). The application of protectants on grain kernels is a preventive tactic used to treat uninfested grain as it is being loaded into bins. Grain protectants guarantee a residual protection of grain; however, they are not effective against all life stages of insects, especially larvae that are developing internally. It is therefore important to kill adults of stored-grain insects before they have had a chance to mate and lay eggs on (internal insects) or within the grain kernels (external insects) (Hagstrum and Subramanyam, 2006). Recently, consumers' growing aversion for chemical residues in food as well as the development of resistance in stored-grain insects has led to exploring alternatives to conventional insecticides (Donahaye 2000, Collins 2006). Fumigation, a rather responsive technique, uses highly-toxic gases (fumigants) that penetrate the entire grain mass to kill all life stages of insects. If properly performed, fumigation successfully manages infestation but lacks residual effectiveness and fumigated grain may become re-infested after the dissipation of the fumigant.

Research to make available innovative, efficacious, cost-effective, and reduced-risk insecticides is needed. Inert dusts are one of the most promising alternatives to traditional contact

insecticides. Inert dusts are dry, chemically unreactive powders of different origins and have various industrial and agricultural uses (Ebeling, 1971). Inert dusts used in stored-product protection can be categorized into four groups (Banks & Fields, 1995). Subramanyam and Roesli (2000) have provided an exhaustive list of inert dusts used for stored-product protection. Briefly, the first group consists of clays, sand, paddy husk ash, wood ash, and volcanic ash. The second group consists of minerals such as dolomite, magnesite, copper oxychloride, katelsous (rock phosphate and ground sulfur), lime (calcium hydroxide), limestone (calcium carbonate), and common salt (sodium chloride). These materials are effective on stored-product insects but at rates (>10 g/kg of grain) too high to be reasonably advocated (Golob, 1997; Golob and Webley, 1980). The third group consists of dusts that contain synthetic silica (silicon dioxide). These materials are light and hygroscopic, and are produced by drying an aqueous solution of sodium silicate (Quarles, 1992). Compounds such as tricalcium tri-silicophosphates (Singh et al., 1984) and silica aerogels (Quarles, 1992) are examples of synthetic silicas. The fourth group consists of dusts that contain natural silica, such as diatomaceous earth (DE), which are made up of fossilized skeletons of diatoms (Calvert, 1930).

Amorphous silica dusts are characterized by their unique ability to reversibly lose or gain water and adsorb molecules of appropriate cross-sectional diameter and exchange their inorganic cations without any major change of their structure (Dakovic et al., 2007). Inert dusts kill insects primarily by desiccation because of the abrasion of insect cuticle. It is believed that once insects come in contact with the inert dust particles, the inherent adsorption properties induce the dehydration of insect pests, keeping them from flourishing in stored-products. The main advantage of inert dusts is their low mammalian toxicity. Besides, inert dusts are effective for long durations and they do not affect end use quality of grain (Fields et al., 2003). Moreover,

treating storage structures and handling machinery with inert dusts is more cost-effective compared with chemical treatments and provides effective, long-term protection (Desmarchelier et al., 1993). Their main limitations are that they create a dusty environment, do not work well at high relative humidity (>60%), and they presumably adversely affect the physical properties of grain such as angle of repose and flowability (Korunic, 1997b).

Literature on zeolites for use in stored-product insect control is scarce compared to that of earthed dusts. There are a limited number of studies that examined the effectiveness of natural zeolites applied to stored grain against stored-product insect pests. Haryadi et al. (1994) showed that a natural zeolite found in Indonesia, applied to maize at the rate of 5% by weight (50 g of zeolite/kg of grain) effectively controlled the maize weevil, *Sitophilus zeamais* (Motschulsky) during three months of storage. This is a very high rate and could result in adverse effects on grain physical properties. Kljajić et al. (2010) reported that natural zeolites originating from Serbia resulted in 97 to 100% mortality of the rice weevil, *Sitophilus oryzae* (L.), and 94 to 100% mortality of the red flour beetle, *Tribolium castaneum* (Herbst), after 21 d of exposure to wheat treated with 0.25, 0.50 and 0.75 g/kg followed by a 7 d recovery period on untreated wheat. Progeny suppression of *S. oryzae* and *T. castaneum* was more than 80% after 21 d of exposure of parental adults to wheat treated with zeolite at 0.75 g/kg. Andrić et al. (2012) also reported 100% mortality of *S. oryzae* and *T. castaneum* after 21 d of exposure to wheat treated with a natural zeolite at 1 g/kg followed by a 7 d of recovery period on untreated wheat. Progeny reduction in the two species ranged from 82 to 97%. A natural zeolite modified by treatment with ammonium (NH<sub>4</sub><sup>+</sup>) ions, applied at the same rate, showed much lower insecticidal potential with 36 to 56% mortality and 62 to 71% progeny reduction in the two species. Earlier studies with natural

zeolites did not evaluate the effectiveness of zeolites applied to concrete surfaces, such as those found in empty grain storage facilities, against stored-product insects.

The objectives of this study were:

- To evaluate the insecticidal activity of three amorphous dusts (a synthetic zeolite and two registered DE dusts, Celite and Diafil) against eggs and adults of seven species of stored-grain insects on wheat and on concrete Petri dishes used to simulate floors of empty bins;
- To compare the insecticidal efficacy of the synthetic amorphous zeolite to two existing and registered DE products, Celite and Diafil; and
- To determine the influence of the rate, and the duration of exposure on insecticidal activity against adults on concrete.

## Materials & Methods

### Organic Wheat

Hard red winter wheat was procured from Heartland Mills (Marienthal, KS, USA). All bags of wheat were frozen at -13°C for at least 48 hours to kill any live insects present. All wheat samples had 11-12 % moisture content. Grain moisture was determined using Moisture Analyzer Model 930 (Shore Sales Co., Rantoul, IL). When wheat moisture was not within that range, an adjustment was performed by subjecting the sample to tempering when grains were too dry, or by keeping it inside a growth chamber (65% r.h., 28 °C) for equilibration, when grains were too humid. The formula used for tempering was as follows:

$$\text{water to be added} = \frac{100 - \text{present \%moisture}}{100 - \text{desired \%moisture}} \times \text{Weight of grain (grams)} \quad (4.1)$$

### Concrete-poured Petri dishes

Ready-mix concrete (Rockite, Hartline Products Co., Inc., Cleveland, OH, USA) slurries were obtained by mixing 3,810 g of concrete with 1,905 ml of tap water. About 100 concrete dishes were made by pouring that mixture into 9-cm diameter, 1.5 cm high and 62 cm<sup>2</sup> area plastic Petri dishes (Fisher Scientific, Denver, CO, USA). Slurry was allowed to dry and the inside walls of the Petri dishes were coated with polytetrafluoroethylene (Insecta-A-Slip, Bio Quip Products, Inc., Rancho Dominguez, CA, USA) to prevent insects from crawling on the sides of dishes and escape.

### Inert dusts

Fresh batches of three commercial inert dusts made up of amorphous silica (Odor-Z-Way®, Celite®610, and Diafil®610) were purchased and kept in air-tight containers until analysis.

Odor-Z-Way is a deodorizer agent and was supplied by a local manufacturer (Odor-Z-Way®, Phillipsburg, KS, USA). Diafil is a diatomite functional filler and Celite is a diatomite filter aid. Celite and Diafil are registered Diatomaceous Earth (DE) products manufactured by Celite Corporation (Lompoc, CA, USA). Odor-Z-Way is not yet approved for grain and structural treatments. All three silica-based dusts were tested for their ability to control eggs and adults of six species of stored-grain insects on wheat kernels and on concrete arenas in 9-cm diameter plastic Petri dishes used to simulate the floor of empty bins.

### **Test insects**

Tests for variability in insects' susceptibility were carried out on populations of seven species of stored-grain insects: the lesser grain borer, *Rhyzopertha dominica* (F.); rice weevil, *Sitophilus oryzae* (L.); maize weevil, *Sitophilus zeamais* Motschulsky; red flour beetle, *Tribolium castaneum* (Herbst); sawtoothed grain beetle, *Oryzaephilus surinamensis* (L.), granary weevil, *Sitophilus granarius* (L.); and the Indianmeal moth, *Plodia interpunctella* (Hubner). All insects were reared on standard diets in a growth chamber at 28°C and 65% r.h. in the Department of Grain Science and Industry, Kansas state University, Manhattan, KS, USA. These species have been in rearing since 1999. Organic white wheat flour (Heartland Mills, Marienthal, KS, USA) plus 5% (w/w) brewer's yeast diet was used for rearing *T. castaneum*. Clean organic hard red winter wheat (Heartland Mills, Marienthal, KS, USA) was used for rearing *R. dominica*, *S. oryzae*, and *S. granarius*. Organic yellow dent corn (Heartland Mills) was used for rearing *S. zeamais*. Rolled oats and 5% (by wt) of brewer's yeast were used for rearing *O. surinamensis*. Unsexed adults of mixed ages were used in all tests.

### **Bioassay on wheat**

#### **Adult mortality and progeny production**

Controls (five replications) consisted of 100 g untreated wheat in 0.45L jars to which unsexed adults (50) aged 1-3 weeks of each insect species were added. Unsexed adults (50) aged 1-3 weeks of each insect species (except the Indianmeal moth, *Plodia interpunctella* (Hubner)) were added to 100 g hard red winter wheat (11-12% r.h.) in 0.45L cylindrical jars mixed with each of three amorphous dusts to provide doses of 0 (control), 0.2, 0.5, 1.0, and 2.0 g/kg. Before adding insects, jars were tightly closed and shaken manually for 3 min to ensure dust particles were uniformly distributed through the entire wheat sample. After adding insects, jars were tightly secured and kept into growth chambers (28°C, 65% r.h.) for 7 and 14 days to determine mortality. Insects were prevented from escaping by screened lid lined with mesh screens and filter papers. Mortality 7-day and 14-day post infestation were determined after separation of insects from wheat, dockage, and residual dust by using pans and aluminum sieves of various diameters. Each combination of species and dose was replicated five times and each replication was treated separately. Live and dead adults were counted, parental adults were discarded and wheat samples were incubated in a growth chamber to determine progeny production at 42 d post-infestation.

#### **Egg-to-adult emergence of four insect species on wheat**

Fifty (50) eggs of the lesser grain borer, *Rhyzopertha dominica* (F.); red flour beetle, *Tribolium castaneum* (Herbst); and the Indianmeal moth, *Plodia interpunctella* (Hubner) and 35 eggs of sawtoothed grain beetle, *Oryzaephilus surinamensis* (L.) were exposed to wheat treated with Odor-Z-Way, Diafil and Celite at 0 (control), 0.2, 0.50, 1.0, and 2.0 g/kg. Only doses of 0.5, 1.0, and 2.0 g/kg were used in tests with *Plodia interpunctella*, while doses of 0.2 and 0.5 g/kg were used in tests with *Rhyzopertha dominica* (F.), *Tribolium castaneum* (Herbst), and *Oryzaephilus*

*surinamensis* (L.). The numbers of emerged larvae and adults were assessed after 21 and 42 d. Each treatment was replicated five times.

### **Bioassay on concrete arenas**

Concrete-poured arenas were sprinkled with each of three amorphous silica dusts (Odor-Z-Way, Celite, and Diafil) to provide deposits of 0 (control), 1, 2, and 5 g/m<sup>2</sup>. Adults (50) of six insect species were added to untreated and amorphous dust-treated concrete arenas. The six insect species used in bioassay on concrete arenas were as follows: the lesser grain borer, *Rhyzopertha dominica* (F.); rice weevil, *Sitophilus oryzae* (L.); maize weevil, *Sitophilus zeamais* Motschulsky; red flour beetle, *Tribolium castaneum* (Herbst); sawtoothed grain beetle, *Oryzaephilus surinamensis* (L.), and granary weevil, *Sitophilus granarius* (L.). Adults were exposed for 24 and 48 h. After each exposure time, adults were carefully removed from Petri dishes and transferred onto clean, HRW wheat (11-12% moisture) in 0.45 L glass jars fitted with wire mesh screens and a filter paper. Adults were placed in a growth chamber at 28°C and 65% r.h. for 48 h of recovery and the wheat with insects was sifted to separate insects from the wheat using a 0.21 µm round holed aluminum sieve. The number of live and dead insects was counted in each jar and insects unable to respond when gently prodded with a camel's hair brush were considered dead. Mortality and knockdown percentages were determined 24 and 48 h post-exposure to the amorphous dusts.

### **Statistical analyses**

Mortality in treatments was corrected when mortality in controls exceeded 10% (Abbott, 1925). Abbott's formula for correction of mortality in treatment is expressed as follows:

$$\text{Corrected mortality} = 100 \times \left[ \frac{\% \text{ mortality in treatment} - \% \text{ mortality in control}}{100 - \% \text{ mortality in control}} \right] \quad (4.2)$$

Mean mortality and associated standard errors were calculated. Percent mortality was calculated from the number of dead insects out of the total exposed. Each combination of exposure time and/or dose was replicated five times, and independent samples were examined over time.

## Results & Discussion

### Adult mortality on wheat

The mean adult mortality on untreated wheat ranged between  $2.8 \pm 1.0$  and  $13.4 \pm 4.6\%$  at 7 d post-infestation and between  $2.8 \pm 1.5\%$  and  $60.4 \pm 4.6\%$  at 14 days post infestation (Table 5.1). On untreated wheat, adult mortality of each insect species was significantly higher 14 d post infestation compared to 7 d post infestation ( $P=0.23$ ). The corrected mean adult mortality on wheat is presented in Table 5.2. In case of *S. granarius*, 0.5 g/kg Celite caused 100% adult mortality 7d post infestation. Complete adult mortality with Diafil was achieved using 2.0 g/kg. When *S. granarius* adults were exposed for 14 days to Celite and Diafil, only 0.5 g/kg was required to achieve 100% mortality. *R. dominica* adults were more susceptible to Celite followed by Odor-Z-Way and Diafil. In fact, when *R. dominica* adults were exposed for 7d to 0.5 g/kg of Celite, Odor-Z-Way, or Diafil, mortality was respectively  $70.1 \pm 1.8$ ,  $35.6 \pm 8.6$ , and  $1.04 \pm 1.04\%$ . The adults *R. dominica* were generally not very susceptible to Diafil. Even 2g/kg of Diafil caused only  $49.7 \pm 1.6\%$  adult mortality at 7d post infestation. Extending the exposure duration from 7d to 14d increased adult mortality to only  $69.6 \pm 3.2\%$ . As for *S. zeamais*, 100% adult mortality was achieved 7d post infestation using 1g/kg of Celite, Diafil, or Odor-Z-Way, whereas 0.25 g/kg of Celite was able to achieve 100% mortality at 14d post-infestation. In case of *T. castaneum*, 0.5g/kg of Celite at 14 d post infestation, or 1g/kg at 7d post infestation yielded 100% adult mortality. When adults of *T. castaneum* were exposed to 2.0g/kg of Diafil, 100% mortality was achieved at 14d post-infestation. *S. oryzae* adults were very susceptible to Odor-Z-Way. In fact, only 0.5 g/kg of Odor-Z-way was required to achieve 100% mortality, while 1g/kg of Celite or Diafil was required to kill 100% of *S. oryzae* adults exposed to these dusts for 7d. Similarly to previous observations with *S. zeamais* and *T. castaneum*, a prolonged exposure of *S.*

*oryzae* adults from 7d to 14d reduced the dose required to achieve 100% mortality from 1.0 to 0.5g/kg of Celite or Diafil. Finally, *O. surinamensis* adults were susceptible to all three silica dusts, especially to Celite as just 0.5g/kg of Celite achieved 100% adult mortality 7d post infestation. A similar dose of Diafil caused 100% adult mortality, but only after 14 d of exposure. More than 95% of *O. surinamensis* adults exposed for 7d to 0.5g/kg of Odor-Z-Way were killed.

### **Progeny production on wheat**

Progeny production on wheat was determined for each of five species of stored-grain insects (Table 4.3). Progeny production relates to the ability of insects adults to mate, lay eggs and sustain infestation before they are killed by the grain protectant. As expected, progeny production on untreated wheat was generally higher than on wheat treated with the silica dusts. No progeny of *O. surinamensis* was produced on untreated wheat. Besides, no progeny data was recorded for *S. zeamais* due to cross contamination between jars inside the growth chambers. Progeny produced was  $51.6\pm 6.8$ ,  $238.6\pm 13.6$ , and  $239\pm 35.9$ , respectively for *S. granarius*, *R. dominica*, and *T. castaneum*.

On wheat treated with Celite and Diafil, progeny production generally decreased with increasing dose. Progeny production data was consistent with data on adult mortality. Complete progeny production suppression in *O. surinamensis*, *S. oryzae*, *T. castaneum*, *S. granarius* was achieved using only 0.5 g/kg of Celite. In case of *R. dominica*, 2.0 g/kg was required for complete progeny suppression. With Diafil, only the maximum dose (2.0 g/kg) achieved complete progeny suppression in *R. dominica*, *S. granarius*, and *T. castaneum*, although complete progeny suppression was not achieved in *S. oryzae* (Table 4.4).

### **Egg-to-adult emergence on wheat**

Celite and Diafil's influence on egg-to-adult emergence on wheat was determined for *P. interpunctella*, *R. dominica*, *T. castaneum*, and *O. surinamensis*(Table 4.5). Generally, larval counts and adult emergence decreased with increasing doses of Celite or Diafil. In case of *P. interpunctella*, 0.5 g/kg of Celite or Diafil was enough to prevent larval and adult emergence. Larval and adult emergence were also prevented in *T. castaneum* and *O. surinamensis* using 0.5g/kg and 0.2 g/kg of Celite, respectively. Doses of 0.2 and 0.5 g/kg of Diafil could not prevent larval and adult emergence in *R. dominica*, *T. castaneum*, and *O. surinamensis*.

### **Adult mortality on concrete**

Corrected mortality over time on concrete sprinkled with different rates of Celite, Diafil, and Odor-Z-Way was determined for *S. granarius*, *R. dominica*, *S. zeamais*, *T. castaneum*, and *O. surinamensis* (Table 4.6). On concrete arenas, adult mortality generally increased with increasing duration of exposure and dose. Odor-Z-Way at 5g/m<sup>2</sup> was successful at controlling all insect species within 24h of exposure. Celite (1g/m<sup>2</sup>) killed 100% of adults of *S. oryzae* and *R. dominica* within 24h, and adults of *S. granarius*, and *O. surinamensis* within 48h. Diafil was less successful at controlling adults of *S. granarius*, *R. dominica*, *S. zeamais*, *T. castaneum*, and *O. surinamensis*. When these species were exposed to the maximum dose of Diafil (5g/m<sup>2</sup>) during 24h, adult mortality was respectively 59.5±6.0, 11.9±0.7, 22.4±6.8, and 75.2±7.1%. Extending the duration of exposure from 24 to 48h did not yield 100% adult mortality. Two exceptions to this observation were encountered with 100% adult mortality of *S. oryzae* and *R. dominica* after 48 h exposure to 1 g/m<sup>2</sup> and 2 g/m<sup>2</sup>, respectively.

## Conclusions

The susceptibility to Celite, Diafil, and Odor-Z-Way varied among stored-product insect species and also among the type of substrate (wheat or concrete). Adults of the lesser grain borer, *Rhyzopertha dominica*, were generally least susceptible to all three amorphous silica dusts; however, a complete suppression of progeny production was possible using Celite. Adult emergence was generally not prevented by Celite, Diafil, and Odor-Z-Way which suggested a lower insecticidal efficacy of the three dusts against early developmental stages. On concrete, Odor-Z-way was particularly effective at controlling all stored-product insect species after 24 h of exposure. Odor-Z-Way has potential to control several insect species on wheat and would prove ideal for the treatment of surfaces of empty bins or grain processing facilities. Further research will investigate the impact of Odor-Z-Way on the efficacy of a heat treatment.

## References

- Abbott, W. S. 1925. A method for computing the effectiveness of an insecticide. *J. Econ.Entomol.* 18: 265-267.
- Andrić, G. G., Marković, M. M., Adamović, M., Daković, A., Golić, M. P., & Kljajić, P. J. (2012). Insecticidal potential of natural zeolite and diatomaceous earth formulations against rice weevil (Coleoptera: Curculionidae) and red flour beetle (Coleoptera: Tenebrionidae). *Journal of economic entomology*, 105(2), 670-678.
- Banks, J. H., and P. G. Fields. 1995. Physical methods for insect control in stored-grain ecosystems, pp.353-409. In D. S. Jayas, N. D. G. White, and W. E. Muir [eds.], *Stored-Grain Ecosystems*. Marcel Dekker, New York.
- Calvert, R. 1930. *Diatomaceous Earth*. American Chemical Society Monograph Series, J. J. Little and Ives Company, New York.
- Collins, P. J. (2006, October). Resistance to chemical treatments in insect pests of stored grain and its management. In *Proceedings of the 9th International Working Conference on Stored Product Protection* (Vol. 15).
- Daković, A., Matijašević, S., Rottinghaus, G. E., Dondur, V., Pietrass, T., & Clewett, C. F. (2007). Adsorption of zearalenone by organomodified natural zeolitic tuff. *Journal of Colloid and Interface Science*, 311(1), 8-13.
- Desmarchelier, J. M., Wright, E. J., & Allen, S. E. (1993). Dryacide (R): a structural treatment for stored-product insects.
- Desmarchelier, J. M., & Dines, J. C. (1987). Dryacide treatment of stored wheat: Its efficacy against insects, and after processing. *Australian Journal of Experimental Agriculture*, 27(2), 309-312.

Donahaye, E. J. (2000). Current status of non-residual control methods against stored product pests. *Crop Protection*, 19(8-10), 571-576.

Ebeling, W. 1961. Physicochemical mechanisms for the removal of insect wax by means of finely divided powders. *Hilgardia* 30: 531-564.

Ebeling, W. (1971). Sorptive dusts for pest control. *Annual review of entomology*, 16(1), 123-158.

Fields, P.G., Allen, S., Korunic, Z., McLaughlin, A., Stathers, T., 2003. Standardized testing for diatomaceous earth, In: Credland, P.F.A., Armitage, D.M., Bell, C.H., Cogan, P.M., Highley, E. (Eds), *Proceedings of the Eighth, International Working Conference on Stored-product Protection*, 22-26 July 2002, York, UK, CAB International, Wallingford, UK, pp. 779-784.

Golob, P. (1997). Current status and future perspectives for inert dusts for control of stored product insects. *Journal of Stored Products Research*, 33(1), 69-79. Golob, P. 1997. Current status and future perspectives for inert dusts for control of stored-product insects. 1997, *J. Stored Prod. Res.* 33, 69-79

Golob, P. A. V., & Webley, D. J. (1980). *The use of plants and minerals as traditional protectants of stored products*.

Haryadi, Y., Syarief, R., Hubeis, M., Herawati, I., 1994. Effect of zeolite on the development of *Sitophilus zeamais* Motsch, In: Highley E., Wright, E.J., Banks, H.J., Champ, B.R. (Eds), *Stored Products Protection. Proceedings of the Sixth International Working Conference on Stored-product Protection*, 17-23 April 1994, Canberra, Australia, CAB International, Wallingford, UK, pp. 633-634.

Hagstrum, D. W. and Bh. Subramanyam. 2006. Fundamentals of Stored Product Entomology, AACC International, St. Paul, Minnesota.

Kljajić, P., Andrić, G., Adamović, M., Bodroža-Solarov, M., Marković, M., Perić, I., 2010. Laboratory assessment of insecticidal effectiveness of natural zeolite and diatomaceous earth formulations against three stored-product beetle pests. *Journal of Stored Products Research* 46, 1-6.

Korunic, Z. (1997a) Rapid assessment of the insecticidal value of diatomaceous earths without conducting bioassays. *J. Stored Prod. Res.* 33, 219-229.

Korunic, Z. Diatomaceous earths, a group of natural insecticides. 1998, *J. Stored Prod. Res.* 34, 87-97.

Korunic, Z., Fields, P. G., Kovacs, M., Noll, J. S., Lukow, O. M., Demianyk, C. J., & Shibley, K. J. (1997b). The effect of diatomaceous earth on grain quality. *Postharvest Biology and Technology*, 9(3), 373-387.

Quarles, W. 1992. Silica gel for pest control. *IPM Practitioner* 14 (7): 1-11.

Singh, K., H. M. Bhavnagary, and S. K. Majumder. 1984. Silicophosphate as new insecticide. I. 18 Evaluation of silicophosphates for the control of stored grain pests in milled rice. *J. Food Sci. Technol.* 21: 302-307.

Subramanyam, Bh., Roesli, R., 2000. Inert dusts, In: Subramanyam, Bh., Hagstrum, D.W. (Eds), *Alternatives to Pesticides in Stored-Product IPM*. Kluwer Academic Publishers, Boston, USA, pp. 321-380.

White, N.D.G., Leesch, J. G., 1996. Chemical control. In: Subramanyam, Bh., Hagstrum, D.W. (Eds.), *Integrated Management of insects in Stored Products*. Marcel Dekker, Inc., New York, Basel, Hong Kong, pp. 399-408.

**Table 4.1** Mortality of adults of six species of stored-grain insects after 7 and 14 days on untreated wheat.

Insect species	Mortality (% mean $\pm$ SE)	
	7 days	14 days
<i>S. granarius</i>	13.4 $\pm$ 4.6	17.6 $\pm$ 4.0
<i>R. dominica</i>	3.3 $\pm$ 1.4	0.0 $\pm$ 0.0
<i>S. zeamais</i>	6.2 $\pm$ 0.3	9.9 $\pm$ 2.2
<i>T. castaneum</i>	2.8 $\pm$ 1.0	4.3 $\pm$ 1.4
<i>S. oryzae</i>	4.1 $\pm$ 1.1	2.8 $\pm$ 1.5
<i>O. surinamensis</i>	11.0 $\pm$ 3.4	6.4 $\pm$ 4.6

Each mean is based on  $n = 5$  replications. In each replication, 50 adults of a species were used.

**Table 4.2** Corrected adult mortality on wheat of six species of stored-grain insects exposed to various doses of Celite, Diafil, and Odor-Z-Way.

Species	Treatment	Dose	Corrected mortality* (% mean $\pm$ SE)	
			7 days	14 days
<i>S. granarius</i>	Celite	0.5	100 $\pm$ 0	100 $\pm$ 0
		1	100 $\pm$ 0	100 $\pm$ 0
		2	100 $\pm$ 0	100 $\pm$ 0
	Diafil	0.5	93.2 $\pm$ 2.5	100 $\pm$ 0
		1	98 $\pm$ 1.4	100 $\pm$ 0
		2	100 $\pm$ 0	100 $\pm$ 0
	Odor-Z-Way	0.5	-	-
		1	-	-
		2	-	-
<i>R. dominica</i>	Celite	0.5	70.1 $\pm$ 1.8	88.8 $\pm$ 2.1
		1	94.5 $\pm$ 1.5	99.2 $\pm$ 0.8
		2	95.9 $\pm$ 1.1	97.5 $\pm$ 1.5
	Diafil	0.5	1.04 $\pm$ 1.04	5.1 $\pm$ 1.4
		1	9.2 $\pm$ 4.2	40.4 $\pm$ 4.8
		2	49.7 $\pm$ 1.6	69.6 $\pm$ 3.2
	Odor-Z-Way	0.5	35.6 $\pm$ 8.6	-
		1	51.1 $\pm$ 4.8	-
		2	72.7 $\pm$ 2.0	-
<i>S. zeamais</i>	Celite	0.2	33.6 $\pm$ 8.4	100 $\pm$ 0
		0.5	97.4 $\pm$ 1.6	100 $\pm$ 0
		1	100 $\pm$ 0	100 $\pm$ 0
		2	100 $\pm$ 0	100 $\pm$ 0
	Diafil	0.2	16.4 $\pm$ 5.8	82.6 $\pm$ 4.7
		0.5	41 $\pm$ 11.9	97.8 $\pm$ 0.7
		1	100 $\pm$ 0	100 $\pm$ 0
		2	100 $\pm$ 0	100 $\pm$ 0
	Odor-Z-Way	0.5	98.6 $\pm$ 1.4	-
1		100.0 $\pm$ 0.0	-	
2		-	-	
<i>T. castaneum</i>	Celite	0.5	99.2 $\pm$ 0.5	100 $\pm$ 0
		1	100 $\pm$ 0	100 $\pm$ 0
		2	100 $\pm$ 0	100 $\pm$ 0
	Diafil	0.5	18.9 $\pm$ 3	67.7 $\pm$ 7.4
		1	34.7 $\pm$ 7.3	94.5 $\pm$ 2
		2	76.7 $\pm$ 8.3	100 $\pm$ 0
	Odor-Z-Way	0.5	94.3 $\pm$ 4.1	-
		1	94.9 $\pm$ 3.0	-

<i>S. oryzae</i>	Celite	2	-	-	
		0.2	92.0 ± 2.6	99.6 ± 0.4	
		0.5	99.6 ± 0.4	100 ± 0	
	Diafil	1	100 ± 0	100 ± 0	
		2	100 ± 0	100 ± 0	
		0.2	20.3 ± 6.4	90.1 ± 6.4	
		0.5	84.5 ± 5.6	100 ± 0	
		1	100 ± 0	100 ± 0	
		2	100 ± 0	100 ± 0	
	Odor-Z-Way	0.5	100 ± 0	-	
		1	100 ± 0	-	
		2	-	-	
<i>O. surinamensis</i>		Celite	0.5	100 ± 0	100 ± 0
			1	100 ± 0	100 ± 0
	2		100 ± 0	100 ± 0	
	Diafil	0.5	93.2 ± 1.9	100 ± 0	
		1	100 ± 0	100 ± 0	
		2	100 ± 0	100 ± 0	
Odor-Z-Way	0.5	95.7 ± 2.7	-		
	1	94.7 ± 5.3	-		
	2	-	-		

---

Each mean is based on  $n=5$  replications. In each replication, 50 adults of a species were used.  
 \* Mortality in treatments was corrected using Abbott's formula when mortality in control exceeded 10%.

**Table 4.3** Progeny production on untreated wheat exposed to six species of stored-grain insects

Insect species	Progeny
<i>S. granarius</i>	51.6 ± 6.8
<i>R. dominica</i>	238.6 ± 13.6
<i>S. zeamais</i>	-
<i>T. castaneum</i>	27.6 ± 2.7
<i>S. oryzae</i>	239 ± 35.9
<i>O. surinamensis</i>	0 ± 0

Each mean is based on  $n = 5$  replications. In each replication, 50 adults of a species were used.

(-) Data was not recorded

**Table 4.4** Progeny production on wheat treated with various doses of Celite and Diafil

Species	Treatment	Dose	Progeny
<i>S. granarius</i>	Celite	0.5	0 ± 0
		1	0 ± 0
		2	0 ± 0
	Diafil	0.5	3.6 ± 0.8
		1	0.2 ± 0.2
		2	0 ± 0
<i>R. dominica</i>	Celite	0.5	7.4 ± 2.7
		1	0.6 ± 0.4
		2	0 ± 0
	Diafil	0.5	243.2 ± 23.3
		1	27 ± 7.8
		2	12.2 ± 2.6
<i>T. castaneum</i>	Celite	0.5	0 ± 0
		1	0.2 ± 0.2
		2	0 ± 0
	Diafil	0.5	3.8 ± 0.7
		1	1.2 ± 0.4
		2	0 ± 0
<i>S. oryzae</i>	Celite	0.2	10.2 ± 5.4
		0.5	2.6 ± 1.1
		1	0 ± 0
	Diafil	2	0 ± 0
		0.2	141 ± 29.8
		0.5	11 ± 6.6
<i>O. surinamensis</i>	Celite	1	5 ± 2.5
		2	5 ± 1.3
		0.5	0 ± 0
	Diafil	1	0 ± 0
		2	0 ± 0
		0.5	0 ± 0

Each mean is based on  $n = 5$  replications. In each replication, 50 adults of a species were used.

**Table 4.5** Egg-to-adult emergence on wheat of four insect species of stored-grain exposed to various doses of Celite, and Diafil.

Species	Treatment	Dose	21 d larval counts	42 d adult emergence	
<i>P. interpunctella</i>	Control	0	31.4 ± 4.7	17.2 ± 2.5	
		Celite	0.5	0 ± 0	0 ± 0
			1	0 ± 0	0 ± 0
	Diafil	2	0 ± 0	0 ± 0	
		0.5	0 ± 0	0 ± 0	
		1	0 ± 0	0 ± 0	
	<i>R. dominica</i>	Control	2	0 ± 0	0 ± 0
			0	–	36.4 ± 3.8
		Celite	0.2	–	25.4 ± 1.4
0.5			–	3.4 ± 1	
Diafil		0.2	–	37.4 ± 4.3	
	0.5	–	31.2 ± 5.6		
<i>T. castaneum</i>	Control	0	43 ± 2.4	46.8 ± 4.4	
		Celite	0.2	7.6 ± 1	2.8 ± 0.6
			0.5	0 ± 0	0 ± 0
	Diafil	0.2	36 ± 3.4	35.6 ± 2.2	
		0.5	25.6 ± 1.6	19 ± 2.7	
<i>O. surinamensis</i>	Control	0	16 ± 2.3	24.6 ± 0.9	
		Celite	0.2	0 ± 0	0 ± 0
			0.5	0 ± 0	0 ± 0
	Diafil	0.2	2.6 ± 0.7	1.4 ± 1.4	
		0.5	0.2 ± 0.2	0.6 ± 0.2	

\_ Data not recorded

Each mean is based on  $n = 5$  replications. In each replication, 50 eggs of a species were used, except for *O. surinamensis* (35 eggs).

**Table 4.6** Corrected percent knockdown of adults of six species of stored-grain insects exposed over time to concrete sprinkled with different rates of Celite and Diafil.

Species	Treatment	Dose (g/m <sup>2</sup> )	24h	48h
<i>S. granarius</i>	Celite	1	20.4 ± 0.4	68.8 ± 3.3
		2	51.6 ± 4.4	74 ± 6.1
		5	43.3 ± 10.1	88.5 ± 7.2
	Diafil	1	11.3 ± 4.1	29.6 ± 3.6
		2	12.2 ± 4.3	24.1 ± 3.5
		5	37.6 ± 1.5	43.2 ± 7.8
<i>R. dominica</i>	Celite	1	67.9 ± 6.4	98.1 ± 1.9
		2	77.4 ± 3.8	95.3 ± 4.7
		5	74.4 ± 4.6	100 ± 0
	Diafil	1	23 ± 6.3	79.9 ± 20.1
		2	24.7 ± 6.3	81.3 ± 4.7
		5	50 ± 4.5	88.1 ± 2.1
<i>S. zeamais</i>	Celite	1	26.8 ± 3.7	68.4 ± 1.9
		2	41.3 ± 3.4	66.1 ± 3.2
		5	57.6 ± 2.5	78.7 ± 3.6
	Diafil	1	15.4 ± 4.7	20.1 ± 6.3
		2	22.1 ± 3.3	29 ± 2.1
		5	25.9 ± 0.7	43.2 ± 2
<i>T. castaneum</i>	Celite	1	8.3 ± 6	10.6 ± 9.2
		2	25.4 ± 1.6	14.5 ± 5.1
		5	16.7 ± 4.4	16.6 ± 4.4
	Diafil	1	6.7 ± 1.7	0 ± 0
		2	13.1 ± 6.1	10 ± 0
		5	11.2 ± 4.1	1.8 ± 1.8
<i>S. oryzae</i>	Celite	1	11.4 ± 4.6	95.2 ± 2.8
		2	15.9 ± 3.8	98.5 ± 1.5
		5	36.6 ± 2.5	93.8 ± 3.1
	Diafil	1	6.5 ± 4.4	31.2 ± 3.4
		2	4.6 ± 2.6	68.3 ± 7.4
		5	12.3 ± 3	65.7 ± 7.2
<i>O. surinamensis</i>	Celite	1	67.5 ± 9.3	98.7 ± 1.3
		2	80.3 ± 5.5	96.8 ± 1.6
		5	97.1 ± 1.5	98.5 ± 1.5
	Diafil	1	26.2 ± 6.4	74.6 ± 4.8
		2	25.5 ± 6	66.2 ± 2.9
		5	45.1 ± 15.5	91.6 ± 6.1

Each mean is based on  $n = 5$  replications. In each replication, 50 adults of a species were used.

**Table 4.7** Corrected mortality of adults of six species of stored-grain insects exposed over time to concrete sprinkled with different rates of Celite, Diafil, and Odor-Z-Way.

Species	Treatment	Dose	24h	48h	
<i>S. granarius</i>	Celite	1	95.2 ± 2.7	100 ± 0	
		2	98.4 ± 1.6	100 ± 0	
		5	98.4 ± 1.6	100 ± 0	
	Diafil	1	40.4 ± 13.1	67.5 ± 6.7	
		2	47.5 ± 0.1	71.1 ± 6.4	
		5	59.5 ± 6.0	89.1 ± 3.1	
		Odor-Z-Way	5	100.0±0.0	-
	<i>R. dominica</i>	Celite	1	100 ± 0	100 ± 0
			2	98.2 ± 1.8	100 ± 0
5			100 ± 0	100 ± 0	
Diafil		1	60.4 ± 11.8	96 ± 4	
		2	76.3 ± 7.4	100 ± 0	
		5	91.5 ± 4.5	100 ± 0	
		Odor-Z-Way	5	100 ± 0	-
<i>S. zeamais</i>		Celite	1	54.1 ± 11.1	88.5 ± 6.1
			2	48.2 ± 1.6	89.3 ± 6.6
	5		59.8 ± 10.8	95 ± .5	
	Diafil	1	4.4 ± 3.2	23.9 ± 5.7	
		2	9.8 ± 4.6	34.8 ± 6.5	
		5	11.9 ± 0.7	51.4 ± 7.4	
		Odor-Z-Way	5	100 ± 0	-
	<i>T. castaneum</i>	Celite	1	21.6 ± 8.4	12.3 ± 9.1
			2	42.9 ± 8.2	23.2 ± 9.7
5			38.3 ± 6	30.8 ± 8.2	
Diafil		1	6.7 ± 1.7	8.1 ± 1.8	
		2	19.4 ± 3.1	16.5 ± 2.8	
		5	22.4 ± 6.8	13.8 ± 3.3	
		Odor-Z-Way	5	100 ± 0	-
<i>S. oryzae</i>		Celite	1	100 ± 0	100 ± 0
			2	100 ± 0	100 ± 0

		5	100 ± 0	100 ± 0
	Diafil	1	61.1 ± 5.7	100 ± 0
		2	75.2 ± 3.3	100 ± 0
		5	90.2 ± 3	100 ± 0
	Odor-Z-Way	5	100.0 ± 0.0	-
<i>O.</i>	Celite	1	87.1 ± 7.6	100 ± 0
<i>surinamensis</i>		2	98.7 ± 1.3	100 ± 0
		5	97.2 ± 1.4	98.5 ± 1.5
	Diafil	1	48.9 ± 9.8	83.8 ± 7.6
		2	47.8 ± 6.7	79.5 ± 8.1
		5	75.2 ± 7.1	95.6 ± 4.4
	Odor-Z-Way	5	100.0 ± 0.0	-

---

Each mean is based on  $n = 5$  replications. In each replication, 20 adults of a species were used.

## General conclusion and Recommendations

According to BET and the IUPAC classifications, Hard Red Winter (HRW) Wheat had typical type II sigmoid shape isotherm, whereas, zeolite powder had a sorption isotherm close to resembling a type IV sigmoid shape isotherm. Type II isotherms are exhibited by nonporous or macroporous solids (pore size  $> 50\text{nm}$ ) and represents unrestricted monolayer-multilayer adsorption, while Type IV isotherms are mostly characteristic of mesoporous solids (pore size 2-50 nm) and are indicative of multilayer adsorption followed by capillary condensation. Full sorption isotherms of zeolite and wheat obtained at 25, 35, and 45°C clearly showed the hysteresis phenomenon, resulting from lower equilibrium moisture contents during adsorption than during desorption. Considering the IUPAC classification of isotherms, the hysteresis loops were of type H3 for HRW, and of type H4 for zeolite powder. Type H3 hysteresis are aggregates of plate-like particles forming slit-like pores, while type H4 hysteresis are narrow slit-like pores, particles with internal voids of irregular shape and broad size distribution, mostly hollow spheres with walls composed of ordered mesoporous silica. Adsorption hysteresis in porous materials such as inert dusts is characterized both by the shapes of the hysteresis loops and by the way in which they depend on temperature. The intensity of hysteresis remained unchanged for HRW, as hysteresis loop height and width did not change with increasing temperatures. Conversely, the intensity of hysteresis decreased with increased temperatures during water adsorption by porous zeolite powder. Sorption experimental data fitted by means of three single-temperature models: Guggenheim-Anderson-de Boer (GAB), Double Log Polynomial (DLP), and Brunauer-Emmet-Teller (BET). Irrespective of sorption direction, DLP model was the best model to estimate zeolite and HRW sorption isotherms, followed by GAB and BET models. As expected, BET model provided almost perfect fitting to sorption data, only in the water activity range 0-0.5.

Monolayer moisture content values ( $m_0$ ) for each sorption direction were provided only by GAB and BET models and indicated a decrease in monolayer moisture content with an increase in temperature. Critical water activity values for zeolite powder increased from 0.639 to 0.657 as temperatures increased from 25 to 45°C. The same trend was observed with HRW wheat as water activity values increased from 0.700 to 0.790 for the same temperature range. The recommended storage moisture contents for inert dust and wheat at different temperatures were determined and a linear relationship between zeolite (Z) and wheat (W) moisture contents was found to be temperature-dependent. A careful examination of optimal moisture contents of zeolites and wheat suggest that the water activity and the non-equilibrium moisture content of zeolite increased with increasing temperatures and wheat moisture content. Water activity was strongly linearly correlated ( $0.995 < R^2 < 0.999$ ) with temperature at constant zeolite or wheat moisture contents. The slopes of the lines obtained by plotting water activity as a function of temperature are higher during desorption than adsorption, which is a mathematical corroboration of the hysteresis phenomenon taking place in both wheat and zeolite samples. The net isosteric heats of sorption and the differential enthalpy of zeolite estimated by the Clausius–Clapeyron equation and determined graphically decreased with increasing moisture content of zeolite. Zeolite dust underwent a spontaneous adsorption process, which corroborates its hygroscopic nature.

The investigation of the effects of moisture content on dust and inert dust-treated wheat showed that within the 2-35% moisture range, surface mean diameter significantly decreased ( $F=331$ ;  $P<.0001$ ) with increasing moisture content. Conversely, volume mean significantly increased ( $F=3807$ ;  $P<.0001$ ) with increasing dust moisture content. Decreases in surface mean diameter values with increasing moisture content suggest the formation of agglomerates. Increases in

volume mean diameter with increasing moisture show that the proportion of large particulates is increasing in the particle size distribution. The particle size distributions of the silica dust reported as percentiles indicated that all three percentiles determined at 35% moisture content were significantly higher than the percentiles determined at 2.0, 6.0, and 10.0% moisture contents, which implies a significant increase in the particle size when dust moisture reaches 35%. No significant difference was found between median particle sizes ( $D_{v50}$ ) at 2% and 6% dust moisture content, but the median particle size at 10% was significantly higher than the median particle sizes at 2% and 6%. Significant changes in the median particle size begin to occur at 10% dust moisture content and the maximum change in particle size occur when the dust is at 35% moisture content, that is, at the time of reception. Also, changes at the extremes of the particle size distribution ( $D_{v10\%}$  and  $D_{v90\%}$ ) could be due to the presence of fewer fines, and more oversized particles or agglomerates, or a loss in texture and structure occurring above the critical water activity. Circularity values were comprised between 0.923 and 0.979 when the moisture of the dust ranged between 2 and 35%. Particles of the amorphous dust were not close to resembling a perfect circle. A significant decrease in circularity values was observed at 10 and 35% moisture contents. No significant difference was observed between circularity at 2 and 6% moisture contents ( $P < .001$ ). Deviation from a perfect circle was significantly higher at 35% moisture content. These changes in circularity suggest possible changes in particle form and/or outline (surface roughness). Aspect ratio ranged between 0.74 and 0.79 within the 2-35% moisture range, implying that the amorphous dust particles do not have regular symmetry, such as spheres or cubes and their shape is closer to ovoid particles. Solidity and convexity data provided more precise information about the outline of the particles. At 2% moisture content, convexity and solidity were respectively 0.977 and 0.978, whereas, at 35% moisture content,

these values dropped at 0.958 and 0.975, respectively. As with circularity, the values determined for aspect ratio, convexity, and solidity did not significantly change at 2% and 6% moisture contents. Aspect ratio, convexity, and solidity values were significantly lower at 35 % moisture content, followed by 10% moisture content. These lower convexity/solidity values show that the amorphous dust particles possess rough outlines and they probably become agglomerated primary particles as moisture increases. Values of static angle of repose can serve as an indirect assessment of flowability because the angle of repose relates to the inter-particulate friction. Changes in the bulk density of wheat were dependent on both the dust moisture and the rate of the application. In fact, the moisture main effect ( $F=2489$ ;  $P<.0001$ ) and the rate main effect ( $F=117$ ;  $P<.0001$ ) were significant at the 5% level of significance. The moisture by rate interaction was also significant at 5% level ( $F=5.0$ ;  $P=.0018$ ). The lowest increase in static angle of repose was observed when wheat was admixed with dust at 2% moisture content and a rate of 0.5g/kg. The highest increase in static angle of repose was observed when wheat was admixed with dust at 35% moisture content and a rate of 2.0 g/kg. Based on Carr's classification of powder flowability, wheat treated with the amorphous silica dust evolved from having "some cohesiveness" into exhibiting "true cohesiveness". Tests on bulk density showed that the moisture main effect ( $F=8248.51$ ;  $P <.0001$ ), the rate main effect ( $F=662.69$ ;  $P<.0001$ ), and the moisture by rate interaction ( $F=57.11$ ;  $P <.0001$ ) were all significant at the 5% level of significance. Similarly, tests on tapped density indicated that the moisture main effect ( $F=50547.8$ ;  $P<.0001$ ), the rate main effect ( $F=3362.64$ ;  $P<.0001$ ), and the moisture by rate interaction ( $F=631.39$ ;  $P<.0001$ ) were all significant at the 5% level of significance. An increase in both the dust moisture and the rate of application significantly decreased wheat bulk density and significantly increased wheat tapped density. Only minimal changes in bulk density

(decrease) and in tapped density (increase) occurred when wheat was mixed with 0.5g/kg dust at 2% moisture content. As with the static angle of repose, the highest increase in tapped density of wheat and the highest decrease in the bulk density of wheat were observed when wheat was admixed with 2.0 g/kg of dust at 35% moisture content. As for Hausner ratio and Carr index, there were a significant moisture main effect ( $F=8248.51$ ;  $P<.0001$ ), a significant rate main effect ( $F=662.69$ ;  $P<.0001$ ), and a significant interaction between moisture and rate ( $F=57.11$ ;  $P<.0001$ ) at 5% level of significance. In general, higher values of CI or HR were observed for combinations of higher dust moisture contents and higher rates of application. An increase in both the CI and the HR are indicative of a cohesive material with a tendency to not flow easily or a tendency to resist flow. Single Kernel Characterization System (SKCS) of wheat treated with dust at various moisture and rates were determined. The two-way analysis of variance did not show any significant difference in wheat kernel diameter ( $F=1.47$ ;  $P=.206$ ), and in wheat hardness ( $F=.37$ ;  $P=.95$ ). However, data on wheat weight and moisture content showed a significant interaction between dust moisture and rate of application ( $P<.05$ ). Wheat moisture and wheat weight were significantly higher when dust moisture was 35%. No significant difference was found in wheat moisture and wheat weight between untreated wheat (control) and all treatments with dust at 2%. Average kernel weight and moisture were similar between all treatments with 2 and 6% amorphous dusts. Permeability was measured as the pressure drop across the powder bed versus normal consolidation stress. A minimal pressure drop (high permeability) across the powder bed was observed for untreated wheat while moderate permeability was observed for wheat treated with each of the three amorphous dusts: Celite, Diafil and Odor-Z-Way. Compression had little or no effect on the permeability of untreated wheat, which is typical of non-cohesive, large particle size or granular material. However,

pressure drop increased with increased compression in all samples of wheat treated with the amorphous dusts, suggesting a reduction in the size and number of available channels for air to pass. Moderate permeability is typical of granular material with some cohesion and a wide particle size distribution. As expected, the conditioned bulk density (CBD) of wheat was significantly lower when wheat was mixed with 1g/kg Celite, Diafil, or Odor-Z-Way. The fine dust particles occupy the voids and small interstices between coarse grains kernels, causing a reduction in the weight of kernels needed to fill the same volume. The bulk density was similar between Wheat+Celite ( $688.03 \text{ kg/m}^3$ ) and Wheat+Diafil ( $697.09 \text{ kg/m}^3$ ), but significantly different to Wheat+Odor-Z-way ( $718.11 \text{ kg/m}^3$ ). Particle sizes and shapes of Celite and Diafil along with a better adhesion on wheat kernels could explain the higher decrease in bulk density of wheat kernels. Among the three dusts, Odor-Z-Way caused the minimum decrease in bulk density which could be explained by a lower adhesion on wheat kernels. According to stability index (SI) classification, untreated wheat (SI=.98) was a robust material, not being affected by being made to flow. The one-way analysis of variance showed a significant difference in SI ( $F=95.61$ ;  $P <.0001$ ). Admixing wheat with Odor-Z-way caused the SI to increase to 1.24. The *p*-values for the pair-wise ANOVA t-tests showed that the SI for Wheat+Odor-Z-Way (SI=1.24;  $P<.0001$ ) was higher than the SI for untreated wheat. The SI of Wheat+Celite (SI= 0.85;  $P=0.0052$ ) was statistically lower than the SI of untreated wheat. The SI of and Wheat+Diafil (SI= 0.94;  $P=0.5504$ ) was not statistically different from the SI of untreated wheat. Treating wheat with each of the three dusts caused wheat to become unstable. The deviation from stability observed in wheat treated with Celite (SI<1) could be attributed to coating of the blade and vessel, causing a reduction in flow energy due to a reduction in friction. On the other hand, the deviation from stability observed in wheat treated with Odor-Z-Way (SI>1) was more likely

caused by segregation (coarser kernels remaining on top and dust particles sinking to the bottom of the test vessel), and moisture uptake by the hygroscopic dust particles. Powders that are hygroscopic may take on moisture during the test, resulting in swelling of particles in size and in an increase in the surface frictional forces due to moisture adhering to the surface of the particles. Wheat mixed with amorphous silica dust is a granular system with a very wide particle size distribution. During the stability test, amorphous dust particles fill the voids between the large kernels, causing the granular system to segregate as a function of particle size. A visual inspection of test vessels showed a less pronounced segregation when wheat was mixed with Celite and Diafil, more likely due to their smaller particle sizes or better adhesion to wheat kernels, which were not determined. The flow rate index of wheat+Odor-Z-Way was 0.97, which is typical of powders with large particle size and insensitive to flow rate. Only wheat+Celite (FRI=0.85) and wheat+Diafil (FRI=0.87) showed pseudoplastic flow rates (FRI<1.0), usually seen in powders with flow enhancers. The flowability of wheat was apparently enhanced by the addition of 1g/Kg of Celite or Diafil. The low adhesion of Odor-Z-Way on wheat kernels as determined by visual evaluation caused most of the dust to sink to the bottom of the test vessel, resulting in a much lower kernel-kernel surface friction but a higher blade-dust friction expressed by higher energy requirements to initiate flow. The specific energy of wheat significantly decreased as a result of being admixed with amorphous silica dusts ( $F=129.85$ ;  $P<.0001$ ). The specific energy measured ranged between 1.94 and 2.33 mJ/mg, indicating that even after treating wheat with amorphous dusts, the cohesion remained low. The observations about the specific energy are consistent with the flow rate index and confirm that the three amorphous dusts somewhat improved the flow performance of wheat by acting as lubricants. In fact, specific energy and flow rate represent true flowability as they relate to the interaction between not only

wheat kernels, but also between wheat kernels and the inner surface of the storage vessel they are interacting with or sliding on.

The ability of powder to become aerated depends heavily on the cohesive forces acting between particles. The Aeration Ratio (AR) measured during the aeration program was respectively 2.19, 2.45, 3.66, and 3.15 for wheat, wheat+Odor-Z-way, wheat+Celite, and wheat+Diafil. Untreated wheat and wheat treated with each of the three amorphous dusts exhibited moderate sensitivity to aeration, which means they did not behave as cohesive materials, nor did they become easily fluidized. In fact, even at maximum air velocity ( $40 \text{ mm}\cdot\text{s}^{-1}$ ), fluidization was never achieved, since the flow energy never stabilized in relation to air velocity. Approximately 98% recovery to the BFE was observed in untreated wheat, after 5 de-aeration cycles, while 68-80% recovery was observed in wheat treated with the amorphous dusts. Despite having similar permeability, the dusts caused wheat to exhibit different de-aeration patterns. BFE generally increased with increased number of de-aeration cycles. Differences in de-aeration patterns can be attributed to the level of adherence of dust on wheat kernels, to the porosity of the dust particles, and to the particle size and shape of the different dusts, which were not determined. The tapped consolidated energy increased with increased number of taps and so did the bulk density. The tapped consolidated energy increased by 14.0-25.6% for a corresponding 2-5% increase in bulk density. After 400 taps, the bulk density of untreated wheat increased by 2%, the bulk density of Wheat+Odor-Z-Way increased by 4%, and the bulk density of both Wheat+Celite and Wheat+Diafil increased by about 5%. Similarly, the direct pressure consolidated energy increased with increased direct pressure, and so did the bulk density measured after direct pressure. The direct pressure consolidated energy increased by 21-47% for a corresponding 9-14% increase in bulk density. Changes in flow energy and bulk density were higher after direct

pressure (3-15Kpa) than after tapping (0-400 taps). The changes in flow energy measured after tapping and direct pressure simulate the change in flow energy that would occur after vibration or mechanical oscillation (like during transportation, process, and storage) or during storage in hopper under different normal stress. The magnitude of increase in bulk density was dissimilar to the magnitude of change in flowability.

The investigation of the insecticidal activity of the dust showed that the susceptibility to Celite, Diafil, and Odor-Z-Way varied among stored-product insect species and also among the type of substrate (wheat or concrete). On wheat, the adults *R. dominica* were generally not very susceptible to Diafil. Even 2g/kg of Diafil caused only 49.7±1.6% adult mortality at 7d post infestation. Extending the exposure duration from 7d to 14d increased adult mortality to only 69.6±3.2%. As for *S. zeamais*, 100% adult mortality was achieved 7d post infestation using 1g/kg of Celite, Diafil, or Odor-Z-Way, whereas 0.25 g/kg of Celite was able to achieve 100% mortality at 14d post-infestation. In case of *T. castaneum*, 0.5g/kg of Celite at 14 d post infestation, or 1g/kg at 7d post infestation yielded 100% adult mortality. When adults of *T. castaneum* were exposed to 2.0g/kg of Diafil, 100% mortality was achieved at 14d post-infestation. *S. oryzae* adults were very susceptible to Odor-Z-Way. In fact, only 0.5 g/kg of Odor-Z-way was required to achieve 100% mortality, while 1g/kg of Celite or Diafil was required to kill 100% of *S. oryzae* adults exposed to these dusts for 7d. Similarly to previous observations with *S. zeamais* and *T. castaneum*, a prolonged exposure of *S. oryzae* adults from 7d to 14d reduced the dose required to achieve 100% mortality from 1.0 to 0.5g/kg of Celite or Diafil. Finally, *O. surinamensis* adults were susceptible to all three silica dusts, especially to Celite as just 0.5g/kg of Celite achieved 100% adult mortality 7d post infestation. A similar dose of Diafil caused 100% adult mortality, but only after 14 d of exposure. More than 95% of *O.*

*surinamensis* adults exposed for 7d to 0.5g/kg of Odor-Z-Way were killed. On wheat treated with Celite and Diafil, progeny production generally decreased with increasing dose. Progeny production data was consistent with data on adult mortality. Complete progeny production suppression in *O. surinamensis*, *S. oryzae*, *T. castaneum*, *S. granarius* was achieved using only 0.5 g/kg of Celite. In case of *R. dominica*, 2.0 g/kg was required for complete progeny suppression. With Diafil, only the maximum dose (2.0 g/kg) achieved complete progeny suppression in *R. dominica*, *S. granarius*, and *T. castaneum*, although complete progeny suppression was not achieved in *S. oryzae*. Larval counts and adult emergence decreased with increasing doses of Celite or Diafil. In case of *P. interpunctella*, 0.5 g/kg of Celite or Diafil was enough to prevent larval and adult emergence. Larval and adult emergence were also prevented in *T. castaneum* and *O. surinamensis* using 0.5g/kg and 0.2 g/kg of Celite, respectively. Doses of 0.2 and 0.5 g/kg of Diafil could not prevent larval and adult emergence in *R. dominica*, *T. castaneum*, and *O. surinamensis*. On concrete arenas, adult mortality generally increased with increasing duration of exposure and dose. Odor-Z-Way at 5g/m<sup>2</sup> was successful at controlling all insect species within 24h of exposure. Celite (1g/m<sup>2</sup>) killed 100% of adults of *S. oryzae* and *R. dominica* within 24h, and adults of *S. granarius*, and *O. surinamensis* within 48h. Diafil was less successful at controlling adults of *S. granarius*, *R. dominica*, *S. zeamais*, *T. castaneum*, and *O. surinamensis*. When these species were exposed to the maximum dose of Diafil (5g/m<sup>2</sup>) during 24h, adult mortality was respectively 59.5±6.0, 11.9±0.7, 22.4±6.8, and 75.2±7.1%. Extending the duration of exposure from 24 to 48h did not yield 100% adult mortality. Two exceptions to this observation were encountered with 100% adult mortality of *S. oryzae* and *R. dominica* after 48 h exposure to 1 g/m<sup>2</sup> and 2 g/m<sup>2</sup>, respectively. In general, adults of the lesser grain borer, *Rhyzopertha dominica*, were generally least susceptible to all three amorphous silica

dusts; however, a complete suppression of progeny production was possible using Celite. Adult emergence was generally not prevented by Celite, Diafil, and Odor-Z-Way which suggested a lower insecticidal efficacy of the three dusts against early developmental stages. On concrete, Odor-Z-way was particularly effective at controlling all stored-product insect species after 24 h of exposure. Odor-Z-Way has potential to control several insect species on wheat and would prove ideal for the treatment of surfaces of empty bins or grain processing facilities. In view of the bulk and dynamic flow properties, Odor-Z-Way has potential to become a grain protectant provided that segregation and the decrease in bulk density are mitigated and that the insecticidal activity is not adversely affected by the seemingly low adhesion on wheat kernels. Our data also highlight the importance of drying any amorphous dust or allowing a dust to equilibrate at the experiment temperature before conducting tests on physical properties. The improper handling of the amorphous dust before analysis may cause significant bias in the analysis of the flow and the physical properties of amorphous silica dusts and ultimately that of inert dust treated wheat. Further research will investigate the impact of Odor-Z-Way on the efficacy of a heat treatment, the segregation behavior of inert dust, the adhesion characteristics of inert dust with grains, the friction characteristics of inert dusts, the adhesion characteristics of inert dusts with handling equipment, and the cost-effectiveness of a pest management program with Odor-Z-Way in comparison to other treatments like fumigation or chemical grain protectants.